AN ABSTRACT OF THE THESIS OF

Cody VandenRaadt for the degree of Master of Science in Nuclear Engineering presented on May 12, 2022.

Title: Impacts of Prompt Radiation on Nuclear Blast Waves.

Abstract approved:

_____

Camille Palmer

Prompt radiation accounts for 3% of the energy released in a nuclear blast. Simulating the prompt radiation will help identify the potential changes to the ambient temperature and pressure of air around the blast. The changes in ambient conditions may alter blast wave effects. The relationship between the energy deposition of prompt radiation in air and blast wave effects will be further analyzed to improve existing simulations. Existing nuclear blast wave simulations and estimates often rely on assumptions to limit the problem to manageable levels. One assumption used in current blast wave effect simulations is to ignore the prompt radiation from a nuclear blast. If simulating prompt radiation changes blast wave estimates, it may indicate an important correlation.

MCNP6 code was used to simulate the transport of prompt radiation in air. The simulation was conducted for four distinct designs of nuclear devices. The results of the simulation showed that prompt radiation from a nuclear device could potentially heat the air hundreds of degrees (C) as far as 100 meters from the blast. The increase in temperature also increased the ambient pressure of the air. The effects of the changes in ambient conditions were then utilized in analytical solutions to different blast wave effects. The results of these calculations were then compared to STP conditions to see how much blast wave effects changed as a direct result of simulating prompt radiation. It was found that simulating prompt radiation does change blast wave effects. Additionally, the impact of prompt radiation is higher at lower nuclear device yields. This indicates that current blast wave effect analytical solutions should be updated to account for the prompt radiation from a nuclear blast. The updated

solutions would hopefully drive the creation of better tools to increase the ability of civilian leaders to plan and respond to any nuclear weapon disasters.

Impacts of Prompt Radiation on Nuclear Blast Waves

by

Cody VandenRaadt

A THESIS

submitted to

Oregon State University

in partial fulfillment of
the requirements for the
degree of

Master of Science

Presented May 12, 2022
Commencement June 2022

Master of Science thesis of Cody VandenRaadt presented on May 12, 2022

APPROVED:

Major Professor, representing Nuclear Engineering

Head of the School of Nuclear Science and Engineering

Dean of the Graduate School

I understand that my thesis will become part of the permanent collection of Oregon State University libraries. My signature below authorizes release of my thesis to any reader upon request.

Cody VandenRaadt, Author

ACKNOWLEDGEMENTS

The making of this work was not done in a void, it is thanks to the contributions of many people that this work was able to be done. I would not have made it this far without the assistance of Aaron Tamashiro who consistently gave guidance and advice, giving up his own time to help me be successful.

TABLE OF CONTENTS

Page

1 INTRODUCTION 1

1.1 Nuclear Weapon Primary Features 2

1.2 Weapon Types 6

1.3 Prompt Radiation 9

1.3.1 Neutrons 9

1.3.2 Gammas 12

1.3.3 Secondary Photons and electrons 12

1.4 Blast Wave Formation 14

1.4 Research Objective 16

2 Literature Review 16

2.3 Current Nuclear Weapon Models and Simulations 17

2.4 Prompt Radiation Models 20

2.5 Blast Wave Models 24

3 Methods 31

3.3 MCNP 31

3.3.1 Neutron Input and Modeling 35

3.3.2 Gamma and Secondary Radiation Input and Modeling 38

3.3.3 Postproduction of Results 40

4 RESULTS 47

4.3 MCNP Results 47

4.3.1 Neutron Deposition 48

4.3.2 Gamma Deposition 50

4.3.3 Secondary Radiation Effects 54

4.4 Post Production Calculation Results 56

5 Discussion 87

5.1 Expected Results vs. Observed Results 87

TABLE OF CONTENTS (Continued)

Page

5.1.1 MCNP Results 88

5.1.2 Blast Wave Analytical Solution Results 91

5.2 Limitations of Research 99

5.3 Future of Model 101

6 Conclusion 104

References 108

LIST OF FIGURES

Figure Page

1.1 Radiation from nuclear blast at different times…….....…11

1.2 Gamma ray interaction based on energy and Z of molecule ……...…13

1.3 Ideal shock front shape of nuclear blast ……...15

2.1 Dose as a function of slant range of prompt neutrons versus yield …….21

2.2 Prompt gamma ray dose at different ranges and yields…….22

2.3 Neutron energy levels vs yield……...23

2.4 Angular distribution of Hiroshima neutrons……..24

2.5 Estimated temperature changes during radiation expansion period from prompt radiation ……...…….27

2.6 Thermal output of 19 KT blast vs time……..29

2.7 Pictures of 19 KT blast at different peaks……..30

3.1 MCNP6.2 model for prompt radiation transport ……..33

3.2 Three-Dimensional model of shells of air surrounding blast ……...34

3.3 Peak Overpressure versus distance for a 1-KT free air burst for sea-level ambient conditions …….…….....37

4.1 Type 3 device change in air temperature vs. distance …….……56

4.2 Type 5 device change in air temperature vs distance ……..57

4.3 Type 8 device change in air temperature vs. distance……..58

4.4 Type 13 change in air temperature vs. distance…….……..60

4.5 Temperature increase vs distance for all types of weapons devices……...60

4.6 Air temperature after simulating prompt radiation vs STP conditions……...…..63

TABLE OF FIGURES (Continued)

Page

4.7 Change to STP peak overpressure due to prompt radiation……..75

4.8 Change to STP dynamic pressure due to prompt radiation……..76

4.9 Changes to STP shock front density due to prompt radiation……..77

4.10 Change to STP material velocity due to prompt radiation…….……..77

4.11 Change to STP shock front temperature due to prompt radiation……..….78

4.12 Shock Temperature (K) vs Radius (m) …….…….…….……79

4.13 Observed blast temperature vs time…….…….…….…….80

4.14 Pressure vs Temperature of a 20 KT Blast…….…….…….……...81

4.15 Peak overpressure (bars) vs shock front radius…….…….…….…….82

4.16 Relationship between peak overpressure and particle velocity…….……..84

LIST OF TABLES

Table Page

1.1 Weapon types and description …… 08

3.1 Neutron and gamma yields for each device type…….…… 40

4.1 Type 3 average neutron energy deposited in air ……..…….…… .47

4.2 Type 5,8, 13 average neutron energy deposited in air …….…..... 48

4.3 Type 3 average neutron energy deposited in air ……..…..….. 49

4.4 Type 3 gamma energy deposited in air……..... 50

4.5 Type 5 gamma energy deposited in air……..... 50

4.6 Type 8 gamma energy deposited in air……..... 51

4.7 Type 13 gamma energy deposited in air……..…..... 52

4.8 Type 3 gamma energy deposited in air……..…….. 52

4.9 Energy from secondary radiation deposited in air by device type…...…….. 53

4.10 Type 3 secondary radiation energy deposited in air……... 54

4.11 Type 3 device temperature increase as a result of prompt radiation……..… 55

4.12 Type 5 device temperature increase as a result of prompt radiation…….. 66

4.13 Type 8 device temperature increase as a result of prompt radiation…….. 57

4.14 Air temperature changes from prompt radiation from Type 13 device ….….59

4.15 Air temperature changes from prompt radiation of 100 KT Type 3 device…61

4.16 Air temperature changes from prompt radiation of 1 KT Type 3 device……62

4.17 Type 3 initial calculation of peak overpressure at different distance……..64

LIST OF TABLES (Continued)

Page

4.18 Type 3 vs STP ambient pressure and peak overpressure at different distances ……..……...65

4.19 Type 3 STP vs. prompt ambient and shock front density…….…....66

4.20 Type 3 STP vs. prompt material velocity and dynamic pressure ……...…67

4.21 STP vs prompt shock front temperature……...……...68

4.22 Changes (%) in STP blast wave effects due to prompt radiation of 100 KT blast ……..…....69

4.23 Constant pressure blast wave effects……..….....71

4.24 Blast wave effects at STP conditions from a 1 KT blast..….....72

4.25 Blast wave effects after simulating prompt radiation from a 1 KT blast 73

4.26 Changes (%) in STP blast effects due to prompt radiation from 1KT blast……..…….....74

LIST OF APPENDICES

Appendix Page

Appendix A: MCNP Input Card Examples……..107

Impacts of Prompt Radiation on Nuclear Blast Waves

1 INTRODUCTION

This research aims to simulate and analyze the impacts of prompt radiation from the detonation of a nuclear weapon. This includes the effects on temperature, pressure, and most importantly, blast wave formation. While mathematical models do exist that estimate the range of values of nuclear weapons effects, they are limited in their ability to handle the impacts of prompt radiation on blast wave formation [2]. Many of these models utilize standard temperature and pressure (STP) conditions for air as their initial ambient conditions. Prompt radiation can change the ambient conditions, which may impact blast wave formation specifically. Prompt neutrons and gamma rays leave the initial blast area significantly quicker than the blast wave is formed. This initial radiation interacts with the environment around the blast significantly increasing the air temperature and pressures as the blast wave is being formed. In order to establish a baseline for the importance of this modeling, a literature review was conducted of relevant weapons effects. The majority of available prior research is based on empirically gathered information that can describe the individual events of a blast but not holistically describe the source of effects or how they effectively tie together. To better understand the impacts of this prompt radiation, Monte Carlo N-Particle Transport Code (MCNP6.2) was used to simulate the absorption of energy in open air [7]. The results of the MCNP predictions were then utilized in previously existing analytical solutions for blast wave formation. These results were compared to the historical models for blast wave effects. Additionally, the blast solutions will be calculated at STP conditions to give a reference point for how much the energy deposited from prompt radiation can change solutions.

The specific objectives for the model are:

- Use MCNP6.2 to estimate the energy deposition in air from prompt neutrons of a blast at different distances for various special classes of nuclear weapons
- Use MCNP 6.2 to estimate energy deposition in air from prompt gamma radiation at different distances for various special classes of nuclear weapons
- Estimate the change to blast wave effects such as peak overpressure, dynamic pressure, shock front density, material velocity, and shock front temperature using available analytical solutions compared to standard temperature and pressure conditions

MCNP will help determine how much ambient conditions can change by effectively modeling energy deposition in air. If the change to ambient conditions of air drives a change in the analytical solutions of blast wave effects, it may imply a more direct relationship between prompt radiation and blast wave effects. It may also indicate that improved predictions of blast wave effects may be possible by including more prompt radiation simulations. This would have multiple benefits including more accurately modeling the total radius of a blast front, predicting the optical signal of the blast, and accurately predicting the impacts of the blast wave at different distances. These models would be extremely useful in the civil planning and preparation for response to a nuclear detonation event. Additionally, this lays the groundwork for future work with more complicated ground blast wave formation analysis.

1.1 Nuclear Weapon Primary Features

Nuclear weapons are unique from conventional weapons in many different important areas. These features will be introduced here as basic overviews to increase general understanding of the interaction of the observed weapons effects and the research being produced. Understanding all the different interacting components of a nuclear blast is vital to understanding and modeling the effects of those forces.

The two primary sources of energy that contribute to a nuclear blast are fission and fusion. The primary differences between fission and fusion are the total amount of energy available in the blast and the spectrum of the energy of the radiation released in the blast. Fusion reactions in a weapon significantly change the amount of prompt radiation released and the energy spectrum of the prompt radiation released in the blast. For this current research, multiple types of devices using both fission and fusion will are analyzed. Once the device types are compared, a single device type is selected for further analysis of blast wave effects.

Fission weapons utilize the power of nuclear bonds in fissile isotopes to create a significant release of energy. Fissile isotopes like U-235 and Pu-239 can undergo fission by neutrons at all energies [1]. There are also fissionable isotopes like U-238 that can only undergo fission by neutrons at very high energies [1]. To produce a nuclear blast, the fission events must be in a chain reaction which must occur rapidly. If the chain reaction rate is too slow, the materials will blow apart causing a fizzle blast. The state of a systems fission reaction is described using the term criticality [1]. Neutrons from fission are created in groups called generations. Generations are groups of neutrons created around the same time. Criticality describes the difference between the number of neutrons in a current generation relative to the number of neutrons released in the next generation. A reaction that has an increasing number of neutrons released is called supercritical [1]. If the number of neutrons released is constant it is called a critical reaction. Finally, when the number of neutrons in each subsequent generation is decreasing it is called a sub-critical reaction.

If enough fissile material is collected into a small amount of space, it creates a supercritical environment. The mass of fissile material required to create these conditions is called a supercritical mass [1]. The supercritical mass is different for different fissile materials. When a supercritical mass of fissile isotope is achieved, multiple increasing generations of neutrons are quickly generated. For each fission event, approximately 200 MeV of energy is released [1]. This energy is distributed between fission fragments, 2-3 neutrons released per fission, gamma rays, and thermal radiation [1]. That means each atom of fissionable material contains vast

amounts of releasable energy per unit mass. The critical mass of different isotopes varies significantly with geometry and other factors. These factors are not of great importance to the simulation being conducted. The MCNP simulation only relies on the total energy spectrum of the released prompt radiation not the amount of initial material or efficiency with which it is consumed.

Fusion is the second important nuclear force utilized in nuclear weapons. Fusion involves the nuclei of two smaller isotopes such as deuterium and tritium (H-2 and H-3) that under high temperature and pressure conditions are forced together to create one new heavier element (He in D-T reactions) [1]. The difference in binding energies between the two smaller nuclei and the new larger one is released as energy into the area around the reaction. The reaction release approximately 17.6 MeV as well as additional energy stored in an ejected neutron and thermal radiation. The energy of this neutron (up to 14 MeV) can be much higher than a neutron created as a result of fission (up to 10 MeV). As a result, fusion neutrons can be used to cause secondary fission events in fissionable materials like U-238 [1]. These fission events would otherwise be impossible due to the relatively low energy level of neutrons created in a fission event.

While the 17.6 MeV may not seem like a significant amount compared to the 200 MeV released in fission, it is in fact significantly higher. When the per unit mass is compared, fusion releases about four times as much energy as fission per unit mass. While fusion releases more energy per unit mass, it often only accounts for about half of the overall energy of a modern nuclear weapon[1]. Fission is still a primary driver and initiator of the overall reaction. Fusion does change the average energy of neutrons released in the overall reaction, as well as the amount of gamma radiation produced in secondary fission events. Fusion occurs on the same time scale as fission, around 1 microsecond. Prompt radiation produced in fusion has the same interactions as those from fission. All radiation produced in fusion will either help initiate more fission events, be absorbed or scattered in weapons material, or escape into the air surrounding the blast.

The neutrons released in fission and fusion can cause more fission events in the remaining fissionable isotopes, be absorbed in materials surrounding the weapon core, scatter off different materials surrounding the reaction, or can escape into the environment outside the weapon materials as initial or prompt radiation [1]. Radiation travels at the speed of light between collisions with other atoms making all these processes extremely fast relative to other weapon effects like blast wave formation [2]. There are secondary decay events that take place inside weapon materials that become excited in a high energy environment. The secondary decays do release large amounts of energy, but at later points of time a blast than prompt radiation [1]. The prompt radiation is released near instantaneously, making it the most important factor to this research. The prompt radiation that escapes will drive the energy available to be deposited in the air surrounding the detonation. The total amount of energy accounted for as prompt radiation is estimated around 3% of the total energy released in a nuclear blast [1]. This is a small amount of energy compared to the overall energy released in a blast. However, it is still a significant amount of energy that can potentially travel thousands of meters in air. As prompt radiation moves through air it interacts with the air molecules potentially heating the air to millions of degrees (K) close to the blast [2]. real impact on the area surrounding a nuclear blast, as well as shaping many of the blast effects that follow.

In addition to the initial radiation released in the blast, nuclear weapons also have unique blast and shock effects that are distinctly different from conventional high explosive weapons [2]. These effects include the highly destructive wave of air that precedes the thermal radiation from a blast moving through an area. This wave of air is called the shock or blast wave. The blast wave is one of the most destructive effects of a nuclear weapon [1]. Simulating blast wave is very difficult due to the extremely high temperatures and pressures involved in a nuclear blast [2]. This very difficult simulation is treated as a point source hydrodynamic expansion in currently existing analytical solutions [2]. These solutions will be integrated into the simulation being conducted to understand how they are affected by prompt conditions. Most analytical models only begin being relatively accurate at distances far enough away

from the blast the state of air returns to relatively normal conditions [2]. It is due to the difficulty of these analytical simulations accounting for the conditions close to the blast that it is believed including the conditions created by the prompt radiation will help improve the common understanding of this powerful force.

There is one additional phenomenon that is worth consideration within the scope of this research. The luminosity of the prompt radiation and shock front is a primary consideration in measuring the energy release of a nuclear blast [2]. It has been observed that there are two peaks of light in nuclear explosions called the two pulse phenomena [8]. While technically the two pulse phenomena is a combination of many of the effects already discussed, it is important to consider on its own as it is from the combination of prompt radiation and blast wave analysis that creates the first pulse of light seen in a nuclear blast. The visible light makes it possible to measure the expansion velocity of the blast wave and the difference in time between the two peaks allows for a measurement of the amount of energy potentially released in a blast. Determining the amount of energy released in a nuclear blast can be extremely important from a civil response perspective. There is the potential that in better understanding prompt radiation and blast wave interactions that better models can be developed to determine the amount of energy released. Once the energy can be accurately determined civil response teams can better plan for their response based on potential weapon effects modeled on the energy release alone.

Lastly, nuclear weapons also have unique effects of thermal radiation, electromagnetic radiation (EMP), and residual nuclear radiation or “fallout”. These effects describe the amount of energy released in the form of heat due to thermal radiation, highly ionizing radiation, and the release of radioactive materials into the environment surrounding the blast respectively [1]. These effects occur minutes to days after the initial blast [2]. Since they occur at a time that is relatively much later than prompt radiation these effects are not important to the current simulation. The effects to be studied occur in the first few milliseconds of the blast [1]. These effects are powerful but have little relationship to prompt radiation simulations.

1.2 Weapon Types

To more accurately simulate the energy released from nuclear weapons it is important to analyze a few different types of weapons that have historically been modeled. It is beneficial to define how these different weapon types will be referred to. Additionally, it is important to see what differences in radiative outputs different design types may have. All weapon types will be based on general features as defined in the Northrop "Handbook of Nuclear Weapon Effects: Calculation Tools Abstracted from DSWA's Effects Manuel One (EM-1)" book [3].

The first device type given in Northrop is a Type 3 device [3]. The key feature of this device is that it is based entirely on fission utilizing an implosion style device [3]. The features described in Northrop are for an unboosted fission implosion weapon that has a contemporary design [3]. Contemporary design means that it is relatively recent, but not the most modern design available. Contemporary designs generally use PU-239 in implosion configurations as the primary trigger for the device [1]. The Type 3 device also has no additional radiation boosting from fusion. The outputs of neutron and gamma radiation are thus smaller and more limited in energy range due to the limited potential of fission alone. These types of devices are also generally limited in scope to around 100 KT which sets a solid maximum energy value to analyze across all device types [1]. There is also a significant amount of historical research available on fission spectrums from this device type making it useful in simulating energy deposition.

The second device type that will be simulated is called a Type 5 device. This is listed in Northrop as a boosted fission implosion weapon with a modern design in the Handbook of Weapons Effects [3]. This means the weapon uses a small amount of fusion materials in order to boost the overall fission rate as well, and was the newest available by 1997 when the book was published. In addition to the increase rate of fission, the energy spectrum of neutrons that will be released will be based on the fusion neutron spectrum [3]. However, the yield of prompt radiation is smaller than other devices with fusion due to most of the energy still coming from the fission reaction.

The third type of device that will be simulated is a Type 8 thermonuclear secondary device [3]. This device type will simulate a primary fission initiated reaction, with a large fusion secondary that significant raises the number and energy of prompt neutrons and prompt gammas that escape from the device. The source of energy release is even between the fusion and fission in the device. The key differentiation is the amount of prompt radiation that escapes [3]. This device is unique in that implementing a secondary fusion reaction as a large source of energy also raises the mass of the weapons material. This increase in mass absorbs more of the prompt radiation than smaller device designs [3]. This causes a loss of prompt radiation that will be reflected in the calculations of energy deposition.

The final type of weapon analyzed is a Type 13 enhanced radiation thermonuclear secondary [3]. This device is also based in equal distributions of energy between fission and fusion like the Type 8 design. However, this design has been optimized to increase the amount of prompt radiation released [3]. This implies that the weapon is made with less mass available to absorb prompt radiation. The output of prompt radiation that escapes the devices is the highest of the device types. The energy spectrum used in the simulation will be from fission and fusion. The average energy level of the prompt gamma radiation released by this device is also the highest of all the designs. Gamma radiation is more heavily absorbed in dense weapons materials. The more efficient size of this design allows for more gamma rays to escape with fewer scattering or absorption events than other device types. All four weapon types are displayed with a brief description in Table 1.1 below:

Table 1.1 Weapon types and description

Device Name	Device Description	Source of Energy
Type 3	Contemporary implosion device	Fission
Type 5	Fusion boosted modern implosion device	Fission/Fusion
Type 8	Thermonuclear secondary with implosion trigger	Fission/Fusion
Type 13	Thermonuclear secondary	Fission/Fusion

	optimized for radiative release	

Table 1.1 is a useful reference with consolidated device descriptions. These devices will be discussed extensively throughout the research. It will be important to be able to effectively distinguish between designs. The primary differences in design will be the amount of prompt radiation released.

1.3 Prompt Radiation

Prompt radiation is the radiation that is released as a direct result of fission or fusion in nuclear weapon. A large portion of the prompt radiation energy is absorbed in the dense materials of the weapon itself. Neutrons are used to continue the fission chain reaction and are lost. Despite the losses in the weapons materials, a significant amount of radiation does escape and interacts with the environment surrounding the device. These interactions all occur within approximately .01 μs of the supercritical mass forming [3]. This is source of energy that can be deposited in air prior to the blast wave forming. MCNP will be utilized to simulation how this prompt radiation will travel and distribute energy into open air. The energy deposited in air will caused an increase in both ambient temperatures and pressures ahead of the blast wave. Prompt radiation includes three important types of radiation that will be simulated and contribute to the energy deposition in air.

1.3.1 Neutrons

Neutrons are produced when fission occurs in fissionable isotopes. The average number of neutrons produced on average varies with the material but is between 2 and 3 for each fission event. The energy spectrum of these neutrons can vary from .988 up to 10 MeV [1]. The majority of these neutrons are born fast with energies above 1 MeV [1]. These energy levels have important impacts on the probabilities of particle interactions like scattering or absorption of occurring. Many of these neutrons are captured by fissionable material around the reaction or absorbed in the super dense materials used in nuclear weapons. As a result, only a fraction of the neutrons produced in the initial supercritical mass escape the immediate area of the blast [1]. Empirical data gathered on open air tested weapons has shown estimates of

approximately how many neutrons escape per KT of a fission source blast [3]. For example, it is estimated that in an unboosted fission implosion device approximately $2.7x10^{23}$ neutrons per KT are released [1]. Out of these initially produce neutrons, only a portion make it outside the weapons immediate area. The fraction that escapes into air is highly dependent on weapon design [2]. It is the transport of these neutrons in air that will be handled in the MCNP simulation.

Prior to escaping the device many of these neutrons will interact via elastic and inelastic scattering. As a result of these interactions, many fast neutrons lose energy. As neutrons begin to lose energy the chance of them interacting with particles of air increases [1]. These low energy neutrons are called thermal neutrons [1]. Neutrons lose their energy more quickly than gamma radiation and do not travel as far in air as a result. In the MCNP simulation this may impact the amount of energy deposited at different distances. Neutrons will have a larger impact initially, and as the range increases it would be expected to decrease.

One interesting exception to the impact of thermal neutrons comes from neutron capture by nitrogen. When nitrogen absorbs a high energy neutron above 10 MeV it can create the isotope N-16 [2]. This element decays by emitting gamma radiation at energies as high as 7.1 MeV [2]. This is a relatively energetic gamma ray that causes an increase in dose to anyone in the area. This decay interaction takes almost 7 seconds which is too long to significantly impact blast wave effects [1]. It is more impactful for dose calculation.

As these neutrons move through air, they will experience both elastic and inelastic scattering. Inelastic scattering is the most important interaction mechanism to the MCNP predictions as energy is being physically imparted to the air which would results in both an increase in temperature as well as pressure. These neutron interactions will also cause significant excitation in materials in the air. This is particularly true for oxygen and nitrogen which are abundant in air. Inelastic scattering becomes a significant source of gamma radiation as well as impacting the optical edge of light that preempts the full spectrum of light that is produced in a

nuclear blast. All these interactions occur extremely fast as shown in Figure 1.1 below.

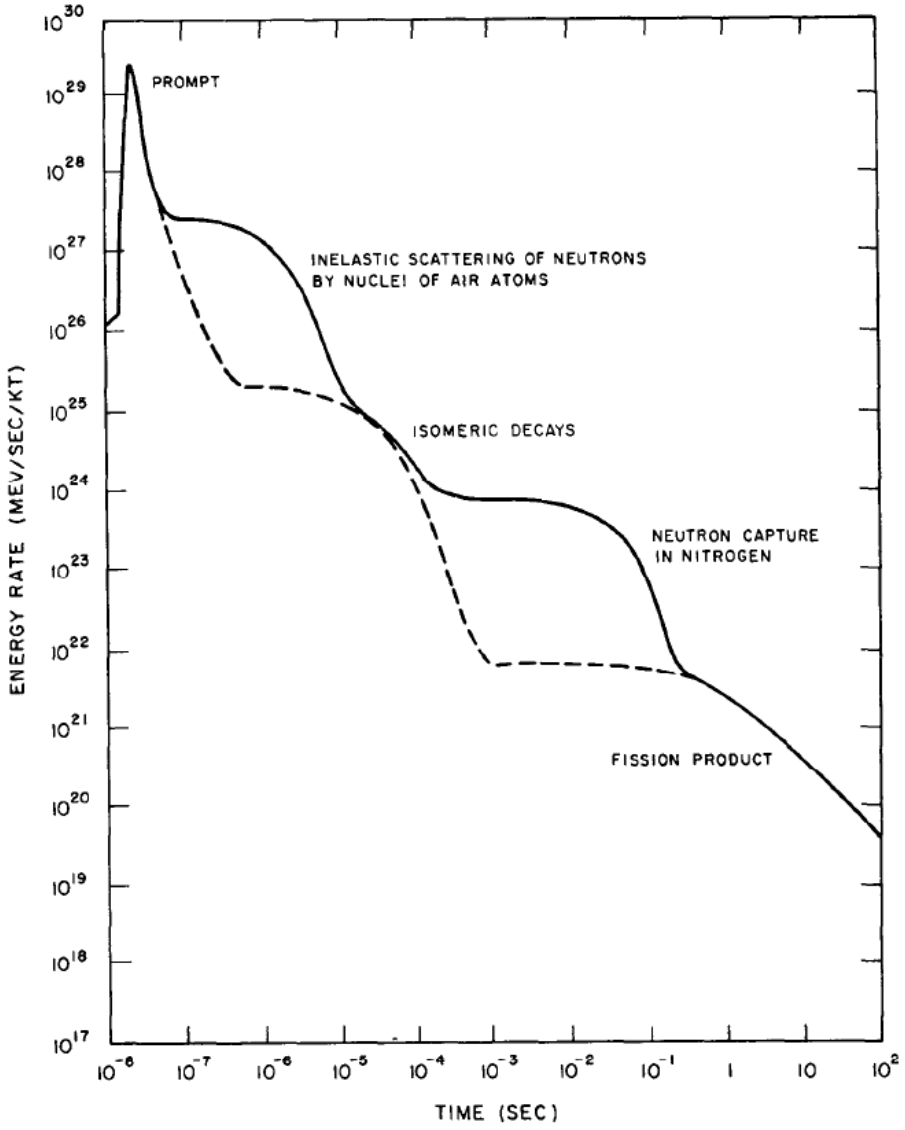

Figure 1.1 Radiation from nuclear blast at different times

The significance of prompt radiation starts to decrease with time as other blast effects like the shockwave and thermal radiation begin to dominate. The neutrons quickly undergo most of the relevant energy transfer events by .1 seconds after the blast occurs. MCNP will allow us to simulate how much energy can be transferred in this short amount of time. This will represent the total change in air temperature caused by neutrons released in prompt radiation.

1.3.2 Gammas

Along with neutrons, gamma rays are also released during fission and fusion events in a nuclear blast. These gamma rays are created at .01 μs as seen in Figure 1.1. This is the same time scale as prompt neutrons. The gamma rays are created with an average energy of 6.6 MeV [1]. Because they are created so quickly, these gamma rays interact strongly with the dense weapons materials that still surround the weapon core prior to being vaporized. As a result, a large portion of these gamma rays are absorbed prior to escaping the weapon itself. The amount that escape is highly dependent on weapon design. Gamma rays are created at an estimated rate of about 4.92×10^{21} MeV/nsec-KT resulting in a total of about 9.8×10^{22} MeV/KT of gamma radiation being released in the form of prompt radiation alone in a standard modeled implosion device [3].

The amount of gamma radiation increases dramatically when fusion is utilized in the making of the device. Modern calculations have shown that as much as 6.70×10^{23} MeV/KT of gamma ray energy can be released in enhanced fusion weapons [3]. This is roughly ten times the amount of gamma rays created in pure fission. Gamma rays travel further in air then neutrons and may have more impacts on air temperature, pressure, as well as air density. These are ambient conditions that are influential on blast wave effects like peak overpressure, shock front density, and shock temperature. This will be especially interesting to simulate as distance increases and radiation has potentially more impact on blast wave effects.

1.3.3 Secondary Photons and electrons

When prompt gamma rays escape from the weapons material into the surrounding air, a number of significant interactions begin to occur that are important to account for. First, for prompt gamma radiation above 10 MeV, pair production is an important effect to consider. Figure 1.2 below shows the dominant way gamma rays interact with different materials as a function of energy and atomic number of the material.

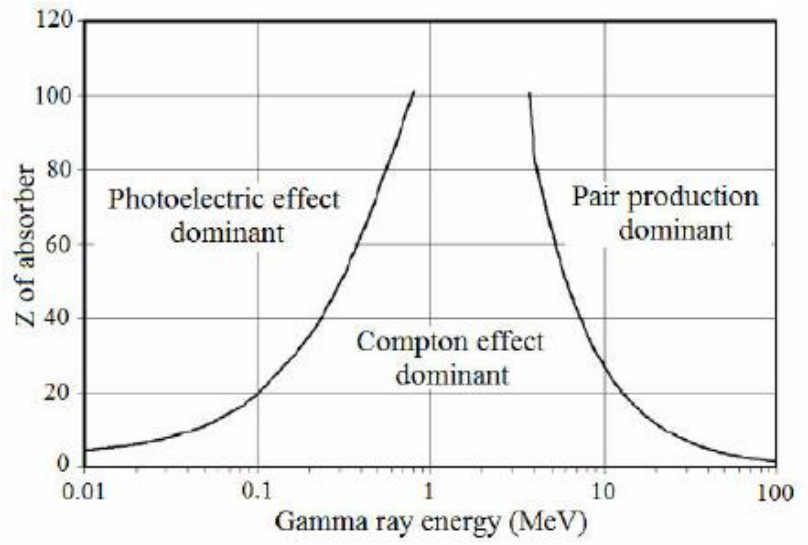

Figure 1.2 Gamma ray interaction based on energy and Z of molecule

The element with the largest atomic number (Z) in air is oxygen(8). That means at high energies pair production begins to dominate the gamma ray interaction spectrum. That does not mean pair production cannot occur at lower energies. For pair production to occur the gamma ray only needs to exceed 1.022 MeV[1]. For every gamma above the minimal threshold of 1.022 MeV it is possible that they will interact with the air molecules resulting in the production of a positron and electron. The positron will then travel until it interacts with a free electron. At this point they will annihilate releasing 1.022 MeV into the surrounding air [1]. This is a significant amount of energy that will add to the already high levels of energy being deposited in the immediate area surrounding a detonation.

It has been estimated that the lowest average energy of gamma rays that escape from weapons materials of a Type 3 device is approximately 1.5 MeV [3]. At this energy level, it is apparent that this interaction can and will occur in the air surrounding the weapons material and must be considered in any simulation. This does not mean that pair production will be the dominant form of interaction.

Air consists of nitrogen, oxygen, carbon, and argon amongst trace amount of other elements. The majority of air is nitrogen with a very low atomic mass. Based on Figure 1.2 this means that gamma interactions in air will be mostly Compton

scattering events. However, while pair production is not dominant, it is possible at energy levels above 1.02 MeV and will add measurably significant amounts of energy into the air as a result of prompt radiation. MCNP is able to account for these interactions, making it extremely valuable in estimating energy deposition.

1.4 Blast Wave Formation

The blast wave of a nuclear weapon is one of its most destructive features. It begins when the rapid release of energy from fission is transferred into materials surrounding the fissile core of the weapon. This energy creates a large increase in both temperature and pressure in those materials, quickly converting the solid materials in hot gas compressed at extremely high pressures [1]. As these temperatures and pressures, gases expand rapidly initiating a shock wave. This shock wave is referred to as a blast wave when the medium is air because it is also accompanied by a strong wind front [1].

As the blast wave expands out from the blast, a shock front is formed where the pressure is significantly higher than the ambient pressure of the air in front of the shock front. The shock front expands to this lower pressure region causing significant damage in areas it passes through by means of its overpressure and high dynamic pressure. Overpressure is the amount in which the peak pressure in the shock front exceeds the ambient pressure in the air immediately in front of the shock front. Dynamic pressure is the associated force of the velocity of the air moving just behind the shock front. This is commonly seen as the strong wind force that develops in an above ground blast [3]. The pressure in the shock front over distance is displayed in Figure 1.3 below.

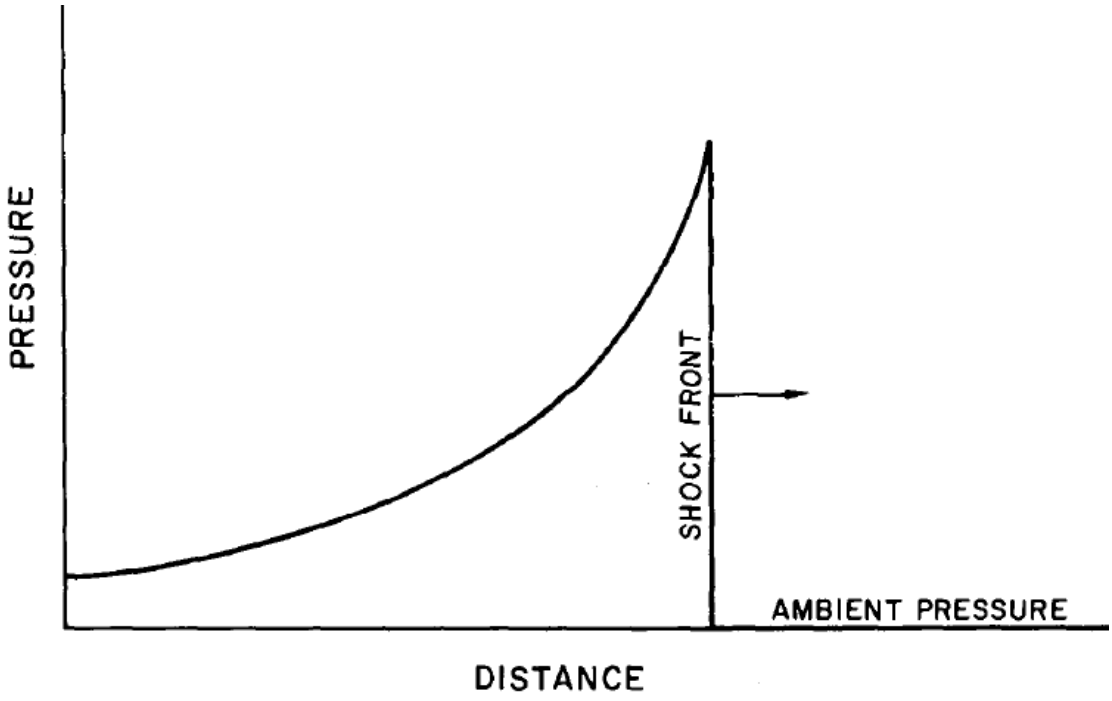

Figure 1.3 Ideal shock front shape of nuclear blast [1]

The velocity of the shock front as well as the velocity of the air particles are both associated directly with the blast wave. The shockwave velocity is the rate at which a blast wave can propagate through space [3]. This is directly influenced by the peak overpressure of the shock front, the medium through which it is travelling, as well as the altitude of the blast.

The blast wave forms on approximately 0.1ms after the initial blast. It continues to increase in temperature and pressure as it expands through approximately 1s. There is a point in the blast when the thermal radiation from the blast moves faster through the air than the shock front and the two separate fronts merge. However, the timescale of that merger happens on the scale of seconds which is far beyond the timescale of this research. For the purpose of this research the blast wave formation is of primary importance. Additionally, there is a shock front phenomenon known as breakaway which is when the shock front breaks away from the fireball[1]. This occurs when the shock front cools to approximately 300,00K [2]. The distance that

breakaway occurs will change with the yield of the device which heavily influences the shock front temperature [3].

1.4 Research Objective

The goal of this research is to simulate and analyze the impacts of energy deposited in air from prompt radiation of a nuclear blast. This energy is expected to increase the temperature and pressure of ambient air which will impact different blast wave effects. The results may be influenced by weapons type. To account for weapon design, four different weapon types at the same yields will be simulated. This will allow the comparison of the effects of weapon types at the same yields. The yield used will initially be 100 KT which is the approximate upper limit of unboosted fission implosion weapons of contemporary designs [1]. Once it is determined which device will be best to use for simulation of blast wave effects the simulation for that device type will be ran again to a larger distance. The temperature and pressure changes from the MCNP simulation will analyzed at yields of 100 KT and 1 KT. The outputs from these calculations will then be substituted into analytical solutions to different blast wave effects. The objectives of each simulation have been previously stated and are shown below.

- Use MCNP6.2 to estimate the energy deposition in air from prompt neutrons of a blast at different distances
- Use MCNP 6.2 to estimate energy deposition in air from prompt gamma radiation at different distances for various types of nuclear weapons
- Estimate the change to blast wave effects such as peak overpressure, dynamic pressure, shock front density, material velocity, and shock front temperature using available analytical solutions compared to standard temperature and pressure conditions

2 Literature Review

A significant amount of work has been done previously to observe and analyze the effects of nuclear weapons. As early as 1947 reports and mathematical projections were being used to theorize and quantify the effects of nuclear explosions. Empirically gathered information drove the earliest days of weapons effects analysis throughout the early years of US testing [1]. Weapon tests were conducted in a variety of conditions in order to fully understand the release of high amounts of energy and radiation in the very small time frame of nuclear weapons. However, by 1963 it was becoming apparent that open air testing was having a significant impact on the earths global environment and a treaty was entered into that limited all testing to underground testing [1]. At this point and time computer simulations for open air detonations became even more important for new weapon designs which could only then be tested underground. The early models and simulations of weapon effects were significantly limited by the lack of modern technology to produce advanced models or run more complicated calculations [2]. As a result, many models were simplified mathematic expressions of the physics of individual features of a blast that did not accurately reflect the interaction of the many different blast features simultaneously. As modern technology advanced better models and predictions were made. However, even in the current era with access to multiple advanced radiation modeling codes and hydrodynamic codes there is still a distinct lack of cohesive modeling of weapons effects available for uses in civilian sectors for the purposes of planning civil response to a nuclear weapon detonation [6]. To understand the importance of a continuing efforts to modernize simulations the history of simulations must first be considered.

2.3 Current Nuclear Weapon Models and Simulations

Modeling the prompt neutrons released as a result of a nuclear blast is a critical aspect of analyzing nuclear weapons effects. While prompt neutrons do not travel as far as prompt gamma radiation, the shear amount of neutrons released give this particle a significant impact. The threat of a nuclear weapon being used is a terrifying prospect due to the shear destructive capability of such weapons. According to one comprehensive review of nuclear weapons titled, “Report of the Defense Science

Board Task Force on Nuclear Weapons Effects Test, Evaluation, and Simulation" released by the Defense Science Board (DSB), the likelihood of a nuclear weapon being used has increased since the end of the Cold War era [6]. The increase is largely due to the proliferation of nuclear technology around the world [6]. Smaller nations seek nuclear weapons to counter the increasingly superior conventional forces of major countries like the United States [6]. The additional threat of terrorist organization that desire to acquire and use a nuclear weapon provide another additional third party actor of importance [6]. As a result of the real threats, the DSB ordered an in depth review of all aspects of nuclear weapons including the current efforts to model simulate weapon effects.

The purpose of this particular review was to ensure the US is aware of the threat and have the military capabilities to operate in a nuclear environment [6]. However, this information is equally as important to the civil response community planning. Major cities around the US are burdened with the difficult task of planning a response to any major disaster including a worst case scenario involving nuclear weapons in a civilian area. Information on weapons effects can help civil leaders plan appropriately to respond to a nuclear weapons event regardless of the elevation, device type, or any other factors. It is through the lens of civil response that this research is oriented. The factors described in the report provide a baseline for the current capabilities of government entities to model and simulate weapons effects [6].

The report assesses the current US model for acquiring next generation technology that is hardened against nuclear weapons effects. The "hardness" of a material refers to its ability to withstand high amounts of radiation resulting from prompt radiation, thermal radiation, and the electromagnetic pulse generated by nuclear weapons [6]. Prompt radiation is broken down into three categories, neutron, gamma, and x-ray. The categories are unique due to the unique testing environments required for each source. Additionally, there are special testing facilities for EMP and blast wave testing [6]. The current sources of testing will be explored along with the efforts to conduct models and simulations of each weapons effect.

One important critique of the report is the relatively low fidelity of weapon output calculations currently available in controlled weapon codes [6]. The high degree of variability in design is considered but no recommendations were made to improve simulations. It is concluded that there is an extreme need for better codes with better resolution on the real effects of nuclear weapons [6]. This is evidenced in the gap between real world models or tests and computer simulations of wider effects. The report references that neutron, gamma, and x-ray prompt radiation are accounted for in different individual tests.

Prompt Neutron environments are modeled from a limited perspective utilizing three fast burst reactors. The Sandia Pulse Reactor III at Sandia National Labs, Army Pulse Reactor Facility at Aberdeen Proving Grounds, and the Fast Burst Reactor (Molly-G) at White Sands Missile range are the only reactors capable of modeling sustained neutron or gamma ray environments similar to the neutrons released in a nuclear blast. These reactors can test material response to prompt radiation at small scales [6]. They cannot however simulate the widespread release of prompt neutrons into a larger city environment. While these environments are useful for determining if individual pieces of equipment are properly hardened, they do not help the civil response community plan for response to a detonation in a civilian area. For modeling a wider scale release of neutrons, advanced computer codes are needed that will be talked about more later. In addition to the ability to simulate small scale neutron interactions, there currently exists a strong capability to simulate high intensity gamma ray environments.

Prompt Gamma ray environments are modeled in the High-Energy Radiation Megavolt Electron Source (HERMES) at Sandia National Laboratories. This facility can simulate real world high doses of gamma radiation significantly beyond what most materials would experience as the result of a nuclear detonation. The extreme dose of this facility is unique and excessive for most gamma simulations. As a result, there are multiple alternative facilities used to simulate prompt gamma ray dose. Facilities like the PulseRad 1150 at Titan International, Relativistic Electron Beam Accelerator (REBA) at White Sands Missile Range, as well as a number of electron

linear accelerators (LINACs) all allow for the small scale testing of materials [6]. This is done by doing live tests of materials interacting with high energy gamma rays. The gamma rays in the tests are at similar energy levels to those that can be produced in a nuclear blast [6]. These facilities account for individual material interactions with prompt radiation but fail to model the full release of radiation in a blast. For these larger scale calculations, only computer simulations begin to approach an adequate solution [6].

One significant shortcoming of some current computer models is the ability to handle the full radiation transport in complex environments [6]. The use of computers is extremely important to fill the knowledge gap of how a nuclear blast will interact with its environment on a broad scale. While the Department of Defense (DoD) has some legacy codes like MCNP to help assist in some of this modeling, these are severely limited in being mostly one dimensional [6]. The Department of Energy (DoE) which is more directly responsible for monitoring nuclear weapons in the US, has more robust computing capabilities. These computer codes require significantly more advanced computers than DoD models but they provide more realistic three dimensional modeling of nuclear weapons effects [6]. The civil community, much like the DoD, would benefit from collaboration with the DoE community. While these codes have extremely important implications in modeling survivability of conventional military forces, they could also be applied to civil response.

These models would be valuable for civil defense planning by providing a larger degree of resolution on the impact of weapons in urban and rural city environments. However, they are highly restricted due to being based on US weapons rather than adversary weapons. The high resolution provided would be invaluable to planning civil response in the US, it would however pose a defense risk if acquired by an adversary. As a result, the civil community only has access to limited resources to understand and plan for a nuclear weapon detonation.

2.4 Prompt Radiation Models

Some of the first estimates of prompt radiation made by LANL scientists in 1947 estimated that its impacts were so small that they would have almost no impact on blast wave formation [2]. As time progressed and weapons testing increased, other handbooks were made that primarily simulated or measured prompt radiation primarily to determine how much dose was received at different distances. This was seen as being the primary impact of prompt radiation at any distance early in weapons history [1]. Figure 2.1 below gives an example of the dose measurements being made in the 1950s.

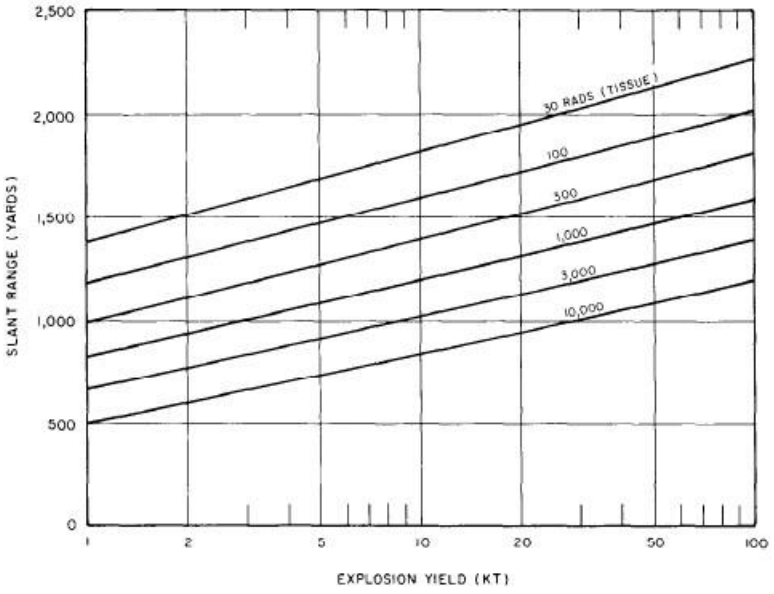

Figure 2.1 Dose as a function of slant range of prompt neutrons versus yield [1]

What was clear to early nuclear scientists was that gamma rays and neutrons escaping from the blast could travel extremely far causing extremely high doses of radiation. This dominated the early field of prompt radiation models that were concerned with radiation transport which is an important aspect of prompt radiation. It does travel extremely far in air, especially gamma radiation shown in Figure 2.2 below.

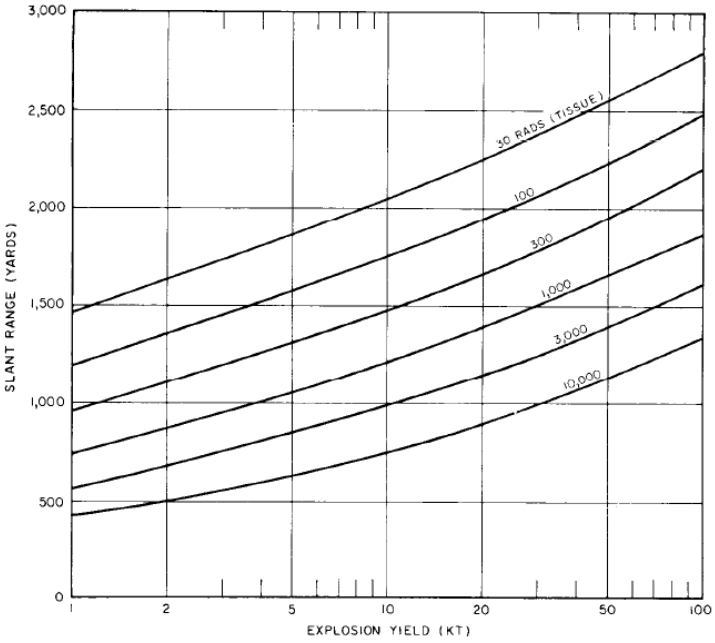

Figure 2.2 Prompt gamma ray dose at different ranges and yields [1]

The gamma radiation gives a higher dose at closer distances than neutrons. It is expected that as distance increases gamma radiation will steadily become more important to dose as gamma radiation can travel much farther in air [2]. Dose was a dominant conversation for nuclear weapons for so long that very little available work focused on working out the potential impacts prompt radiation might have on other blast effects.

As time progressed scientist started to recognize that some of the oldest models for the first nuclear detonations ever dropped in conflict. In 1994 LANL publish a report on the Nagasaki Fat Man and Hiroshima Little Boy prompt radiation called "Source and Replica Calculations" that outlined some of the discrepancies [4]. Previous calibrations to radiation models had been made but according to the report so much testing followed the original bombs that there was little thought given to the need to adjust any calculations made for those original devices [4]. Most calculations done were simply to account for dose. What is notable about this report is that it mentions the use of MCNP codes in order to do neutron and gamma radiation transport calculations [4]. The first important thing that comes out of these

calculations is the energy range of neutrons and gamma rays escaping the devices. The outputs are shown in Figure 2.3 below for both devices compared to normal fission spectrums.

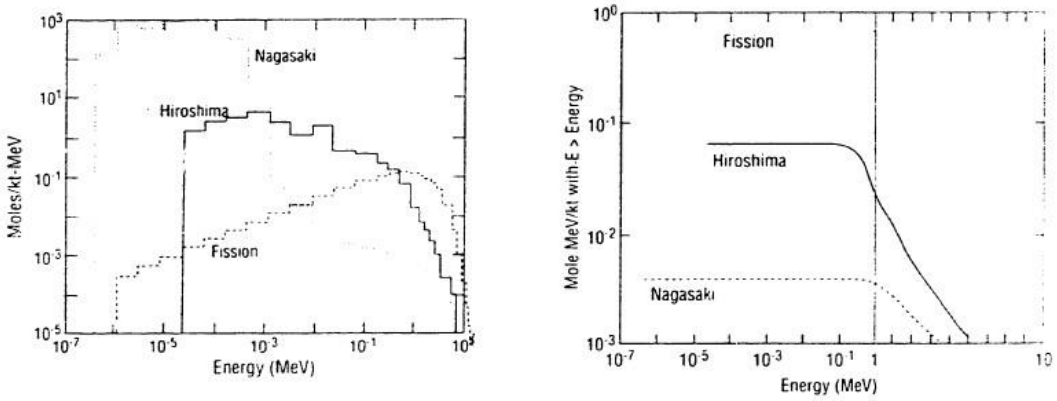

Figure 2.3 Neutron energy levels vs yield [4]

This is the first available fission spectrum for neutrons after they leave a nuclear device. This is important for modeling prompt radiation as it is not possible for calculations made in this research to be able to account for weapons designs the way this LANL report has. One important note from the research is that the Fat Man device, which was a plutonium implosion design, had a significantly more thermal neutron spectrum than the gun type Little Boy device [4]. This is important since this research will assume that the source of neutrons is from a plutonium implosion trigger. Another important output is the angular distribution of neutrons. While this research assumes that prompt radiation is isotropic that is not the case in real world releases of radiation. The results in Figure 2.4 below show the angular distribution of neutrons in a simulated nuclear device.

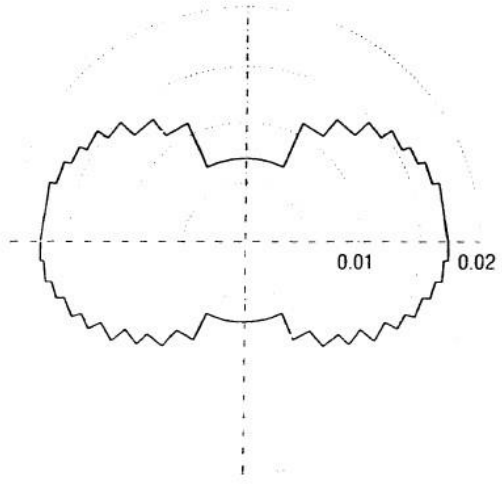

Figure 2.4 Angular distribution of Hiroshima neutrons [4]

This change in angular distribution is largely what was believed to have caused problems with some of the original calculations of the dose received at different distances from the original two devices [4]. This is useful in helping understand the possible error introduced into the current efforts to simulate prompt radiation isotropically. Luckily, parallel efforts by the Northrop "Handbook of Weapons Effects" utilize similar models contemporary with the LANL research that helps mitigate this problem. Northrop's research generated Tables 8.5 and 8.6 which list the neutron and gamma spectra and outputs for various weapon types[2]. They also Generate Figure 8.2 in their handbook which shows the fluence of prompt radiation at different energies. These results are deliberately made to be usable as tools to model prompt radiation that is escaping from the device isotropically in air [3]. These outputs will act as valuable inputs later on in the research.

Overall, there is little available information on any efforts to accurate measure the impact of prompt radiation directly on blast wave effects. The general belief seems to hold through even reports in the early 2000's that the primary impact of prompt radiation of import is the dose received [6]. It is the purpose of this research to explore this gray area in nuclear science to see if there is anything worth adding to existing models and simulations.

2.5 Blast Wave Models

The earliest available blast wave simulations were made in 1947 by a team of scientists consisting of Hans Bethe, Klaus Fuchs, Joseph Hirschfelder, John Magee, Rudolph Peierls, and John Von Neumann who all were working for Los Alamos National Lab and reported their results in a report title “Blast Wave” [2]. This team of extremely accomplished scientists, mathematicians, and chemists worked from an extremely limited perspective while trying to qualify and quantify the blast wave effects of nuclear weapons. At the time they wrote their report, the only significant computing device was an early era IBM computer [2]. Despite the lack of available technology, this team was still able produced the first collective projections of a nuclear blast wave effects. This report was specifically focused on blast wave effects and so does not consider the impacts of radiation on either blast wave formation, propagation, or dose. As a result of these deliberate limitations in scope, the team was able to make a reasonable simulation

At the time of writing, this team of scientists had only the Trinity nuclear test and measurements to compare to their theoretical work[2]. Despite this, they reasonably concluded that they could model their simulation of nuclear blast effects on regular High Explosive (HE) blast waves which were better understood and studied at the time. There were some key differences that were of note to the project. First, the pressure of a nuclear explosion of the same power of an HE has higher pressures at small distances. Second, the pressure of a nuclear explosion is lower at large distance than HE. Finally, the radiation emitted in a nuclear detonation is significantly greater and therefore the heating aspect of a nuclear detonation is significantly greater. This last effect is most easily seen as a normal chemical HE only reaches internal temperatures around five thousand degrees. A nuclear explosion reached an estimated (at the time) internal temperature of well over fifty million degrees. Because of this extremely high temperature and pressure in such a small mass, the team was able to conclude that a nuclear explosion could be modeled as a point source which made the modeling of a nuclear blast more simple [2]. Additionally, due to the significant difference in yields of a nuclear detonation it was noted that the

duration of the blast was significantly longer than a normal HE blast. As a result, the criteria for assessing the damage of a nuclear blast was the peak pressure instead of the blast impulse which was used in normal HE models for damage effects. This is significant for blast wave models especially at longer distances as the area of damage would only increase at a rate of two-thirds the energy released in a nuclear blast compared to four-thirds increase in a HE blast.

The group made several key findings regarding blast waves that were highly influential in the development of future models. They noted that the shock wave will start inside the mass of the weapon and spread to the surrounding air and continue expanding spherically in undisturbed air around the device [2]. From a mathematical standpoint this is important to support the use of the point source equation as the driving force for the blast wave analysis. Also important to note is the admitted shortcomings of the project in dealing with radiation. It is stated that radiation could potentially heat the air by millions of degrees. However, it was not yet understood how much of an impact the radiation would have on the transport of energy from the weapon. What was clear at the time was that after a certain amount of time, the air shock wave properties still resembled point source calculations. They concluded that the radiation would have significant impacts at early time stages of blast formation but that at longer distances blast wave calculations would conform to simple point source models [2].

The point source calculations were handled by John Von Neumann who was one of the most prominent mathematicians of his era. He observed that due to multiple changing variables in the shock front velocity and trajectory as well as the continuous flow of air behind the shock front that exact analytical solutions were not possible. Instead general solutions were required to estimate the forces in the shock front [2]. The solution to this problem of limited analytical techniques was to treat the problem as a point source. That means that all of the energy going into the blast comes from a very small point. This model supports that as the volume goes to zero the pressure approaches infinity, a condition that may be uniquely possible in the vast amounts of energy released in nuclear explosions. Von Neumann's mathematical contributions

showed that a point source calculation was valuable for shock wave analysis. Other members of the team used Von Neumann's initial work as support for their own work. This is seen in the thermal and prompt radiation models completed by Hirschfelder and Magee.

Hirschfelder and Magee worked extensively on solving the problem of the prompt and thermal radiation released in a nuclear blast. They also tried to show the relationship between the prompt radiation and the location the shock front forms. They approximated that while the exact location of the formation may be irrelevant in longer time scales, that it is still tied to a characteristic of the blast and should be determined. They estimated that the shock front would form around the region of air with a temperature at or just below three hundred thousand degrees kelvin. They estimated the temperature of air from prompt radiation versus radius to show the expected area the shock front would form as shown in Figure 2.1 below [2].

SOME PROPERTIES OF THE BLAST WAVE DURING RADIATION EXPANSION PERIOD

R, cm	E_{rad}/E_{int}	$\dot{R}$, cm/sec	T, °K	$\bar{\gamma} - \gamma$
841	0.0035	4.8×10^6	492,500	0.28
1015	0.00123	3.8×10^6	328,300	0.032
1122	0.00052	3.3×10^6	246,250	0.0058
1271	0.00022	2.6×10^6	180,000	0.0011

Figure 2.5 Estimated temperature changes during radiation expansion period from prompt radiation [2]

Here in Figure 2.1, it is seen that around 10-12 meters the temperature in air drops below the determined threshold of approximately three hundred thousand kelvin allowing for shockwave formation. This was modeled off the release of a 20KT blast and used and equation of the state of air that was generated in earlier parts of the

research by Fuchs, Kynch, and Peierls [2]. It should be noted that this estimate is extremely rough since they could not fully account for particle interactions in air due to limited available technologies and limited knowledge of particle cross sections [2]. However, this gives a general assessment of the amount of energy deposited in air prior to shockwave formation which is useful for modern simulations. This work shows the limitations of early models that required multiple assumptions due to large amounts of limitations and constraints.

There were multiple assumptions needed to simplify the research being conducted that correlated directly with assumptions often needed today. First, it is significant that much of the research was conducted assuming standard pressure, density, and temperature conditions in an infinite homogeneous atmosphere. It must be noted that in later parts of the research that blast wave characteristics change significantly once the environment around the detonation is changed. This is most evident in blast wave analysis involving reflection from the ground [2]. Reflection causes significantly higher pressures in the blast wave in addition to impacting the reflection of radiation back into the air. Because of the complex environment created by reflection, there had been little work done in the field resulting in extreme difficulties even interpreting the images of the Trinity explosion [2]. Additionally, it could be seen that increasing pressure from reflection would also increase the shock wave velocity. These properties, while significant, were not fully able to be modeled due to the complex nature of the calculations and again the limited availability of modern technology. The shock wave characteristics were extremely important in understanding nuclear weapon effects on targets so further investigation was necessary both then and now.

In addition to the limited ability to fully analyze shock wave formation, the prompt radiation piece of the equation was another significant hole in the research as it was not yet understood or able to be modeled effectively. There was no effort made to distinguish between prompt radiation and thermal radiation as those terms had yet to be fully understood. However, most of the description in the research to early radiation is easily attributable to prompt radiation escaping from the device.

However, it was noted that due to the high temperatures in and behind the shock front the vast majority of thermal radiation remaining in the fireball behind the shock front would be absorbed until the front dropped below a sufficient temperature. They theorized that there could be a very early phase of the blast, ahead of the shock front forming, in which radiation could propagate significantly faster than the shock front. This phase would be short lived and representative of prompt radiation which was estimated to be limited in significance to a distance of around 10 meters [2]. The estimates were based on the projected distance that the radiation might be able to heat the air up to at least 1 million degrees kelvin. At the point heating the air to that temperature is no longer possible, the expanding sphere of prompt radiation would slowly become more normalized and have significantly less of an impact on shock wave propagation [2].

Another aspect that prompt radiation might impact in blast wave formation is the luminosity. A Los Alamos National Lab report titled "Light Flash Produced by an Atmospheric Nuclear Explosion" explores how nuclear blasts have a characteristic light flash with two peaks [8]. These peaks shown in Figure 2.6 below correspond to the hottest points of the shock wave as well as the point that the shock wave cools enough that the inner fireball becomes visible [8].

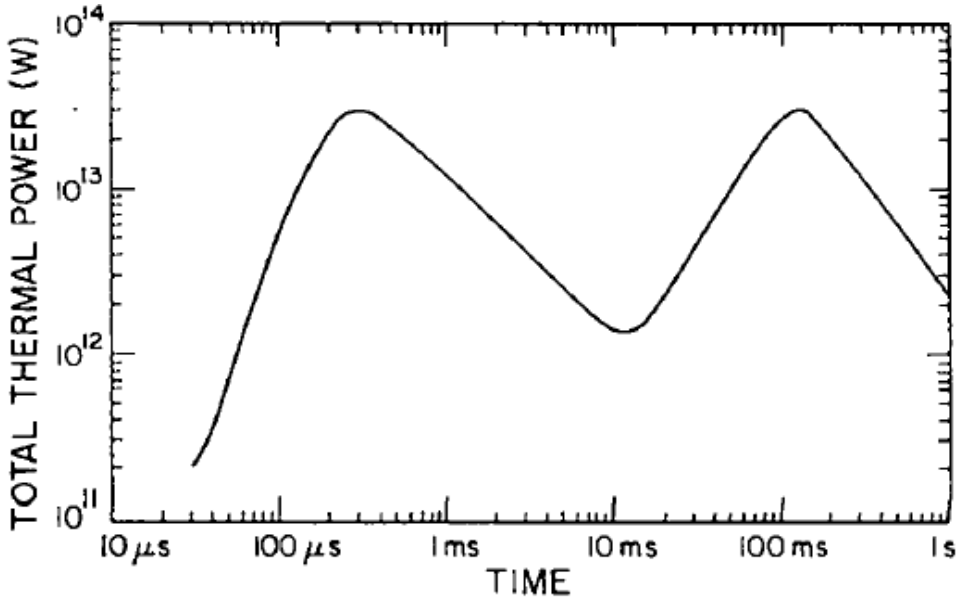

Figure 2.6 Thermal output of 19 KT blast vs time

The difficulty is in determining where the source of the luminosity was coming from [2]. It was estimated in a previous LANL report that as long as the temperature inside the shock front was above five thousand degrees it would have severely high opacity light from the thermal radiation behind the shock front [2]. It is important to define the moment at which the luminosity seen is changing from the shock front to the thermal radiation. The first peak seen in Figure 2.6 is caused by the shock front temperature [8]. The minimum between the two peaks represents the shock front cooling off. The point that the slope begins to rise again is where the shock front cools sufficiently allowing the fireball to be seen. At this point the fireball is already starting to cool which is why the thermal power does not seem to be much greater despite the fireball containing as much as 80% of the blast energy [8]. The second peak however lasts almost 10 times as long as the first peak [8]. The timing is important because the area under the respective peaks is used to estimate blast yield. It was found that through optical observance of luminosity as shown in Figure 2.2 that the power of the blast is proportional to the fireball brightness times the area of the surface. The is shown in Figure 2.7 below with pictures taken at different optical peaks of Figure 2.6:

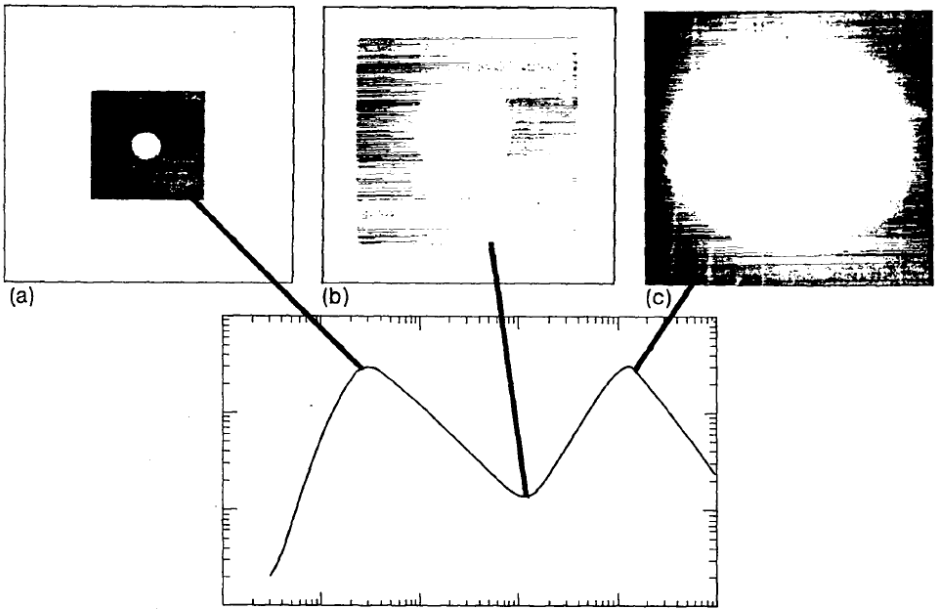

Figure 2.7 Pictures of 19 KT blast at different peaks

What can be seen in picture (a) of Figure 2.7 is the visibility due to the expanding shock front. Picture (b) shows the minimum where the shock front is cooling and thermal radiation from the fireball is starting to be seen through light still coming off the shock front. Finally, in picture (c) of Figure 2.7 the fireball is visible [8]. The first longer the first peak shields the second peak, the more distorted the yield of the blast would become as the time between peaks decreases. The importance of this as it relates to prompt radiation is that if prompt radiation heats air up to appreciable levels it may have multiple impacts. First it may be shielding the blast wave from optical observation by absorbing radiation in heated air just as the blast wave shields the inner fireball. Second, the prompt radiation may be impacting the temperature and rate of expansion of blast wave generated by the nuclear blast.

3 Methods

The following section will list in detail the methods used to produce a simulation of initial radiation released in a nuclear blast. The outputs of this simulation will be the inputs of previously generated analytical solutions to blast wave effects to attempt show the impact changing initial conditions has on blast wave propagation.

3.3 MCNP

The unique problem of radiation transport could have been modeled using multiple different computer-based codes. For this research MCNP version 6.2 was chosen due to the historical use of MCNP in these types of calculations. Version 6.2 is the most recent code that is reliable and has a large library of material cards and cross sections. MCNP is also optimized for radiation transport problems giving fast computational time for simple simulations like the research being conducted. An example of the MNCP cards used can be viewed in Appendix A. In all, there were 8 different variations of the simulation run to account for differences in the device types simulated as well as two final simulations that were ran for greater distances. All the radiation talked about for this will be considered to be prompt radiation from the

source of the blast. The only secondary radiation considered will be electrons produced as a results of gamma ray interactions in air outside of the weapons materials. These secondary particles will be included in the definition of prompt radiation as the time it takes for these interactions is still significantly faster than the formation of the shock front. MCNP is a unique radiation transport code that has large libraries of particle interactions previously generated and stored [7]. This allows the code to calculate particle interactions in various materials across a large spectrum of energy at very fast computational rates. This feature will be leaned on heavily to generate results of prompt radiation that some of the earliest models of weapons effects could not handle due to limited computational abilities [2].

The goal of utilizing MCNP is to utilize the energy tally function to simulate how much energy particles released in a blast would then deposition in the air around the device. In order to accomplish this goal a number of limitations and constraints must be observed. Due to the general nature of this simulation, weapon designs are not being modeled. All particles are being treated as having already escaped the surface of the highly dense weapons materials. Due to this constraint, there must be multiple considerations for the energy spectrum used which will be addressed in each particle's respective sections.

Next, the simulation is ran using spherical coordinates. Despite some of the literature showing that the prompt radiation is not released in a perfect sphere, it is important to consider the release spherically [3]. This supports both the shock front formation which is handled spherically and mitigates the problem of trying to model weapons materials. The hydrodynamic expansion of the shock front is simulated in analytical models as spherical, so it is mutually beneficial and economical to run the problems from a similar perspective. The overall environment is treated as a homogenous infinite air problem so the composition of air the prompt radiation interacts with is uniform in all directions. This limits the need to model the direction of radiation release and allows the problem to be treated as a uniform sphere. It is known that the high density of weapons will significantly affect the direction of prompt radiation [1]. Future simulations may be able to handle this more adequately.

For now the research will be limited with the understanding that the results generated may be the smallest results possible. This is still an effective result as it establishes a foundation for what may be possible for future simulations to build on.

The first component of the simulation design that is important is to outline the physical space of the environment. As previously stated, the particles will be treated as if they have already left the dense weapons materials and are just entering into open air. As a result, it is possible to define the source of the problem as a .5 meter radius spherical void that will emit the source particle uniformly in all directions. The isotropic source will be contained within expanding concentric spherical rings of standard modeled air which accounts for the infinite homogeneous assumption. The surface of each cell of air will start at a radius of 1 meter and increase in 1 meter intervals out to 10 meters. This will give 10 cells of air surrounding one internal surface as show in Figure 3.1 below.

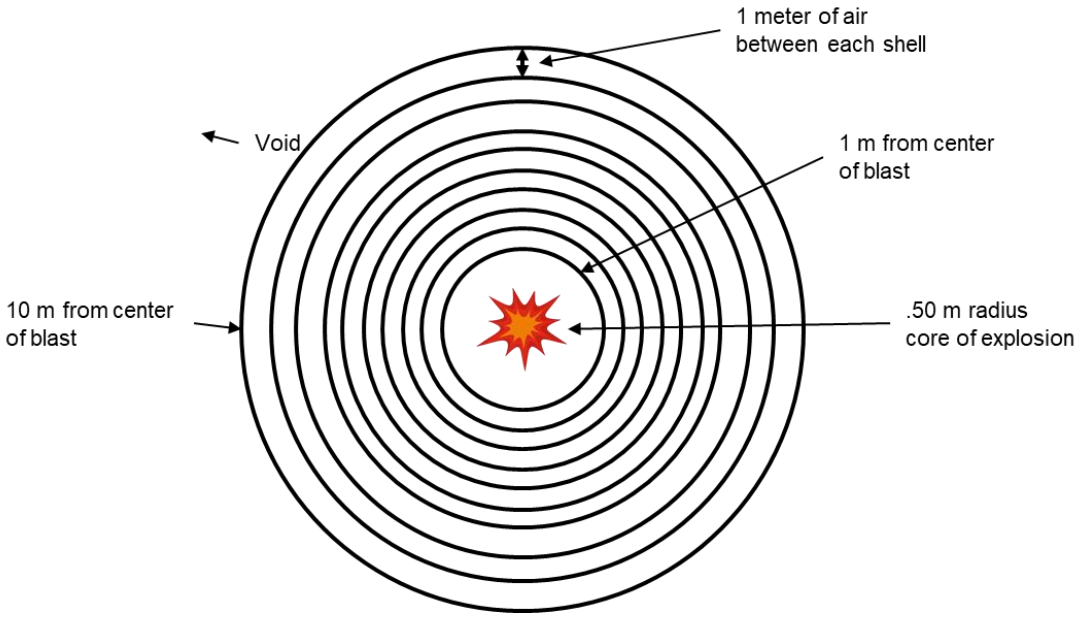

Figure 3.1 MCNP6.2 model for prompt radiation transport

Outside of the last cell is a void so there will be no scattering back into the problem. The structure of this surfaces was meant to be simple and easy to modify to larger scale simulations as needed. Once the outputs are all compared within ten meters it will be possible to compare the outputs of the different weapon types. It

will be important to see if there is any significant variance in outputs based on designs of older and more modern designs. The simulated energy is not being simulated in two dimensions. MCNP allows for three dimensional shapes so results will be given within shells of air as show in Figure 3.2 below:

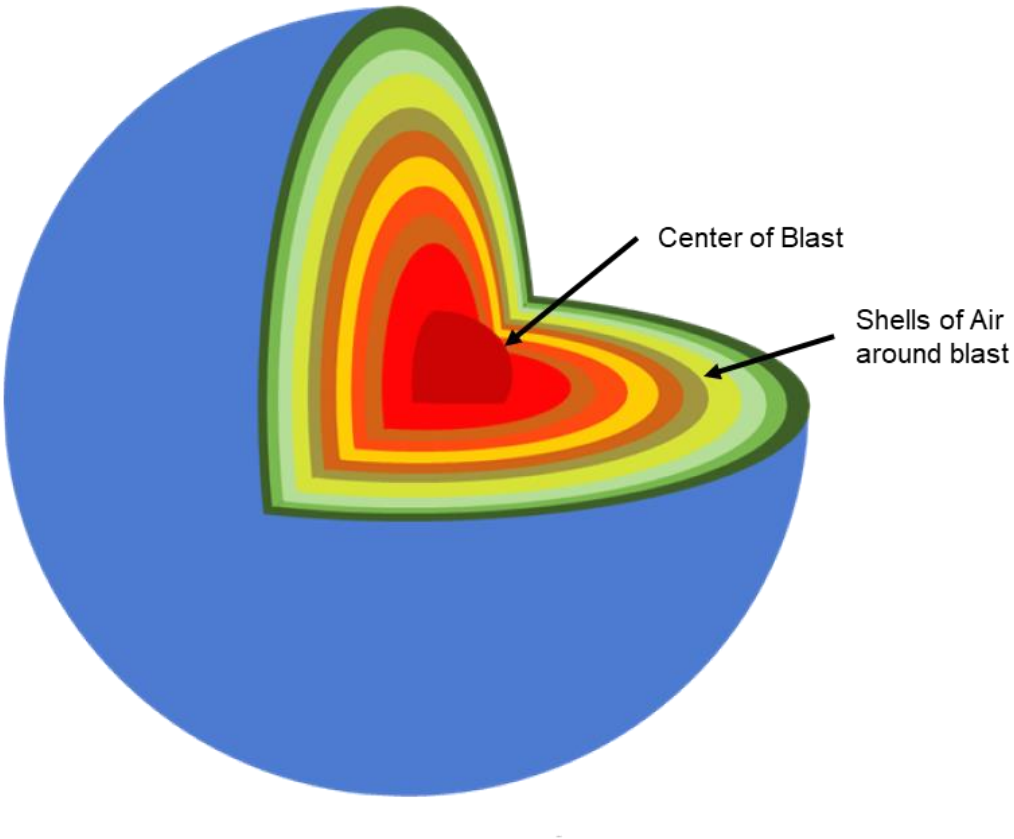

Figure 3.2 Three-Dimensional model of shells of air surrounding blast

The F4 and F6 tallies already contained within MCNP code will be utilized to analyze the particle flux and energy deposition respectively. F4 tallies analyzes the track length of particles or how far they travel within each shell [7]. This will simply be used to make sure particles are moving within each shell at reasonable rates and that there are no large, unexpected variations. The F6 tallies track energy deposition of particles in materials [7]. For this research, the F6 tallies are the most important output of the MCNP 6.2 code. The particles will be simulated over a standard one hundred thousand histories to reduce the relative error below .05. This relative error

is the minimum requirement for MCNP to consider the results as valid and usable [7]. The medium surrounding the weapon will use the MNCP material table for standard air which accounts for nitrogen, oxygen, a small amount of argon, and carbon [7].

Finally, to capture the different radiation energy levels and distributions of the different weapon types being analyzed, eight different simulations will be conducted. Neutrons and gammas will be analyzed separately in order to better isolate energy deposited as a result of the respective radiation as well as to reduce run times as combining multiple radiation sources into one code quickly becomes more computationally expensive. Each card will be explained more in detail within the respective sections below. Two separate simulations were run for neutron simulations and four separate simulations were used for the gamma rays. In addition to these simulations that are used for comparing weapon outputs, two more final simulations are ran for the purpose of generating inputs for the blast wave analytical models. These simulations will have the same source as a Type 3 device but will be model to a higher distance of 100m. The purpose of using a Type 3 device is that it is the most basic design and may give the best comparable results to current blast wave analytical models.

3.3.1 Neutron Input and Modeling

MCNP6.2 is very effective at simulating the radiation transport of neutrons. Previously explored models have handled neutron transport in a large variety of complex scenarios that outline the overall effectiveness of the code [5]. For the particular problem of modeling neutrons being created in weapons, a few adjustments to how the code is ran must be made.

First, the energy spectrum used will be a Watt spectrum library that already exists within the MCNP library [7]. The Watt function is meant to estimate the probability of a neutron being produced at different energies within a standard fission spectrum range. The Watt spectrum is however meant for the modeling of fission U-235, and during this simulation the primary source of neutrons will be Pu-239. The difference

in materials is not of great significance as the variation in the energy of neutrons produced is not significant enough to impact overall results. The MCNP code will analyze individual transportation of neutrons to estimate the average energy deposited in air. The difference in source materials would primarily impact the total number of neutrons produced as Pu on average produces more neutrons than U during fission. To account for the difference, the total amount of neutrons will later be manually assigned in the postproduction of the MCNP results. It is at that point that the type of source material will be of more importance. The total amount will be derived from historical studies of nuclear blasts.

Second, the energy spectrum range will be limited from 0.988-10 MeV for the Type 3 device run, and 0.988-15 MeV for the other device types that utilize fusion in their overall yield. The Watt spectrum is meant to account for fission events only, by extending it to include the energy range from fusion some error will be introduced into the results. However, the overall profile of energy distribution will average out the same and allow for this usage of the Watt spectrum.

Understanding these initial conditions is important in effectively simulating neutron transport using MCNP. It is also important to control the environment being created in the simulation. The overall model for the environment follows what has been described previously. The neutrons are emitted from small .50 m spherical void meant to simulate the interior of the weapon. These neutrons will then be transported by the code into expanding spheres of air at standard sea level altitude, temperature, and pressures. This process will be repeated in all simulations one hundred thousand time. The purpose of generating this many histories is minimizing the error associated with the tally counts. The result of the simulation will be normalized for each particle simulated.

The final step for the neutrons is to count the amount of average energy deposited as a result of each history. For this simulation, F4 and F6 tallies are both used in order to track the motion of the neutrons through air as well as the amount of energy being deposited. The F6 tally is the primary results needed to further analyze the impacts of the radiation on air temperature as it will give the amount of energy

deposited in each defined region in units of MeV/g along with the calculated mass of the region in grams [7]. The F4 tallies will simply be used to capture any problems in the system design by ensuring particles move normally within each region of air.

Of the devices being studied only the Type 3 device is purely based on fission. Many of the available tables and figures in prior existing research were generated using fission devices [1]. As such two simulations were dedicated to this device type with a neutron energy range from .998-10 MeV as mentioned above. The first simulation was run out to 10 meters just like the fusion outputs. The second simulation had the same shape inside 10 meters. After 10 meters, more shells of air are added into the simulation every 10 meters out to 100 meters. The results from this simulation were used in the postproduction of the Type 3 outputs exclusively. This allowed an equal comparison of the different device types. The fission based outputs were the primary outputs used to compare current results to historical results. In order to compare to historical results, it becomes more important to generate results out to a higher distance. Many historical models only start measuring many key weapons effects at distances as great as 100 meters as show in Figure 3.3 below [1]:

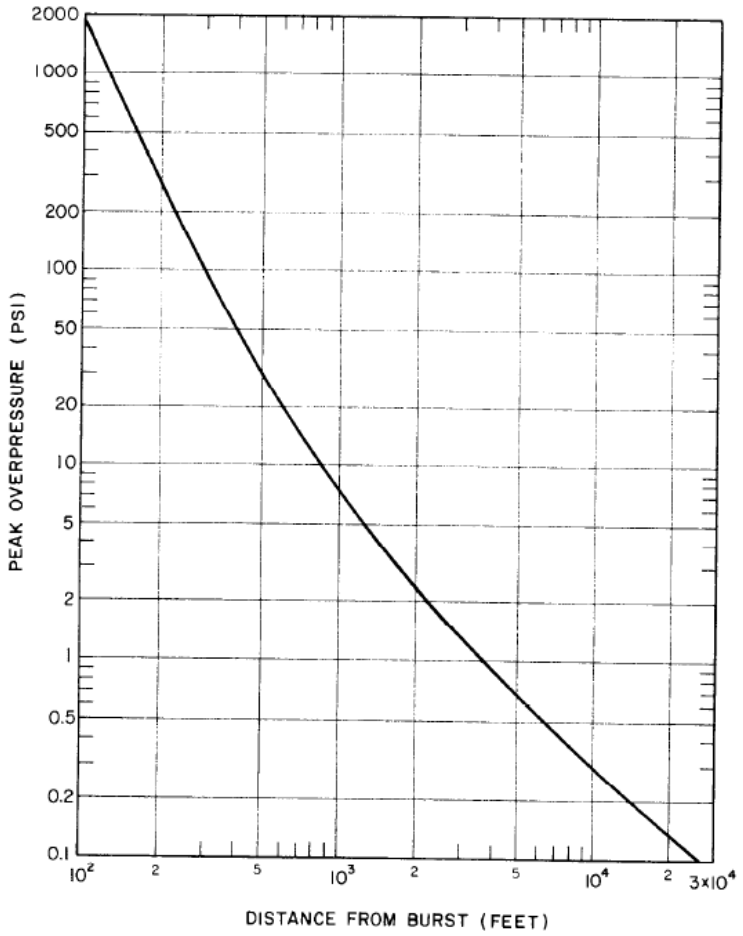

Figure 3.3 Peak Overpressure versus distance for a 1-KT free air burst for sea-level ambient conditions [1]

For the remaining three devices the same fusion spectrum was utilized and only one simulation was conducted. The results of the MCNP simulation for fusion were applied in postproduction to the remaining device types. It is in the calculations used in postproduction that the greatest differences occur because the devices. This difference will be discussed in greater detail in the results of the simulation. It is expected that the temperature change as a results of energy deposition for each device will vary based on the radiative yield of each device. The next step is to simulate the prompt gamma rays that are released in each device type.

3.3.2 Gamma and Secondary Radiation Input and Modeling

Gamma radiation and the electrons created by its interaction with air, are of great importance to measuring total prompt energy deposition in a nuclear blast. The prompt gamma radiation that is able to escape the extremely dense weapons material may represent less than 1% of the total energy of the blast. However, gamma rays are able to thousands of meters in air and convey large amounts of energy through Compton scattering and pair production in the air around the blast [1]. However, there are some unique features of gamma radiation that places constraints on the simulation.

First, the gamma radiation will be modeled isotropically just as the neutrons in the previous simulation. Previously it was discussed how prompt gamma rays that do escape the dense weapons materials do so at angle that is highly influenced by weapon design. For this simulation, the dense weapons materials are not being included. Gamma rays may in reality have higher directional yields for different devices designs [6]. The results here are intended to be as general as possible and not tied to any specific weapons design feature. As a results, the gammas and any secondary radiation they produce will be simulated as if escaping at all angles uniformly into a sphere of air.

Second, it is known that gamma rays produced as prompt radiation will escape at various energy levels due to the extremely dense materials around the weapon [1]. This research is reliant upon gamma ray energy levels extracted from previous studies. As a result, rather than modeling the gamma radiation using a fission spectrum like the neutrons, all prompt gamma rays are assumed to have escaped with an average energy given in Northrop's "Handbook of Nuclear Weapon Effects" [3]. The average energy is listed by device type with Type 3 devices have an average gamma radiation of 1.5 MeV, Type 5 is 1.6 MeV, Type 8 is 1.63, and Type 13 is 2.00 MeV [3]. While the variation is not significantly large, this is the best estimate of the average energy of the gamma radiation after it has escaped from the heavy weapon materials surrounding the fission and fusion events. As stated previously, gamma radiation is significantly influenced by weapon design, so it is important to use a known quantity and energy level produced in historical results as a baseline for

analysis [3]. Each weapon simulated has a given average gamma ray energy. To account for the different energy levels, separate simulations were conducted for each device design. The results were then utilized in the postproduction calculations of each specific device type. A final gamma simulation was run for the Type 3 device out to 100 meters like the neutron simulation.

One key difference between the neutron simulation and the gamma simulation besides the energy production, is the ability of gamma radiation to produce electrons through ionizing particles in air. This is primarily accomplished through pair production at higher energies and Compton scattering at lower energies. This additional energy increases the overall contribution of gamma rays to the temperature of the air surrounding the blast. MCNP6.2 can simulate and tabulate energy deposition of secondary particles as part of the codes intended function [7].

Similar to the neutron modeling, the gamma rays and the electrons they produce must be counted in MCNP. The F4 and F6 tallies function the same for these particle types as they do for the neutrons. They will yield the track length of the particles as well as the energy they deposit in air [7]. Gamma rays will be the only source particle, so all electrons counted will be as a direct result of the gamma ray interaction in air. The energy deposited will be tallied separately and later combined during the postproduction of the MCNP results. This requires only additional lines added into the input card to account for secondary particles. This also requires adding a second tally of energy deposition shown in the Appendix A gamma card as an F16 tally. The total energy deposited from gamma and electrons will later be added together to calculated how much temperature change each escaped gamma can generate in air.

3.3.3 Postproduction of Results

Once a simulation is run in MCNP an output file is created. This output file contains many useful pieces of information including the mass of material in each cell, the volume of each cell, and the energy deposited in units of MeV/gram. With this information it is possible to begin calculating the impact of the energy on the temperature and pressure of air. Once the increase in air temperature and pressure

over distance is determined, it becomes possible to start using existing analytical models to solve for blast wave solutions at set distances.

The first step is to take the output of the F6 tallies which are in units of MeV/gram and multiply the result by the mass of air for each shell. This generates the average energy deposited in each cell of the model by each neutron generated.

Next, the energy must be scaled to the total amount of neutrons that would be in the system. The table below contains historical estimates of the yield of neutrons from different weapon types for every KT of energy. Increasing yield increases the number of particles in a linear relationship so a standard yield of 100 KT will be utilized across all of the different devices. This represents the upper limit pure fission devices in terms of yield as well as a relatively comparable value to historical results which have often been modeled at or near this value. Table 3.1 below shows the different expected outputs of prompt neutrons and gamma rays. The one exception to the scaling of yield is for the Type 8 device. This device type represents a thermonuclear secondary which impacted the scale of the device. As a result, the gamma radiation released must be adjusted by a factor of "W" which is the yield of the device prior to being multiplied by the overall yield of the device. This is show in Table 3.1 below:

Table 3.1 Neutron and gamma yields for each device type[3]

Weapon Type	Neutrons/KT	MeV/KT	Yield (KT)
3	$2.7\text{x}10^{23}$	$9.8\text{x}10^{22}$	100
5	$3.38\text{x}10^{23}$	$1.04\text{x}10^{23}$	100
8	$1.95\text{x}10^{23}$	$3.55\text{x}10^{23}\text{x}W^{-.29}$	100
13	$1.77\text{x}10^{23}$	$6.70\text{x}10^{23}$	100

The results of this calculation yield the amount of energy deposited in each cell of the problem as shown in Equation 3.1 below:

$$E = F6\,Tally\ \left(\frac{MeV}{g}\right) * mass(g) * \#\,particles\ \left(\frac{n}{KT}\right) * Yield\ (KT) \quad \text{EQN 3.1}$$

EQN 3.1 generates energy in MeV which needs to be converted to Joules. This is a simple conversation shown in EQN 3.2 below. Once the energy is in Joules it is possible to calculate temperature change using the heat transfer equation show in EQN 3.3 below.

$$E = 1\ MeV = 1.602 * 10^{-13} J \qquad \text{EQN 3.2}$$

$$\Delta T = \frac{E(J)}{c_p\left(\frac{J}{g-C}\right) * mass(g)} \qquad \text{EQN 3.3}$$

The result of putting the results from EQN 3.2 into EQN 3.3 will yield the temperature increase in air in degrees C as a result of energy deposition in air for each cell. It is important to note that the specific heat capacity of air(c_p) does change with temperature in this calculation. In order to do this calculation, the assumption was made that the average heat capacity of air is approximately 1.4 (J/g-C). Previous research has shown that this assumption is safe up until the temperature begins to exceed 1 million K [2]. At this point air no longer behaves normally and it is difficult to accurately assess its ability to absorb energy [2]. The average specific heat capacity of air was assumed to be usable even at high temperatures. Although temperatures are expected to reach well into the millions of K at close ranges, they quickly drop below a million Kelvin after the first few meters. This means the error introduced by this assumption will likely have a minimal impact over the majority of the analyses.

Once this assumption is made, the temperature change from prompt radiation energy is given in degrees Celsius. To use this temperature in further calculations, it must be converted from C to K. This is done using the output of Equation 3.3 and converting it from Celsius to Kelvin using Equation 3.4 as shown below:

$$T(K) = \sum \Delta C + 20(C) + 273.15 \qquad \text{EQN 3.4}$$

In EQN 3.4 the sum of the temperature change is from the energy of all prompt radiation. The 20 degrees C is included to accounted for the ambient temperature of air that is assumed as part of the STP conditions. The output of EQN 3.4 is the total change in temperature in air in units of Kelvin. This method of

calculating temperature was applied to all the simulations of different devices at all distances. The temperatures generated can be used to calculate the change to ambient pressure as well. This will be done in the next section where ambient pressure becomes more important. The temperature can also be used as input into existing analytical solutions of blast wave formation to determine the change in peak overpressure, dynamic pressure, shock temperature, material velocity, and shock density due to the increased ambient conditions.

3.4 Analytical Solutions to Blast Wave Formation

Multiple sources over the years have tried to generate different formulas for describing the outputs of blast wave formation. General equations used in the 1946 Los Alamos Lab Report described the problem as a point source solution[2]. Glasstone gives multiple equations to describe peak overpressure, shock wave density, and dynamic pressure of the blast wave front[1]. Northrop gives a comprehensive solution to peak overpressure, shock front density, material density, dynamic pressure, and shock front temperature[3]. For the purposes of analyzing the outputs of the MCNP model Northrop's equations were found to be the most suitable and provide the most recent solutions to the complex blast wave models.

In order to generate a baseline of results two separate calculations were conducted. First, standard temperature and pressure conditions were used to generate results for a 100 KT blast in order to generate a baseline of results with which to compare the results from the MCNP model of prompt radiation. This same process will later be repeated for a yield of 1 KT. Second, the same equations are utilized with the added initial temperature and pressure conditions created by the prompt radiation of the blast with a yield of 100 KT. This will be done again with a yield of 1 KT. The results of these calculations can then be compared to one another as well as historical observations to analyze their accuracy.

The first central driving equation utilized describes the peak overpressure as a function of radius for a 1-KT blast is shown below in Equation 3.4.

$$\Delta p(R) = \frac{3.04*10^{11}}{R^3} + \frac{1.13*10^9}{R^2} + \frac{7.9*10^6}{R*\left[\ln\left\{\left(\frac{R}{R_o}\right)+3*e^{-\frac{1}{3}*\left(\frac{R}{R_o}\right)^{\frac{1}{2}}}\right\}\right]^{\frac{1}{2}}} \qquad \text{EQN 3.4 [3]}$$

In this Equation R is the radius of a 1 KT blast, R_o is a constant value of 445.52 meters. To use this equation which is designed with a 1-KT blast, the blast radius of yields over 1 KT must first be scaled using scaling laws. The scaling law is shown in Equation 3.5 below:

$$\frac{d_2}{d_1} = \frac{W_2^{\frac{1}{3}}}{W_1^{\frac{1}{3}}} \qquad \text{EQN 3.5 [3]}$$

In this equation d_2 is distance (radius) from the analyzed burst, d_1 is the distance for the reference burst, W_2 is the yield of the analyzed burst (100 KT) and W_1 is the yield of the reference burst (1 KT). This is solved for the distance of the reference bust so we can use Equation 3.4 to yield appropriate peak overpressure values. This is shown in Equation 3.6 below:

$$d_1 = d_2 * \left(\frac{W_1^{\frac{1}{3}}}{W_2^{\frac{1}{3}}}\right) \qquad \text{EQN 3.6}$$

The radius of each cell is scaled using equation 3.6 and plugged into equation 3.4 in order to generate the peak overpressure of the 100 KT blast at each cells max radius. It must be noted that Equation 3.4 is recommended for use at distances greater than 10 meters/($KT^{1/3}$). For the highest yield being analyzed (100 KT) this means the equation is most useful outside of 2.15 meters. This equation will still be used inside of the recommended radius for both standard conditions and those created by the prompt radiation. This will introduce some error into results inside of 10 meters. Outside of 10 meters the 100 KT blast scales down to more than 2.15 meters which is the most acceptable tolerance of the equation[3]. With the results in hand a second adjustment must be made. For all peak overpressures over 2 MPa the real gas properties of air must be included [3]. Results from a 100KT are expected to exceeded 2 MPa out to a significant distance so an adjustment must be made. To

account for the properties of air Northrop requires that the peak overpressure be added to the ambient pressure of the air as shown in Equation 3.7 below:

$$p_s = \Delta p_s + p_o \qquad \text{EQN 3.7}$$

In this equation Δp_s is the output of equation 3.4 and p_o is the ambient pressure of air which must be calculated to solve for p_s which represents the peak overpressure of the blast wave. To calculate the ambient pressure of air the Ideal Gas Law is used. The Ideal Gas Law was used historically to handle pressure changes in a nuclear blast [2]. For the standard temperature and pressure conditions air is at 293 degrees Kelvin and 101,325 Pascals at all distances. For the prompt simulations, the temperature outputs from Equation 3.4 are used in Equation 3.8 below to generate pressure in Pascals.

$$P(Pa) = n(moles)xR\left(\frac{J}{Kxmoles}\right) * T(K)/V(m^3) \qquad \text{EQN 3.8}$$

The values for n is given by the mass of air(g) divided by the molar mass of air 28.7(moles/g). Volume (V) is given as an output from the MCNP 6.2 results but can be verified using Equation 3.9 below

$$V_x = \left(\frac{4}{3}\right) * \pi * r_x^3 - \left(\frac{4}{3}\right) * \pi * r_{x-1}^3 \qquad \text{EQN 3.9}$$

In this equation V_x is the volume of the current cell, which is a function of the current radius (r_x) minus the volume from the previous cell which is a function of the previous radius (r_{x-1}). The R in Equation 3.8 is the Gas Constant and is equal to 8.314 (J/mol-K). The resulting pressure is in units of J/m^3 which is equal to Pascals. Equation 3.9 gives us the ambient pressure of air as a result of the temperature change caused by the prompt radiation. This ambient pressure is then used in Equation 3.7 which gives us the expected peak overpressure of the blast wave at different distances. With the pressure of the blast wave known it is possible to calculate the density of the shock front. The equation for this density is given in Equation 3.10 below:

$$\rho_s = \left(\frac{\{[(\gamma_s+1)*p_s+(\gamma_s-1)*p_o]*(\gamma_o-1)\}}{\{[(\gamma_o-1)*p_s+(\gamma_o+1)*\gamma_s]*(\gamma_s-1)\}}\right) * \rho_o \qquad \text{EQN 3.10[3]}$$

In this equation γ_s and γ_o represent the ratio of the specific heat capacities of air. Since we are assuming ideal are conditions, these values are both set equal to 1.4. A key variable in this equation will be ρ_o which is the ambient density of air. For standard pressure and temperature conditions this is a known value of 1.225 kg/m^3. However, in order to determine the density of the air after the addition of prompt radiation the Ideal Gas Law must again be utilized. Below in Equation 3.11 the ideal gas law is expressed in order to solve for density of air as a ratio of pressure, temperature, and the specific gas constant ($R_{specific}$):

$$\rho_o = \frac{P}{R_{specific} * T} \qquad \text{EQN 3.11}$$

$R_{specific}$ is the specific gas constant of a mixture of gases and is equal to 287.058 J/kg-K for dry air. The result of Equation 3.11 is that the ambient density of air is dependent on a ratio between the pressure and temperature caused by the prompt radiation. If the ratio between those two factors remained constant the density of air would not change. Next, the ambient density of air from Equation 3.11 is used in Equation 3.10 to generate the density in the shock front at different distances. With this value known the next value that can be calculated is the material velocity at the shock front as shown in Equation 3.12:

$$u\left(\frac{m}{s}\right) = \left[\frac{\Delta p * \Delta \rho}{\{\rho_o^2 + \Delta \rho * \rho_o\}}\right]^{\frac{1}{2}} \qquad \text{EQN 3.12[3]}$$

It can be seen from Equation 3.12 that the material velocity will depend heavily on the ambient pressure and density of air. These are the key variables between the STP and the prompt radiation outputs. With the material velocity calculated for each shell of air, those outputs can be used to calculate the dynamic pressure as shown in Equation 3.13 below:

$$q_s = \left(\frac{1}{2}\right) * \rho_s * u^2 \qquad \text{EQN 3.13[3]}$$

In Equation 3.13, q_s is the dynamic pressure given in units of Pascals, ρ_s is the shock front density(kg/m^3), and u is the material velocity (m/s). This gives the pressure immediately behind the shock front. Finally, the last value that may be

useful in analyzing the impacts of the prompt radiation is the shock temperature. The equation to give shock front temperature is given in Equation 3.14 below:

$$T_s = T_o * \left(\frac{p_s}{p_o}\right) * \left[\frac{2*\gamma+(\gamma-1)*\left(\frac{\Delta p}{p_o}\right)}{2*\gamma+(\gamma+1)*\left(\frac{\Delta p}{p_o}\right)}\right] \quad \text{EQN 3.14[3]}$$

Equation 3.14 uses the outputs of ambient pressure and shock front pressure from Equations 3.8 and 3.7 as well as the ambient temperature from Equation 3.4. The γ is the same constant used in Equation 3.10 and is equal to 1.4. This gives the temperature of the materials inside the shock front at different distances from the center of the blast. It must be noted that this equation was intended to be used at ranges where the difference between the shock front pressure and the ambient pressure is less than 2 MPa. It is still useful in giving an estimate of shock temperature at higher pressures but the results will be less reliable.

4 RESULTS

The results of the MCNP simulation will be listed below in order to show the energy and temperature change from neutron, gamma, and secondary radiation deposition. The outputs of the MCNP 6.2 code were utilized in previously generated analytical solutions to multiple blast wave factors in the Northrop book on nuclear weapon effects. These outputs were compared to standard temperature and pressure conditions to analyze the impact changing conditions with prompt radiation had on overall blast wave effects.

4.3 MCNP Results

The results of each simulation will be displayed here in detail to show how each process effectively fed the overall results of the research. The MCNP simulations produced the average energy deposited in air in units of MeV/g as well as a calculated mass of each region given in grams. This information was the primary output of each simulation. The uncertainty associated with the simulation was generated as part of

the code. Increasing the number of histories decreases the relative uncertainty of the tallies generated. For each simulation, 100,000 histories were generated. This resulted in a relative uncertainty of .0018. The is significantly below the value of .05 that is required by MCNP to be considered valid results [7]. There are an additional 10 error checks that must be passed in each simulation [7]. The results for each simulation passed all 10 checks indicating the results are considered valid by the code.

4.3.1 Neutron Deposition

There were two simulations produced to model neutrons released from a nuclear blast into infinite, free air. The first simulation conducted involved prompt neutrons produced as a result of fission. The energy distribution was pulled from a watt spectrum with an energy range limit of 10 MeV. The results of the first fission simulation are shown in Table 4.1 below:

Table 4.1 Type 3 average neutron energy deposited in air

Shell (region)	Inner Radius (cm)	Outer Radius(cm)	Energy deposited (MeV/g)	Mass of air in region (g)
2	50	100	6.76E-07	4.49E+03
3	100	200	1.70E-07	3.59E+04
4	200	300	6.27E-08	9.75E+04
5	300	400	3.22E-08	1.90E+05
6	400	500	1.96E-08	3.13E+05
7	500	600	1.31E-08	4.67E+05
8	600	700	9.39E-09	6.52E+05
9	700	800	7.03E-09	8.67E+05
10	800	900	5.46E-09	1.11E+06
11	900	1000	4.34E-09	1.39E+06

The results for the devices that utilize fusion were ran next. This simulation accounts for the higher energy spectrum of fusion neutrons up to 15 MeV. Due to the increase energy of the neutrons the average energy of neutrons escaping the devices would be higher allowing for a larger increase in energy deposited. The results of the simulation are listed in Table 4.2 below:

Table 4.2 average neutron energy deposited in air for type 5, 8, and 13 devices

Shell (region)	Inner Radius (cm)	Outer Radius (cm)	Energy deposited (MeV/g)	Mass of air in region (g)
2	50	100	8.19E-07	4.49E+03
3	100	200	2.05E-07	3.59E+04
4	200	300	7.58E-08	9.75E+04
5	300	400	3.90E-08	1.90E+05
6	400	500	2.36E-08	3.13E+05
7	500	600	1.59E-08	4.67E+05
8	600	700	1.13E-08	6.52E+05
9	700	800	8.50E-09	8.67E+05
10	800	900	6.59E-09	1.11E+06
11	900	1000	5.25E-09	1.39E+06

The energy deposited and the mass of the air in each region or shell be used in later calculations for temperature and pressure. As can be seen, the only variable in these two simulations was the amount of energy deposited. The mass of air is based on the volume of the shells which for this simulation was constant. These results will help analyze the importance of type design in the overall simulation. For the final simulation involving neutrons, the Type 3 device numbers were again used. This simulation went out at far as 100 meters from the blast. The results inside of 10 meters were almost identical to Table 4.1. As a result, the information displayed here will just show the output from 10 meters to 100 meters. The results of the simulation are displayed in Table 4.3 below:

Table 4.3 Type 3 average neutron energy deposited in air

Shell (region)	Inner Radius (cm)	Outer Radius(cm)	Energy deposited (MeV/g)	Mass of air in region (g)
11	900	1000	6.30E-03	1.39E+06
12	1000	2000	6.40E-02	3.59E+07
13	2000	3000	6.53E-02	9.75E+07
14	3000	4000	6.60E-02	1.90E+08
15	4000	5000	6.60E-02	3.13E+08
16	5000	6000	6.53E-02	4.67E+08
17	6000	7000	6.40E-02	6.52E+08
18	7000	8000	6.18E-02	8.67E+08
19	8000	9000	5.93E-02	1.11E+09
20	9000	10000	5.53E-02	1.39E+09

Although the step size is much larger between shells of air, 10 meters instead of 1 meter, the larger volume and mass of air still normalizes the results. Neutrons only cover the first part of the energy deposited in air as a result of prompt radiation. Next, the results of the gamma ray simulations will be shown so that the two types of radiation can be combined in the post production.

4.3.2 Gamma Deposition

The gamma ray simulations were conducted four times to account for the different average gamma ray energies of each device. One final simulation of the Type 3 device was conducted out to 100 meters for use in the final analytical calculations. These values were pulled from historical research that accounts for the average energy of gamma rays that escape the heavy weapons materials. The results of the MCNP F6 tallies are reported with the same units as neutrons (MeV/g). The first simulation conducted was for a Type 3 device which only includes gamma rays created in fission with an average energy of 1.5 MeV, the results are listed in Table 4.4 below:

Table 4.4 Type 3 gamma energy deposited in air

Shell (region)	Inner Radius (cm)	Outer Radius(cm)	Energy deposited (MeV/g)	Mass of air in region (g)
2	50	100	5.22E-07	4.49E+03
3	100	200	1.30E-07	3.59E+04
4	200	300	4.79E-08	9.75E+04
5	300	400	2.45E-08	1.90E+05
6	400	500	1.49E-08	3.13E+05
7	500	600	9.94E-09	4.67E+05
8	600	700	7.10E-09	6.52E+05
9	700	800	5.32E-09	8.67E+05
10	800	900	4.13E-09	1.11E+06
11	900	1000	3.30E-09	1.39E+06

The second gamma ray simulation was for a Type 5 device with an average energy of the gamma rays that escaped being around 1.6 MeV which is slightly higher than Type 3 devices due to the addition of gamma rays produced as a result of fusion. The results are show in Table 4.5 below:

Table 4.5 Type 3 gamma energy deposited in air

Shell (region)	Inner Radius (cm)	Outer Radius(cm)	Energy deposited (MeV/g)	Mass of air in region (g)
2	50	100	5.50E-07	4.49E+03
3	100	200	1.37E-07	3.59E+04
4	200	300	5.05E-08	9.75E+04
5	300	400	2.59E-08	1.90E+05
6	400	500	1.57E-08	3.13E+05
7	500	600	1.05E-08	4.67E+05

8	600	700	7.48E-09	6.52E+05
9	700	800	5.61E-09	8.67E+05
10	800	900	4.35E-09	1.11E+06
11	900	1000	3.48E-09	1.39E+06

The third simulation was for a Type 8 device which would include a larger fusion secondary mechanism that would increase the overall radiation yield of the device. The average energy of the gammas the escape from this device is 1.63 MeV which is only slightly higher than the Type 5 device. The results of the simulation are shown in Table 4.6 below:

Table 4.6 Type 8 gamma energy deposited in air

Shell (region)	Inner Radius (cm)	Outer Radius(cm)	Energy deposited (MeV/g)	Mass of air in region (g)
2	50	100	5.55E-07	4.49E+03
3	100	200	1.38E-07	3.59E+04
4	200	300	5.09E-08	9.75E+04
5	300	400	2.61E-08	1.90E+05
6	400	500	1.58E-08	3.13E+05
7	500	600	1.06E-08	4.67E+05
8	600	700	7.55E-09	6.52E+05
9	700	800	5.66E-09	8.67E+05
10	800	900	4.39E-09	1.11E+06
11	900	1000	3.51E-09	1.39E+06

The final gamma simulation was conducted for the Type 13 device which includes a more advanced design the significant increases the radiative yield of the device. As a result the average energy of the escape gamma rays is higher than all the

previous devices at 2 MeV. The results of the final simulation are shown in Table 4.7 below:

Table 4.7 Type 13 gamma energy deposited in air

Shell (region)	Inner Radius (cm)	Outer Radius(cm)	Energy deposited (MeV/g)	Mass of air in region (g)
2	50	100	6.41E-07	4.49E+03
3	100	200	1.60E-07	3.59E+04
4	200	300	5.89E-08	9.75E+04
5	300	400	3.02E-08	1.90E+05
6	400	500	1.83E-08	3.13E+05
7	500	600	1.22E-08	4.67E+05
8	600	700	8.73E-09	6.52E+05
9	700	800	6.55E-09	8.67E+05
10	800	900	5.09E-09	1.11E+06
11	900	1000	4.06E-09	1.39E+06

Just like with the neutron simulations, these initial results help compare the outputs of the different weapon impacts to measure the importance of weapon design in prompt radiation output. One final simulation was ran for the Type 3 device to simulate the gamma radiation out to 100 meters. The results from this simulation are shown in Table 4.8 below:

Table 4.8 Type 3 gamma energy deposited in air

Shell (region)	Inner Radius (cm)	Outer Radius(cm)	Energy deposited (MeV/g)	Mass of air in region (g)
11	900	1000	3.32E-09	1390570
12	1000	2000	1.27E-09	3.59E+07
13	2000	3000	4.59E-10	9.75E+07

14	3000	4000	2.31E-10	1.90E+08
15	4000	5000	1.37E-10	3.13E+08
16	5000	6000	8.97E-11	4.67E+08
17	6000	7000	6.26E-11	6.52E+08
18	7000	8000	4.56E-11	8.67E+08
19	8000	9000	3.44E-11	1.11E+09
20	9000	10000	2.65E-11	1.39E+09

The results of each of these simulations will be combined with the results of the neutron simulations and the secondary radiation simulations in the post production. It is important to note that these gamma interactions do produce secondary radiation that is captured in the air. MCNP captures these effects in each simulation. The results of the secondary radiation will be listed in the following section.

4.3.3 Secondary Radiation Effects

The four gamma ray simulations each produced a secondary amount of energy that MCNP is able to capture and tally separately. This energy is important to account for because it is lost in when tallying the gamma ray interactions by themselves but in reality it is added to the overall energy captured by the air surrounding a nuclear blast. The results of each simulation will be listed with the same units of energy deposited as the previous simulations (MeV/g) and will be displayed according to the shell and device type as shown in Table 4.9 below:

Table 4.9 Energy from secondary radiation deposited in air by device type

Shell (region)	Type 3 (MeV/g)	Type 5 (MeV/g)	Type 8 (MeV/g)	Type 13 (MeV/g)
2	1.35E-07	1.25E-07	1.27E-07	1.04E-07
3	6.73E-08	6.31E-08	6.14E-08	5.65E-08
4	3.65E-08	3.62E-08	3.60E-08	3.23E-08

5	2.39E-08	2.40E-08	2.38E-08	2.22E-08
6	1.47E-08	1.62E-08	1.64E-08	1.66E-08
7	9.73E-09	1.09E-08	1.10E-08	1.24E-08
8	7.21E-09	7.74E-09	7.90E-09	9.30E-09
9	5.25E-09	5.56E-09	5.61E-09	6.60E-09
10	4.28E-09	4.48E-09	4.53E-09	5.11E-09
11	3.11E-09	3.40E-09	3.37E-09	3.84E-09

The final simulation for the Type 3 device also included secondary radiation created by gamma ray interactions. The information from that simulation is shown in Table 4.10 below:

Table 4.10 Type 3 secondary radiation energy deposited in air

Shell (region)	Inner Radius (cm)	Outer Radius(cm)	Energy deposited (MeV/g)	Mass of air in region (g)
11	900	1000	3.33E-09	1.39E+06
12	1000	2000	1.27E-09	3.59E+07
13	2000	3000	4.58E-10	9.75E+07
14	3000	4000	2.35E-10	1.90E+08
15	4000	5000	1.41E-10	3.13E+08
16	5000	6000	9.22E-11	4.67E+08
17	6000	7000	6.40E-11	6.52E+08
18	7000	8000	4.60E-11	8.67E+08
19	8000	9000	3.46E-11	1.11E+09
20	9000	10000	2.67E-11	1.39E+09

The sum of the energies of the gamma rays and the secondary radiation they produce will be combined into on overall energy used in the post production to calculate the overall energy deposited in air as a result of the gamma simulations. With all of the

simulations completed, the average energy deposited per particle must be converted to temperature change. To do this, average energy deposited in each simulation was used in calculations that will be discussed further in the following section.

4.4 Post Production Calculation Results

One of the most important steps of this research is to quantify the impact of the results of the simulations. The energy deposited from the distribution of prompt radiation in air will have an immediate impact on the temperature and pressure of the air present before the blast wave is formed. The results of the post production show just how much of an impact each device type would have. The results are listed by region to show the relationship between distance from the center of the blast and the temperature increase.

The results of the Type 3 device calculations are listed below in Table 4.11. It is worth nothing that these outputs represent the weakest of the devices in terms of the overall amount of prompt radiation released. It is also the only device with neutrons produced only from fission. This lowers the energy spectrum of neutrons, meaning there was overall less available energy in the simulation.

Table 4.11 Type 3 device temperature increase as a result of prompt radiation

Shell (region)	Inner Radius (m)	Outer Radius (m)	Temp from Neutrons (C)	Temp from Gamma/Electrons (C)	Total Temp (K)
2	.50	1.00	2.09E+06	7.36E+05	2.83E+06
3	1.00	2.00	5.24E+05	2.21E+05	7.46E+05
4	2.00	3.00	1.94E+05	9.46E+04	2.89E+05
5	3.00	4.00	9.96E+04	5.42E+04	1.54E+05
6	4.00	5.00	6.05E+04	3.32E+04	9.39E+04
7	5.00	6.00	4.06E+04	2.20E+04	6.29E+04
8	6.00	7.00	2.90E+04	1.60E+04	4.53E+04
9	7.00	8.00	2.17E+04	1.18E+04	3.39E+04
10	8.00	9.00	1.69E+04	9.42E+03	2.66E+04

11	9.00	10.0	1.34E+04	7.18E+03	2.09E+04

The results of the table are graphed and presented below in Figure 4.1 which shows the temperature vs. distance. A log scale is used to give better resolution of the changes in temperature which is large over the 10 meters of air analyzed.

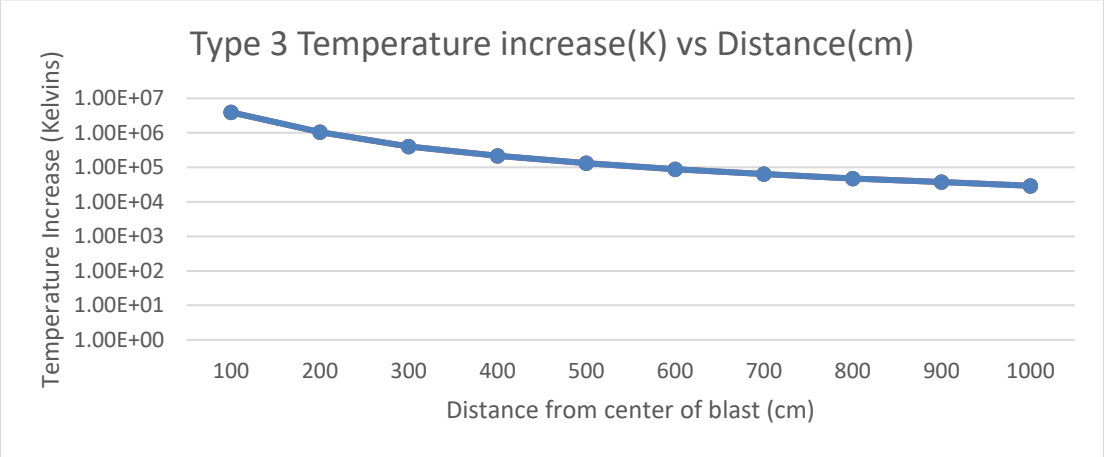

Figure 4.1 Type 3 device change in air temperature vs. distance

The results for a Type 5 device were put through the same calculations as the Type 3 device. The first adjustment made is to account for neutrons from fusion being included in the simulation. The neutrons from fusion increase the energy spectrum of the Watt distribution up to 15 MeV. The second adjustment, is for the variation in the amount of neutrons that on average escape from the device. The Type 5 device has 3.38E+25 neutrons per KT as shown in Table 3.1. The results of the calculations are show in Table 4.12 below:

Table 4.12 Type 5 device temperature increase as a result of prompt radiation

Shell (region)	Inner Radius (m)	Outer Radius (m)	Temp from Neutrons (C)	Temp from Gamma/Electrons (C)	Total Temp (K)
2	.50	1.00	3.16E+06	8.02E+05	3.97E+06

3	1.00	2.00	7.93E+05	2.38E+05	1.03E+06
4	2.00	3.00	2.93E+05	1.03E+05	3.96E+05
5	3.00	4.00	1.51E+05	5.92E+04	2.10E+05
6	4.00	5.00	9.13E+04	3.79E+04	1.29E+05
7	5.00	6.00	6.12E+04	2.54E+04	8.69E+04
8	6.00	7.00	4.38E+04	1.81E+04	6.22E+04
9	7.00	8.00	3.28E+04	1.33E+04	4.64E+04
10	8.00	9.00	2.55E+04	1.05E+04	3.63E+04
11	9.00	10.0	2.03E+04	8.17E+03	2.87E+04

The results from Table 4.12 are graphed vs distance to show the overall drop in temperature from the points closest to the blast out to 10 meters. The results are shown in Figure 4.2 below:

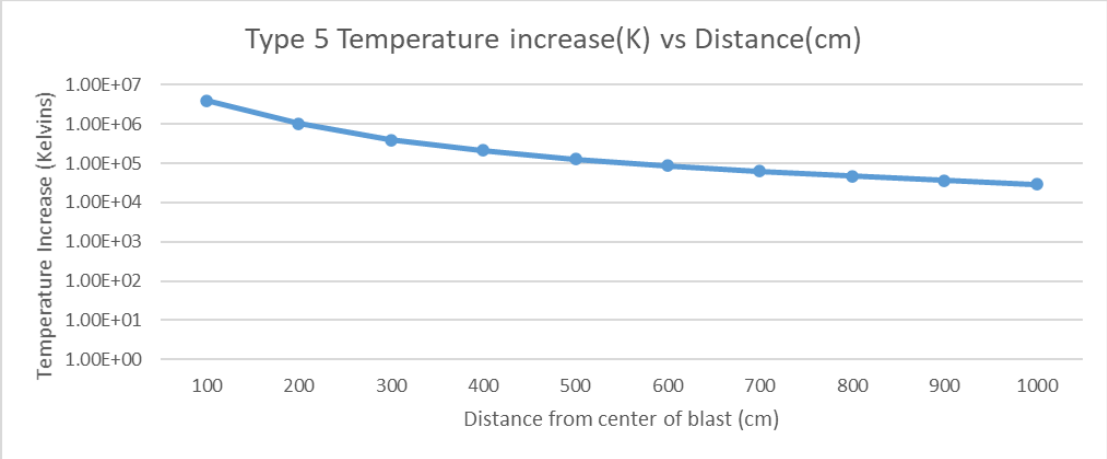

Figure 4.2 Type 5 device change in air temperature vs distance

The next set of calculations that needed to be completed are for the Type 8 device. This device had a unique feature in the radiation yield that caused the average energy deposited to be adjusted as seen in Table 3.1. This was particular important while accounting for the gamma radiation released. Additionally, the Type 8 device released 1.95E+23 neutrons per KT which is lower than the Type 3 or Type 5 device. The results of the temperature increase are showing in Table 4.13 below:

Table 4.13 Type 8 device temperature increase as a result of prompt radiation

Shell (region)	Inner Radius (m)	Outer Radius (m)	Temp from Neutrons (C)	Temp from Gamma/Electrons (C)	Total Temp (K)
2	.50	1.00	1.83E+06	7.28E+05	2.55E+06
3	1.00	2.00	4.57E+05	2.13E+05	6.71E+05
4	2.00	3.00	1.69E+05	9.27E+04	2.62E+05
5	3.00	4.00	8.69E+04	5.32E+04	1.40E+05
6	4.00	5.00	5.27E+04	3.44E+04	8.74E+04
7	5.00	6.00	3.53E+04	2.30E+04	5.86E+04
8	6.00	7.00	2.53E+04	1.65E+04	4.20E+04
9	7.00	8.00	1.89E+04	1.20E+04	3.13E+04
10	8.00	9.00	1.47E+04	9.52E+03	2.45E+04
11	9.00	10.0	1.17E+04	7.34E+03	1.93E+04

The results for this device type were also graphed as a function of temperature and distance as shown in Figure 4.3 below:

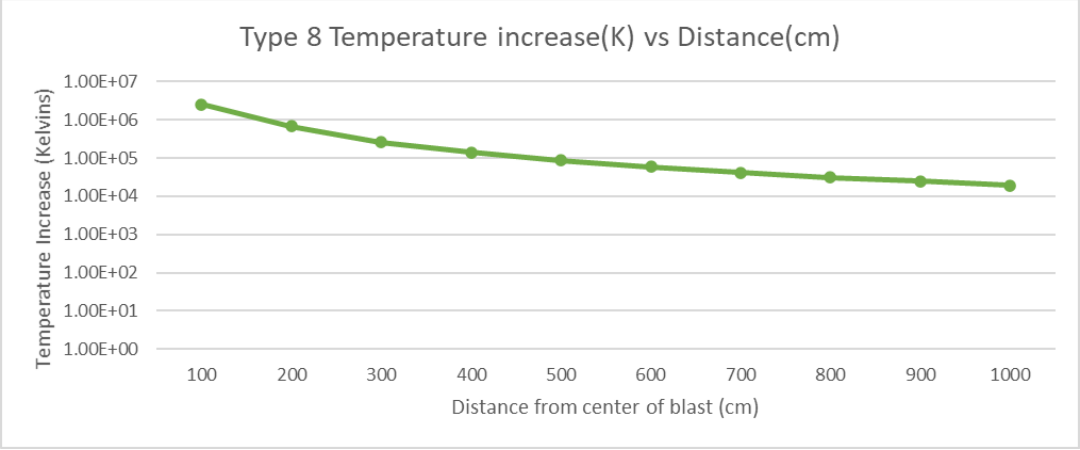

Figure 4.3 Type 8 device change in air temperature vs. distance

The final design type that was analyzed accounted for the largest temperature changes in air. The Type 13 device is the most powerful device with the largest

amount of prompt radiation released. This design type did not have any scaling factors like the Type 8 device. This resulted in the higher production of gamma radiation which is reflected in its significantly higher outputs. However, this design had the lowest radiative yield of neutrons at 1.77E23 neutrons per KT. The results of the post production calculations are shown in Table 4.14 below:

Table 4.14 Air temperature changes from prompt radiation from Type 13 device

Shell (region)	Inner Radius (m)	Outer Radius (m)	Temp from Neutrons (C)	Temp from Gamma/Electrons (C)	Total Temp (K)
2	.50	1.00	1.66E+06	5.77E+06	7.42E+06
3	1.00	2.00	4.15E+05	1.68E+06	2.09E+06
4	2.00	3.00	1.53E+05	7.06E+05	8.59E+05
5	3.00	4.00	7.89E+04	4.05E+05	4.84E+05
6	4.00	5.00	4.78E+04	2.70E+05	3.18E+05
7	5.00	6.00	3.21E+04	1.91E+05	2.23E+05
8	6.00	7.00	2.29E+04	1.40E+05	1.63E+05
9	7.00	8.00	1.72E+04	1.02E+05	1.19E+05
10	8.00	9.00	1.33E+04	7.89E+04	9.25E+04
11	9.00	10.0	1.06E+04	6.12E+04	7.21E+04

The results for the Type 13 device were also plotted as a function of temperature and distance as shown in Figure 4.4 below:

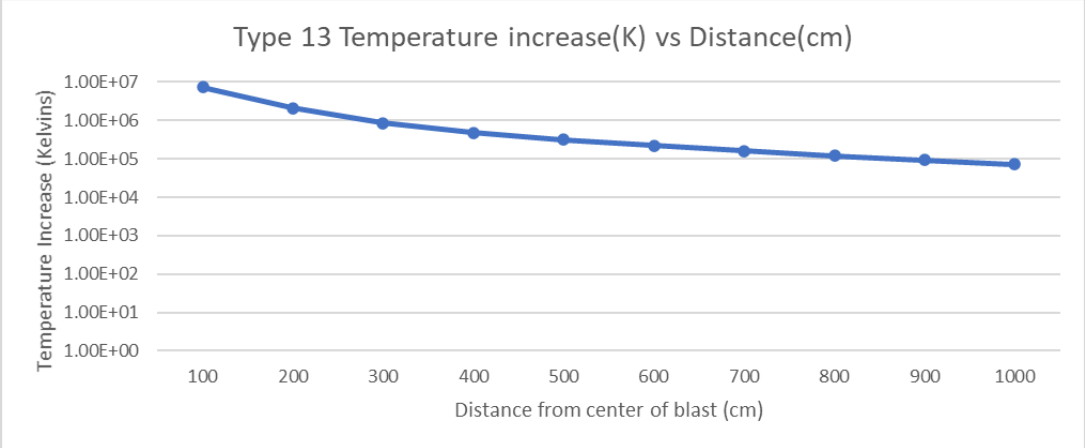

Figure 4.4 Type 13 change in air temperature vs. distance

The results of all the different device types were combined together in Figure 4.5 below in order to show the relative scale of each devices outputs and how they affected the temperature of the air surrounding the device with the same amount of available energy.

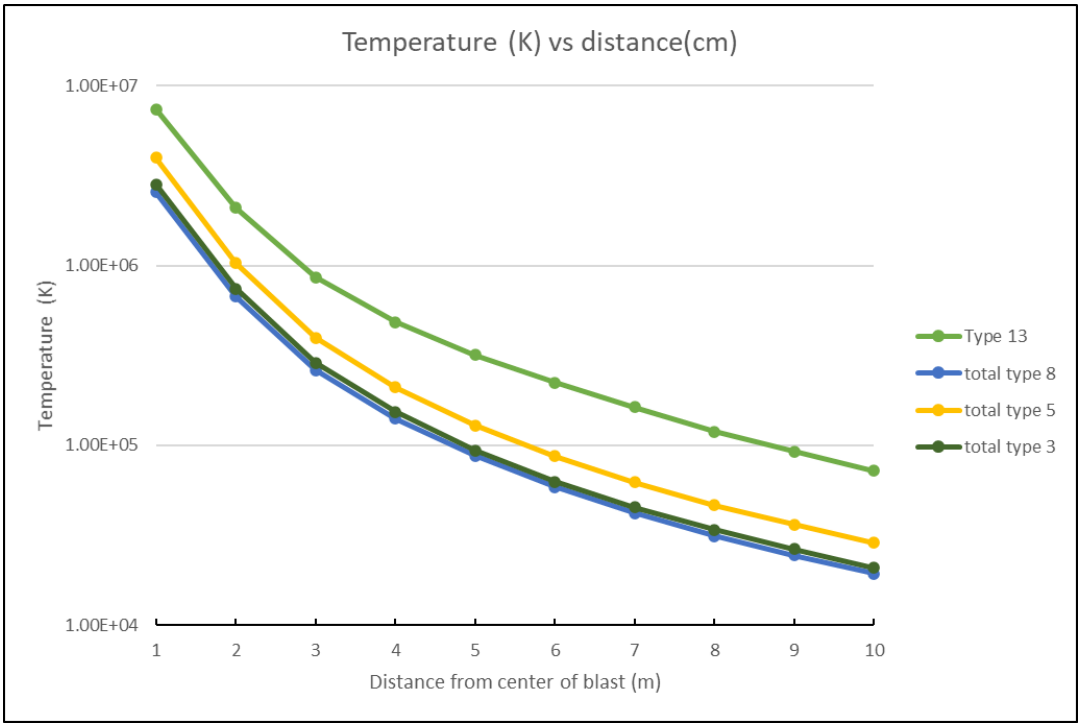

Figure 4.5 temperature increase vs distance for all types of weapons devices

It is important to note that the yields of the Type 3 and Type 8 devices overlapped significantly due to the lower amount of escaped gamma radiation in the Type 8 device. Finally, the results from the final simulation with a yield of 100 KT were modelled out to 100 meters. The results of this simulation were done in increments of 1 meter out to ten meters and after ten meters the shells of air were increased to 10 meter gaps out to 100 meters. The results are displayed below in Table 4.15:

Table 4.15 Air temperature changes from prompt radiation of 100 KT Type 3 device

Shell (region)	Inner Radius (m)	Outer Radius (m)	Temp from Neutrons (C)	Temp from Gamma/Electrons (C)	Total Air Temp (K)
2	.50	1.00	7.36E+03	7.36E+03	2.83E+06
3	1.00	2.00	7.36E+03	7.36E+03	7.43E+05
4	2.00	3.00	7.36E+03	7.36E+03	2.91E+05
5	3.00	4.00	7.36E+03	7.36E+03	1.53E+05
6	4.00	5.00	7.36E+03	7.36E+03	9.44E+04
7	5.00	6.00	7.36E+03	7.36E+03	6.38E+04
8	6.00	7.00	7.36E+03	7.36E+03	4.58E+04
9	7.00	8.00	7.36E+03	7.36E+03	3.46E+04
10	8.00	9.00	7.36E+03	7.36E+03	2.71E+04
11	9.00	10.0	7.36E+03	7.36E+03	2.17E+04
12	10.0	20.0	7.36E+03	7.36E+03	8.64E+03
13	20.0	30.0	7.36E+03	7.36E+03	3.39E+03
14	30.0	40.0	7.36E+03	7.36E+03	1.89E+03
15	40.0	50.0	7.36E+03	7.36E+03	1.26E+03
16	50.0	60.0	7.36E+03	7.36E+03	9.29E+02
17	60.0	70.0	7.36E+03	7.36E+03	7.38E+02
18	70.0	80.0	7.36E+03	7.36E+03	6.16E+02
19	80.0	90.0	7.36E+03	7.36E+03	5.35E+02

20	90.0	100	7.36E+03	7.36E+03	4.75E+02

Table 4.15 gives a complete picture of the increase in air temperature over a distance up to 100 meters as a results of prompt radiation from a 100 KT nuclear blast. These results give a baseline for the air temperatures prior to the blast wave forming. These results will next be directly applied to an analytical model for blast wave formation to estimate the impacts of accounting for simulating prompt radiation in blast wave models. The analytical models will compare the difference in blast wave outputs when calculated with prompt radiation initial conditions from the Type 3 device against standard temperature and pressure conditions.

It can be observed that the difference between the simulation of prompt radiation and standard air temperature start off as high as a million degrees. It is also important to note that the two values quickly converge and by 100 meters the difference in temperatures is only ~182 Kelvin. An additional set of temperature changes was next calculated for a 1 KT blast. The average energy deposited per neutron and gamma ray is does not vary, only the overall numbers of neutrons and gammas available to deposit energy in the system. The results of the 1 KT calculations are summarized in Table 4.16 below:

Table 4.16 Air temperature changes from prompt radiation of 1 KT Type 3 device

Shell (region)	Inner Radius (m)	Outer Radius (m)	Temp from Neutrons (C)	Temp from Gamma/Electrons (C)	Total Air Temp (K)
2	.50	1.00	2.09E+04	7.36E+03	2.86E+04
3	1.00	2.00	5.24E+03	2.18E+03	7.72E+03
4	2.00	3.00	1.94E+03	9.61E+02	3.20E+03
5	3.00	4.00	1.00E+03	5.30E+02	1.82E+03
6	4.00	5.00	6.10E+02	3.32E+02	1.23E+03
7	5.00	6.00	4.11E+02	2.24E+02	9.28E+02
8	6.00	7.00	2.96E+02	1.59E+02	7.48E+02

9	7.00	8.00	2.23E+02	1.20E+02	6.36E+02
10	8.00	9.00	1.74E+02	9.43E+01	5.61E+02
11	9.00	10.0	1.40E+02	7.45E+01	5.07E+02
12	10.0	20.0	5.50E+01	2.85E+01	3.76E+02
13	20.0	30.0	2.07E+01	1.03E+01	3.24E+02
14	30.0	40.0	1.07E+01	5.22E+00	3.09E+02
15	40.0	50.0	6.51E+00	3.11E+00	3.03E+02
16	50.0	60.0	4.32E+00	2.04E+00	2.99E+02
17	60.0	70.0	3.04E+00	1.42E+00	2.97E+02
18	70.0	80.0	2.20E+00	1.03E+00	2.96E+02
19	80.0	90.0	1.64E+00	7.72E-01	2.95E+02
20	90.0	100	1.23E+00	5.96E-01	2.95E+02

The change in STP air temperature varies based on yield. The outputs in Table 4.16 are significantly lower than the outputs for the 100 KT yield shown in Table 4.15. Figure 4.6 shows the temperature changes of both the 100 and 1 KT simulation comparted to STP.

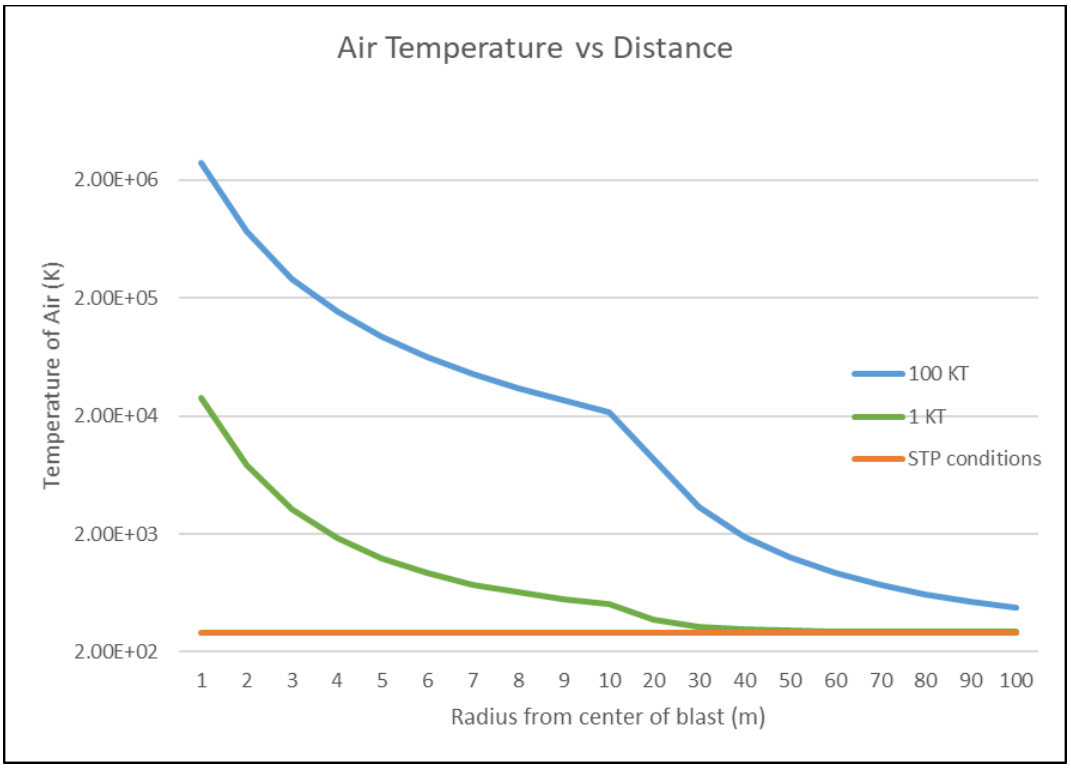

Figure 4.6 Air temperature vs distance of different yields compared to STP conditions

The results of the analytical models will reflect the difference in temperatures as many variables rely on ambient temperature. Next, these initial conditions will be used to solve for the various blast wave outputs such as peak overpressure, dynamic pressure, material velocity, and shock temperature.

4.5 Analytical Results

The results of the temperature increases were introduced as initial conditions into different analytical equations. These same calculations were made at standard temperature and pressures. This allows a direct comparison of results from the prompt radiation simulation. These results can also be compared directly to historical charts and tables. The first calculation made was to determine the peak overpressure in the blast wave using Equation 3.4. In order to make this calculation the radius of the blast had to be scaled from a 100 KT blast to a 1 KT blast as shown in Equation 3.5. There was no variance between the STP and prompt models at this point since

they have the same yield, however both calculations were made for the sake of comparing all outputs. The results of these calculations are shown in Table 4.17:

Table 4.17 Type 3 initial calculation of peak overpressure at different distance

Shell (region)	Radius (m)	Scaled distance (m)	STP Peak Overpressure (Pa)	Prompt Model Peak Overpressure (Pa)
2	1.00	2.15E-01	3.04E+13	3.04E+13
3	2.00	4.31E-01	3.81E+12	3.81E+12
4	3.00	6.46E-01	1.13E+12	1.13E+12
5	4.00	8.62E-01	4.77E+11	4.77E+11
6	5.00	1.08E+00	2.44E+11	2.44E+11
7	6.00	1.29E+00	1.41E+11	1.41E+11
8	7.00	1.51E+00	8.91E+10	8.91E+10
9	8.00	1.72E+00	5.98E+10	5.98E+10
10	9.00	1.94E+00	4.20E+10	4.20E+10
11	10.0	2.15E+00	3.06E+10	3.06E+10
12	20.0	4.31E+00	3.86E+09	3.86E+09
13	30.0	6.46E+00	1.15E+09	1.15E+09
14	40.0	8.62E+00	4.91E+08	4.91E+08
15	50.0	1.08E+01	2.54E+08	2.54E+08
16	60.0	1.29E+01	1.48E+08	1.48E+08
17	70.0	1.51E+01	9.41E+07	9.41E+07
18	80.0	1.72E+01	6.36E+07	6.36E+07
19	90.0	1.94E+01	4.51E+07	4.51E+07
20	100	2.15E+01	3.32E+07	3.32E+07

As can be seen in Table 4.17, the scaled distance does not exceed 21.5 meters. This means the pressure of a 100 KT blast at 100 meters is the equivalent of pressures of a 1 KT blast at 21.54 meters. This is important as it gives an understanding of how weapons effects scale with yield which will be compared in more detail later on. At

this point in the calculation there is no difference between the prompt radiation model and the STP model since the formula used for peak overpressure is purely dependent on radius in open air. However, due to the extremely high pressures present it was necessary to adjust the output of the equation for the pressure of ambient air ahead of the blast wave. This required a calculation to be done for the prompt radiation model to find the ambient pressure as a result of the large temperature change shown in Tables 4.10 and 4.14. With temperatures as high as 3.94E6 Kelvin reached there will be a large impact on pressure. The results of Equation 3.7 and 3.8 are shown in Table 4.18 below:

Table 4.18 Type 3 vs STP ambient pressure and peak overpressure at different distances

Shell (region)	Radius (m)	STP Ambient Pressure (MPa)	Prompt Ambient Pressure (MPa)	STP Peak Overpressure (MPa)	Prompt Peak Overpressure (MPa)
2	1.00	.101325	1.00E+03	3.04E+07	3.04E+07
3	2.00	.101325	2.64E+02	3.81E+06	3.81E+06
4	3.00	.101325	1.03E+02	1.13E+06	1.13E+06
5	4.00	.101325	5.45E+01	4.77E+05	4.77E+05
6	5.00	.101325	3.35E+01	2.44E+05	2.44E+05
7	6.00	.101325	2.26E+01	1.41E+05	1.41E+05
8	7.00	.101325	1.62E+01	8.91E+04	8.91E+04
9	8.00	.101325	1.23E+01	5.98E+04	5.98E+04
10	9.00	.101325	9.62E+00	4.20E+04	4.20E+04
11	10.0	.101325	7.71E+00	3.06E+04	3.07E+04
12	20.0	.101325	3.07E+00	3.86E+03	3.87E+03
13	30.0	.101325	1.20E+00	1.15E+03	1.16E+03
14	40.0	.101325	6.70E-01	4.91E+02	4.92E+02
15	50.0	.101325	4.45E-01	2.54E+02	2.54E+02

16	60.0	.101325	3.30E-01	1.48E+02	1.48E+02
17	70.0	.101325	2.62E-01	9.42E+01	9.44E+01
18	80.0	.101325	2.19E-01	6.37E+01	6.38E+01
19	90.0	.101325	1.90E-01	4.52E+01	4.53E+01
20	100.0	.101325	1.69E-01	3.33E+01	3.34E+01

The produced values for peak overpressure for both the STP and prompt conditions have now both been adjusted for ambient pressure conditions allowing for the calculation of the density in the shock front. Shock front density is a driving force of the material velocity and dynamic pressure. As Equation 3.10 shows shock front density is also dependent on the density of ambient air. This is why Equation 3.11 is needed to calculate the ambient pressure of air while accounting for the temperature change as a result of prompt radiation. The results for these calculations are shown below in Table 4.19:

Table 4.19 Type 3 STP vs. prompt ambient and shock front density

Shell (region)	Radius (m)	STP Ambient Density (kg/m^3)	Prompt Ambient Density (kg/m^3)	STP Shock Font Density (kg/m^3)	Prompt Shock Font Density (kg/m^3)
2	1.00	1.225	1.24	7.35	7.42
3	2.00	1.225	1.24	7.35	7.41
4	3.00	1.225	1.24	7.35	7.41
5	4.00	1.225	1.24	7.35	7.41
6	5.00	1.225	1.24	7.35	7.41
7	6.00	1.225	1.24	7.35	7.41
8	7.00	1.225	1.24	7.35	7.41
9	8.00	1.225	1.24	7.35	7.41
10	9.00	1.225	1.24	7.35	7.41
11	10.0	1.225	1.24	7.35	7.41

12	20.0	1.225	1.24	7.35	7.38
13	30.0	1.225	1.24	7.35	7.37
14	40.0	1.225	1.24	7.34	7.36
15	50.0	1.225	1.24	7.33	7.34
16	60.0	1.225	1.24	7.32	7.32
17	70.0	1.225	1.24	7.30	7.30
18	80.0	1.225	1.24	7.28	7.27
19	90.0	1.225	1.24	7.26	7.24
20	100.0	1.225	1.24	7.22	7.20

It is worth noting that the STP conditions have a lower density in the shock front until the ambient pressure in the prompt conditions begins to drop closer to STP air pressure around approximately 60 meters. The shock front density is used in both Equations 3.12 and 3.13 to generate material velocity and dynamic pressure. The values for both are shown in Table 4.20 below:

Table 4.20 Type 3 STP vs. prompt material velocity and dynamic pressure

Shell (region)	Radius (m)	STP Material Velocity (m/s)	Prompt Material Velocity (m/s)	STP Dynamic Pressure (MPa)	Prompt Dynamic Pressure (MPa)
2	1.00	4.55E+06	4.53E+06	7.61E+07	7.60E+07
3	2.00	1.61E+06	1.60E+06	9.52E+06	9.51E+06
4	3.00	8.76E+05	8.72E+05	2.82E+06	2.82E+06
5	4.00	5.69E+05	5.67E+05	1.19E+06	1.19E+06
6	5.00	4.08E+05	4.06E+05	6.10E+05	6.10E+05
7	6.00	3.10E+05	3.09E+05	3.54E+05	3.53E+05
8	7.00	2.46E+05	2.45E+05	2.23E+05	2.23E+05
9	8.00	2.02E+05	2.01E+05	1.49E+05	1.49E+05
10	9.00	1.69E+05	1.68E+05	1.05E+05	1.05E+05

11	10.0	1.44E+05	1.44E+05	7.66E+04	7.65E+04
12	20.0	5.13E+04	5.10E+04	9.65E+03	9.60E+03
13	30.0	2.80E+04	2.79E+04	2.88E+03	2.86E+03
14	40.0	1.83E+04	1.82E+04	1.23E+03	1.22E+03
15	50.0	1.31E+04	1.31E+04	6.32E+02	6.26E+02
16	60.0	1.00E+04	9.98E+03	3.68E+02	3.65E+02
17	70.0	8.00E+03	7.95E+03	2.34E+02	2.31E+02
18	80.0	6.57E+03	6.54E+03	1.57E+02	1.55E+02
19	90.0	5.53E+03	5.50E+03	1.11E+02	1.10E+02
20	100.0	4.74E+03	4.72E+03	8.12E+01	8.01E+01

Both the material velocity and the dynamic pressure are greater for STP conditions than for prompt radiation conditions. The last blast wave effect to be calculated is the temperature in the shock front. This temperature is dependent on ambient air temperature and pressure as well as shock front pressure as shown in Equation 3.14. The results of the shock temperature is shown in Table 4.21 below:

Table 4.21 STP vs prompt shock front temperature

Shell (region)	Radius (m)	STP Shock Temperature (K)	Prompt Shock Temperature (K)
2	1.00	1.47E+10	1.43E+10
3	2.00	1.84E+09	1.79E+09
4	3.00	5.44E+08	5.30E+08
5	4.00	2.30E+08	2.24E+08
6	5.00	1.18E+08	1.15E+08
7	6.00	6.82E+07	6.65E+07
8	7.00	4.30E+07	4.19E+07
9	8.00	2.88E+07	2.81E+07
10	9.00	2.03E+07	1.98E+07
11	10.0	1.48E+07	1.44E+07

12	20.0	1.86E+06	1.83E+06
13	30.0	5.57E+05	5.47E+05
14	40.0	2.37E+05	2.33E+05
15	50.0	1.23E+05	1.21E+05
16	60.0	7.18E+04	7.08E+04
17	70.0	4.58E+04	4.52E+04
18	80.0	3.11E+04	3.07E+04
19	90.0	2.22E+04	2.19E+04
20	100.0	1.64E+04	1.62E+04

With all of the initial calculations completed the next questions becomes how much did the blast wave outputs change as a result of the prompt simulation? To show the change as a percentage, the STP outputs were subtracted from the prompt outputs and divided by the STP outputs. This gives the percentage in change from STP to prompt blast wave outputs. These changes are shown in Table 4.22 below:

Table 4.22 Changes (%) in STP blast wave effects due to prompt radiation of 100 KT blast

Radius (m)	ΔPeak Overpressure	ΔDynamic Pressure	ΔShock Front Density	ΔMaterial Velocity	ΔShock Temperature
1.00	3.30E-03	-2.31E-02	8.96E-01	-4.57E-01	-2.57E+00
2.00	6.93E-03	-4.85E-02	8.75E-01	-4.59E-01	-2.54E+00
3.00	9.13E-03	-6.39E-02	8.62E-01	-4.60E-01	-2.53E+00
4.00	1.14E-02	-7.98E-02	8.49E-01	-4.61E-01	-2.51E+00
5.00	1.37E-02	-9.57E-02	8.35E-01	-4.63E-01	-2.49E+00
6.00	1.59E-02	-1.11E-01	8.22E-01	-4.64E-01	-2.47E+00
7.00	1.81E-02	-1.27E-01	8.09E-01	-4.65E-01	-2.45E+00
8.00	2.04E-02	-1.42E-01	7.96E-01	-4.67E-01	-2.43E+00
9.00	2.27E-02	-1.58E-01	7.83E-01	-4.68E-01	-2.42E+00

10.0	2.48E-02	-1.74E-01	7.69E-01	-4.69E-01	-2.40E+00
20.0	7.68E-02	-5.34E-01	4.66E-01	-4.99E-01	-1.98E+00
30.0	9.55E-02	-6.64E-01	3.58E-01	-5.10E-01	-1.82E+00
40.0	1.16E-01	-8.03E-01	2.41E-01	-5.22E-01	-1.66E+00
50.0	1.36E-01	-9.38E-01	1.27E-01	-5.33E-01	-1.50E+00
60.0	1.54E-01	-1.06E+00	2.28E-02	-5.44E-01	-1.36E+00
70.0	1.71E-01	-1.17E+00	-6.90E-02	-5.54E-01	-1.23E+00
80.0	1.84E-01	-1.26E+00	-1.42E-01	-5.61E-01	-1.12E+00
90.0	1.96E-01	-1.33E+00	-2.02E-01	-5.68E-01	-1.04E+00
100.0	2.02E-01	-1.37E+00	-2.34E-01	-5.72E-01	-9.94E-01

This data represents the initial scope of the research. In order to fully explore the possibilities of the impacts of prompt radiation on blast wave effects there are two additional case studies that were conducted as alternative solutions. The first alternative solution is to keep pressure constant and allow the density of air to change with temperature. The same calculations were generated under these alternate conditions. This had several impacts on many of the blast wave effects as shown below in Table 4.23:

Table 4.23 Constant Pressure Blast Wave Effects

Radius (m)	Peak Overpressure (MPa)	Dynamic Pressure (MPa)	Air Density (kg/m^3)	Shock Front Density (kg/m^3)	Material Velocity (m/s)	Shock Temperature (K)
1.00	3.04E+07	7.61E+07	1.25E-04	7.49E-04	4.51E+08	1.41E+14
2.00	3.81E+06	9.52E+06	4.75E-04	2.85E-03	8.17E+07	4.65E+12
3.00	1.13E+06	2.82E+06	1.21E-03	7.29E-03	2.78E+07	5.40E+11
4.00	4.77E+05	1.19E+06	2.30E-03	1.38E-02	1.31E+07	1.20E+11
5.00	2.44E+05	6.10E+05	3.74E-03	2.24E-02	7.38E+06	3.79E+10
6.00	1.41E+05	3.54E+05	5.53E-03	3.32E-02	4.62E+06	1.48E+10

7.00	8.91E+04	2.23E+05	7.71E-03	4.63E-02	3.10E+06	6.71E+09
8.00	5.98E+04	1.49E+05	1.02E-02	6.13E-02	2.21E+06	3.40E+09
9.00	4.20E+04	1.05E+05	1.30E-02	7.81E-02	1.64E+06	1.87E+09
10.0	3.06E+04	7.66E+04	1.62E-02	9.74E-02	1.25E+06	1.10E+09
20.0	3.86E+03	9.65E+03	4.09E-02	2.45E-01	2.81E+05	5.49E+07
30.0	1.15E+03	2.88E+03	1.04E-01	6.24E-01	9.61E+04	6.44E+06
40.0	4.91E+02	1.23E+03	1.87E-01	1.12E+00	4.68E+04	1.53E+06
50.0	2.54E+02	6.32E+02	2.81E-01	1.68E+00	2.74E+04	5.26E+05
60.0	1.48E+02	3.68E+02	3.80E-01	2.27E+00	1.80E+04	2.28E+05
70.0	9.42E+01	2.34E+02	4.78E-01	2.85E+00	1.28E+04	1.15E+05
80.0	6.37E+01	1.57E+02	5.73E-01	3.41E+00	9.61E+03	6.53E+04
90.0	4.52E+01	1.11E+02	6.60E-01	3.91E+00	7.54E+03	4.04E+04
100.0	3.33E+01	8.12E+01	7.42E-01	4.38E+00	6.09E+03	2.66E+04

The blast wave effects of this experiment are almost all higher than previously conducted calculations. The sole exceptions are the peak overpressure and dynamic pressure which are not significantly impacted by changing ambient air density based on the equations which were based on energy released in the blast [3]. The ambient air density at constant pressure drops as low as 1.25E-04 (kg/m^3). This is purely based on the calculations and not balanced with the expansion of air that would surely occur in reality. The shock front density likewise decreases to extremely small values as low as 7.49E-04 (kg/m^3). This is smaller than would be expected in reality and will be discussed in the following section. Material velocity increases by an order of magnitude of approximately one hundred. Dynamic pressure does not change significantly. Shock temperature increases by a factor approaching an order of magnitude of one thousand. These are extremely high differences that will be discussed in greater detail in the following sections.

A final alternate case study that is worth exploring is changing the yield from 100 KT to 1 KT and running all the same calculations again. With the lower overall yield of energy from the blasts it could change how impact prompt radiation is on

modeling. For this model no scaling is needed as many of the historical figures and equations are based on 1 KT results. Due to the yield being lower, it first becomes necessary to reestablish the results of the STP model. The results of this calculation are showing in Table 4.24 below:

Table 4.24 Blast wave effects at STP conditions from a 1 KT blast

Radius (m)	Peak Overpressure (MPa)	Dynamic Pressure (MPa)	Shock Front Density (kg/m^3)	Material Velocity (m/s)	Shock Temperature (K)
1.00	3.05E+05	7.63E+05	7.35E+00	4.54E+05	1.47E+08
2.00	3.83E+04	9.57E+04	7.35E+00	1.61E+05	1.85E+07
3.00	1.14E+04	2.85E+04	7.35E+00	8.76E+04	5.49E+06
4.00	4.82E+03	1.21E+04	7.35E+00	5.70E+04	2.33E+06
5.00	2.48E+03	6.20E+03	7.35E+00	4.09E+04	1.20E+06
6.00	1.44E+03	3.60E+03	7.35E+00	3.12E+04	6.95E+05
7.00	9.11E+02	2.27E+03	7.35E+00	2.48E+04	4.39E+05
8.00	6.12E+02	1.53E+03	7.34E+00	2.03E+04	2.96E+05
9.00	4.32E+02	1.08E+03	7.34E+00	1.71E+04	2.09E+05
10.0	3.16E+02	7.88E+02	7.34E+00	1.46E+04	1.53E+05
20.0	4.13E+01	1.01E+02	7.25E+00	5.26E+03	2.03E+04
30.0	1.29E+01	3.03E+01	7.03E+00	2.92E+03	6.57E+03
40.0	5.75E+00	1.26E+01	6.67E+00	1.93E+03	3.13E+03
50.0	3.14E+00	6.16E+00	6.19E+00	1.40E+03	1.87E+03
60.0	1.95E+00	3.35E+00	5.65E+00	1.08E+03	1.30E+03
70.0	1.33E+00	1.95E+00	5.11E+00	8.68E+02	9.95E+02
80.0	9.69E-01	1.19E+00	4.60E+00	7.16E+02	8.20E+02
90.0	7.45E-01	7.65E-01	4.14E+00	6.04E+02	7.09E+02
100.0	5.96E-01	5.09E-01	3.74E+00	5.17E+02	6.36E+02

Table 4.24 gives a different baseline than Tables 4.19, 4.20. and 4.21 for the blast wave outputs at STP. This is needed in order to generate an equivalent baseline

for the 1 KT yield prompt radiation calculations. Once this is baseline has been established it is possible to generate results for 1 KT utilizing the air temperature calculations results shown in Table 4.16. Utilizing these updated temperatures it is possible to calculate the different blast wave effects for a 1 KT blast which are shown in Table 4.25 below:

Table 4.25 Blast wave effects after simulating prompt radiation from a 1 KT blast

Radius (m)	Peak Overpressure (MPa)	Dynamic Pressure (MPa)	Shock Front Density (kg/m^3)	Material Velocity (m/s)	Shock Temperature (K)
1.00	3.05E+05	7.63E+05	7.42E+00	4.54E+05	1.43E+08
2.00	3.83E+04	9.57E+04	7.41E+00	1.61E+05	1.80E+07
3.00	1.14E+04	2.84E+04	7.41E+00	8.76E+04	5.35E+06
4.00	4.82E+03	1.20E+04	7.41E+00	5.70E+04	2.27E+06
5.00	2.48E+03	6.19E+03	7.41E+00	4.09E+04	1.17E+06
6.00	1.44E+03	3.59E+03	7.41E+00	3.12E+04	6.78E+05
7.00	9.11E+02	2.27E+03	7.40E+00	2.48E+04	4.29E+05
8.00	6.13E+02	1.53E+03	7.40E+00	2.03E+04	2.88E+05
9.00	4.32E+02	1.08E+03	7.40E+00	1.71E+04	2.04E+05
10.0	3.16E+02	7.87E+02	7.39E+00	1.46E+04	1.49E+05
20.0	4.13E+01	1.01E+02	7.28E+00	5.26E+03	1.99E+04
30.0	1.29E+01	3.00E+01	7.05E+00	2.92E+03	6.45E+03
40.0	5.76E+00	1.24E+01	6.68E+00	1.93E+03	3.08E+03
50.0	3.15E+00	6.09E+00	6.19E+00	1.40E+03	1.85E+03
60.0	1.96E+00	3.30E+00	5.65E+00	1.08E+03	1.28E+03
70.0	1.33E+00	1.92E+00	5.10E+00	8.68E+02	9.85E+02
80.0	9.73E-01	1.17E+00	4.58E+00	7.16E+02	8.13E+02
90.0	7.48E-01	7.51E-01	4.12E+00	6.04E+02	7.04E+02
100.0	6.00E-01	4.99E-01	3.73E+00	5.17E+02	6.32E+02

STP conditions are useful in helping show the changes between prompt conditions at 100 KT and 1 KT. This is accomplished by calculating the percentage change from STP temperature and shock front outputs the prompt temperature and shock front outputs. If the prompt conditions were higher than the STP the value will be shown as a positive, if the prompt conditions lowered the overall output the results will be shown as a negative percentage. The results for these comparisons are shown in Table 4.26 below:

Table 4.26 Changes (%) in STP blast effects due to prompt radiation from 1KT blast

Radius (m)	ΔPeak Overpressure	ΔDynamic Pressure	ΔShock Front Density	ΔMaterial Velocity	ΔShock Temperature
1.00	3.29E-03	-2.30E-02	8.96E-01	-4.57E-01	-2.57E+00
2.00	6.89E-03	-4.82E-02	8.75E-01	-4.59E-01	-2.54E+00
3.00	9.07E-03	-6.35E-02	8.62E-01	-4.60E-01	-2.53E+00
4.00	1.13E-02	-7.92E-02	8.49E-01	-4.61E-01	-2.51E+00
5.00	1.36E-02	-9.50E-02	8.36E-01	-4.63E-01	-2.49E+00
6.00	1.58E-02	-1.11E-01	8.22E-01	-4.64E-01	-2.47E+00
7.00	1.80E-02	-1.26E-01	8.10E-01	-4.65E-01	-2.45E+00
8.00	2.03E-02	-1.42E-01	7.96E-01	-4.66E-01	-2.43E+00
9.00	2.27E-02	-1.58E-01	7.83E-01	-4.68E-01	-2.42E+00
10.0	2.49E-02	-1.74E-01	7.69E-01	-4.69E-01	-2.40E+00
20.0	7.81E-02	-5.36E-01	4.66E-01	-5.00E-01	-1.98E+00
30.0	1.06E-01	-7.03E-01	3.29E-01	-5.16E-01	-1.79E+00
40.0	1.45E-01	-9.07E-01	1.69E-01	-5.38E-01	-1.57E+00
50.0	1.93E-01	-1.12E+00	9.08E-03	-5.66E-01	-1.34E+00
60.0	2.51E-01	-1.32E+00	-1.31E-01	-5.99E-01	-1.14E+00
70.0	3.18E-01	-1.51E+00	-2.39E-01	-6.37E-01	-9.71E-01
80.0	3.92E-01	-1.66E+00	-3.11E-01	-6.78E-01	-8.38E-01
90.0	4.71E-01	-1.78E+00	-3.51E-01	-7.21E-01	-7.34E-01

100.0	5.53E-01	-1.88E+00	-3.61E-01	-7.65E-01	-6.60E-01

The results from changing the yield were noticeably different in terms of impact than the higher yield. To better show the difference between the different yields, it is beneficial to graph the results of the changes over distance as shown for peak overpressure in Figure 4.7 below:

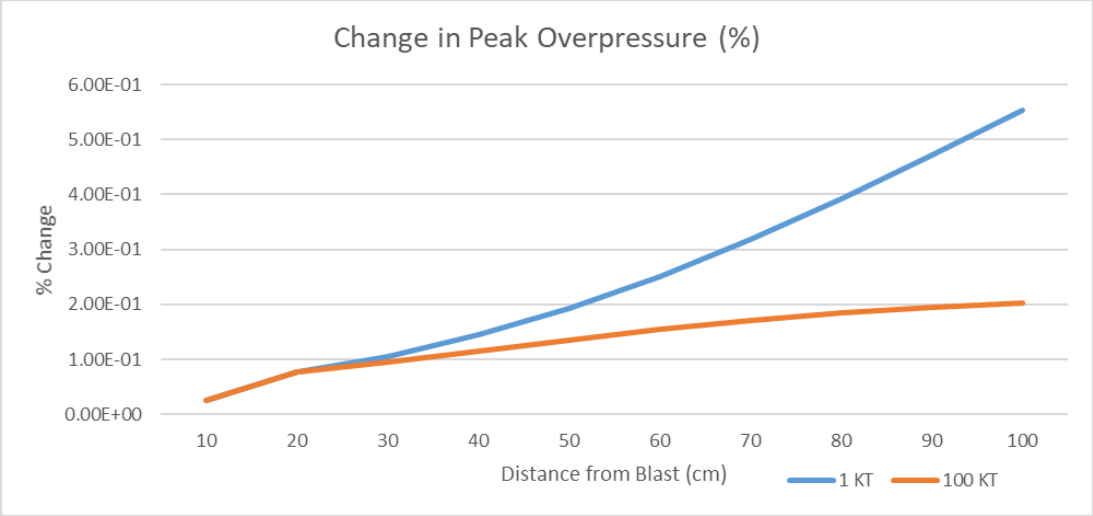

Figure 4.7 Change to STP peak overpressure due to prompt radiation

Figure 4.7 shows that at 100 meters the 1 KT the prompt radiation causes a .55% increase of STP conditions. This is compared to the 100 KT blast which only increases .20% at the same distance. The results for dynamic pressure were also graphed vs distance as shown in Figure 4.8 below:

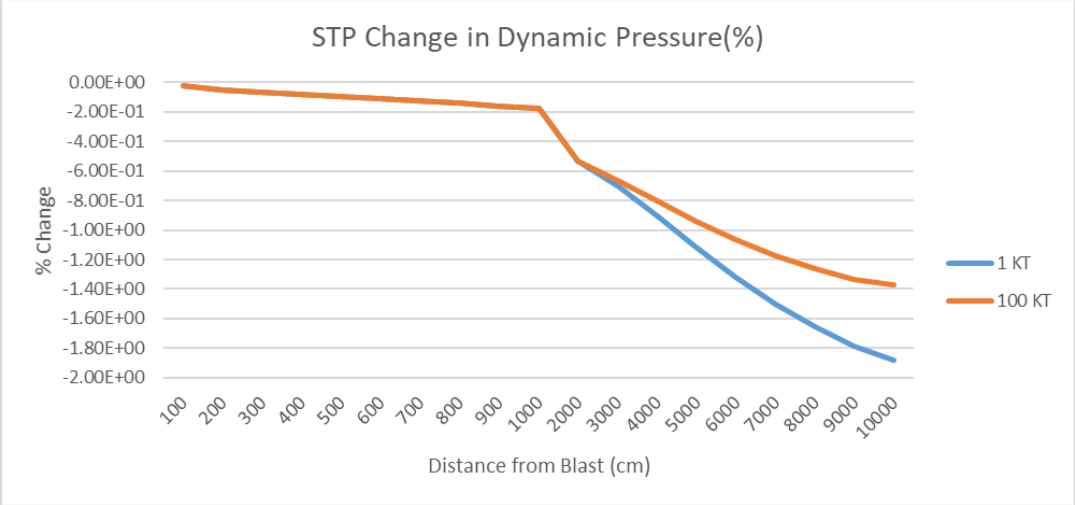

Figure 4.8 Change to STP dynamic pressure due to prompt radiation

Figure 4.8 shows that for the 1 KT blast, the prompt dynamic pressure is -1.88% smaller than the STP dynamic pressure at 100 meters. This is compared to the 100 KT results where the largest change in dynamic pressure from STP to prompt conditions is -1.37%. It is apparent that for the 1 KT blast the dynamic pressure drops faster in the 1 KT calculations than in the 100 KT calculations. The next blast weapon effect to be compared will be the shock front density shown in Figure 4.9 below:

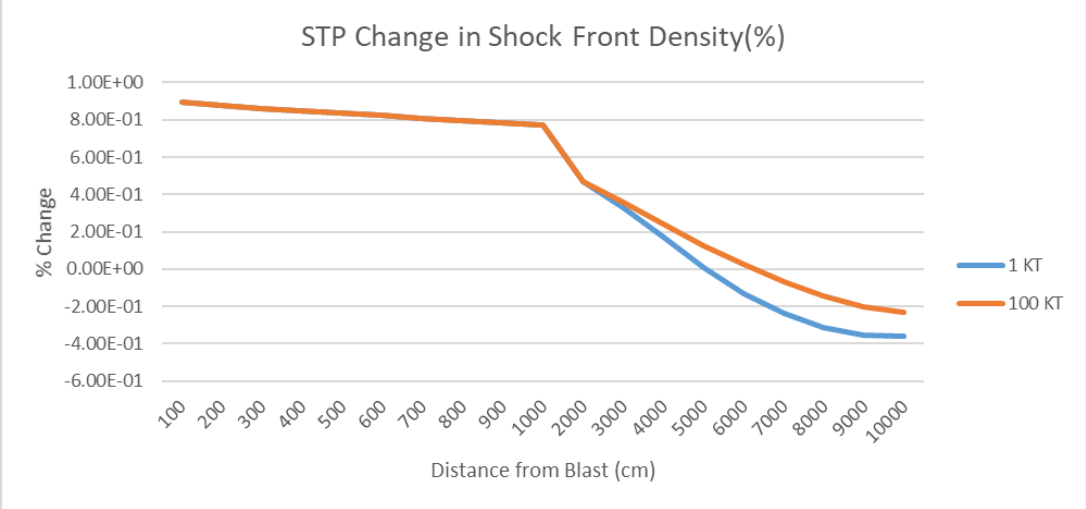

Figure 4.9 Changes to STP shock front density due to prompt radiation

Figure 4.9 shows that for the 1 KT blast the change in shock front density starts off at nearly the same values. At approximately 20 meters the 1 KT prompt shock front density drops below STP conditions much quicky than the 100 KT results. The 1 KT results decrease to a maximum change of -.36% at 100 meters. The 100 KT prompt results result in a similar drop (-.23%) in STP shock front density at 100 meters. Next, the change in STP material velocity will be compared for the 1 KT and 100 KT blast as shown in Figure 4.10 below:

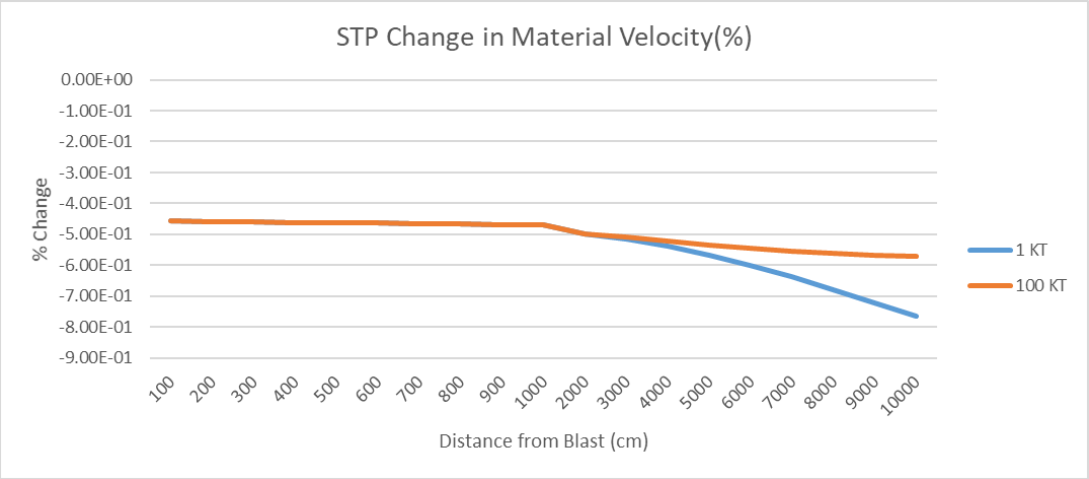

Figure 4.10 Change to STP material velocity due to prompt radiation

The results from the 1 KT calculation show a drop in the STP material velocity from -.46% at 1 meters to a max of -.77% at 100 meters. This is compared to the results from the 100 KT calculation which show a decrease of -.457% at 1 meter to a maximum change of -.57% at 100 meters. The final blast wave effect that was calculated was the shock front temperature. The results in the change to STP shock front temperature are shown in Figure 4.11 below:

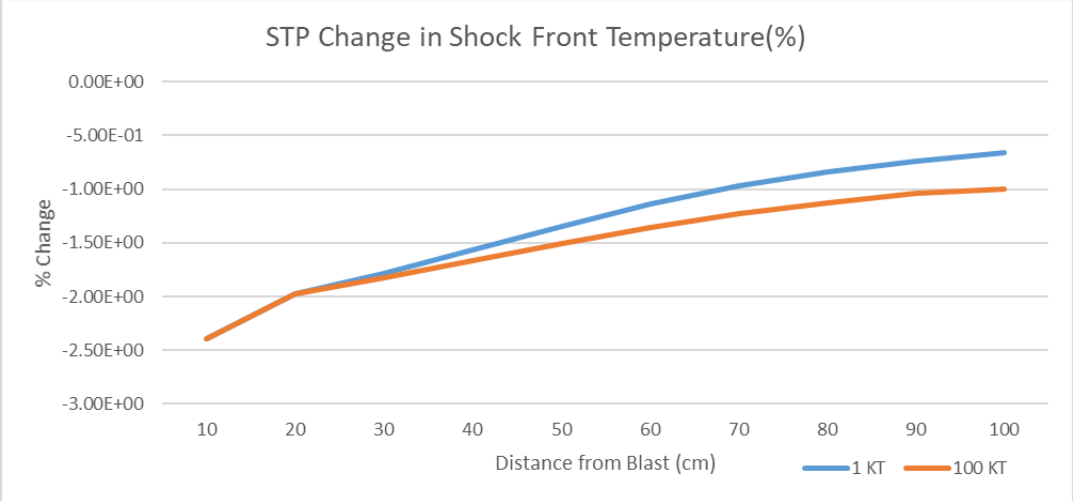

Figure 4.11 Change to STP shock front temperature due to prompt radiation

Figure 4.11 shows that for both yields they decrease the STP shock temperature by -2.57% at 10 meters. The change between STP and prompt shock front temperatures decrease as distance increases. By 100 meters, the 1 KT results are only -.66% below STP results. The 100 KT yield at 100 meters is still -.99% lower than STP conditions. This indicates that the 1 KT yield is having a larger impact on STP at closer distances than the 100 KT yield. These figures give an idea of the difference that yield can make on prompt radiation and blast wave effects.

With these final values calculated it is possible to analyze the results and make observations about the impacts modeling prompt radiation may have on blast wave formation. To verify that the results are relevant, many will have to be compared to historical results. Nuclear weapon effects are a very narrow field with restricted studies available. This makes it necessary to use the best available historical charts and graphics to evaluate modern results. In this case many of the historical results are from very early reports such as the 1947 LANL report “Blast Wave” [2]. For one such comparison of shock temperature vs radius was generated as shown in Figure 4.12 below:

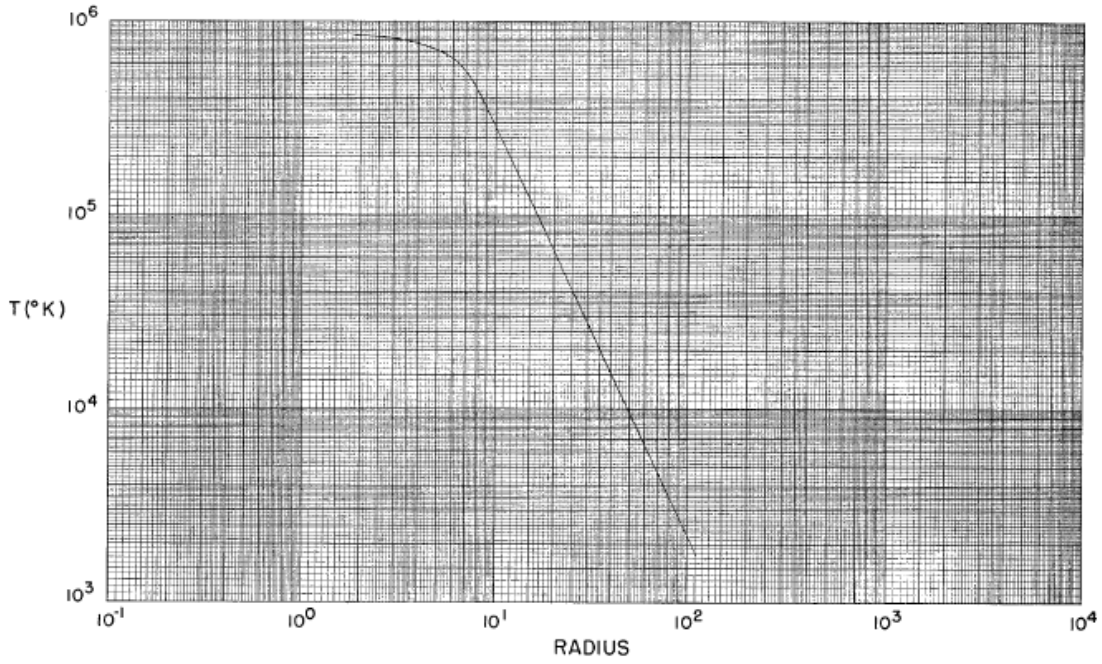

Figure 4.12 Shock Temperature (K) vs Radius (m) [2]

This figure was generated from calculations made for a 10KT blast [2]. The temperature approaches maximum values of 10^6 Kelvin towards the center of the blast. This is significantly lower than the 1.47E+10 K estimated from a 100 KT blast or 1.43E+08 K from the 1 KT blast. However, at a radius of 10 meters the values for shock temperature in the 1 KT blast drop to 1.49E+05 which much closer to the values in Figure 4.12. One newer model from 19747 is available comparing the observed temperature to the calculated or expected temperature. This comparison shown in Figure 4.13, gives an understanding that observed temperatures vary for reasons that might be accounted for by prompt conditions [1].

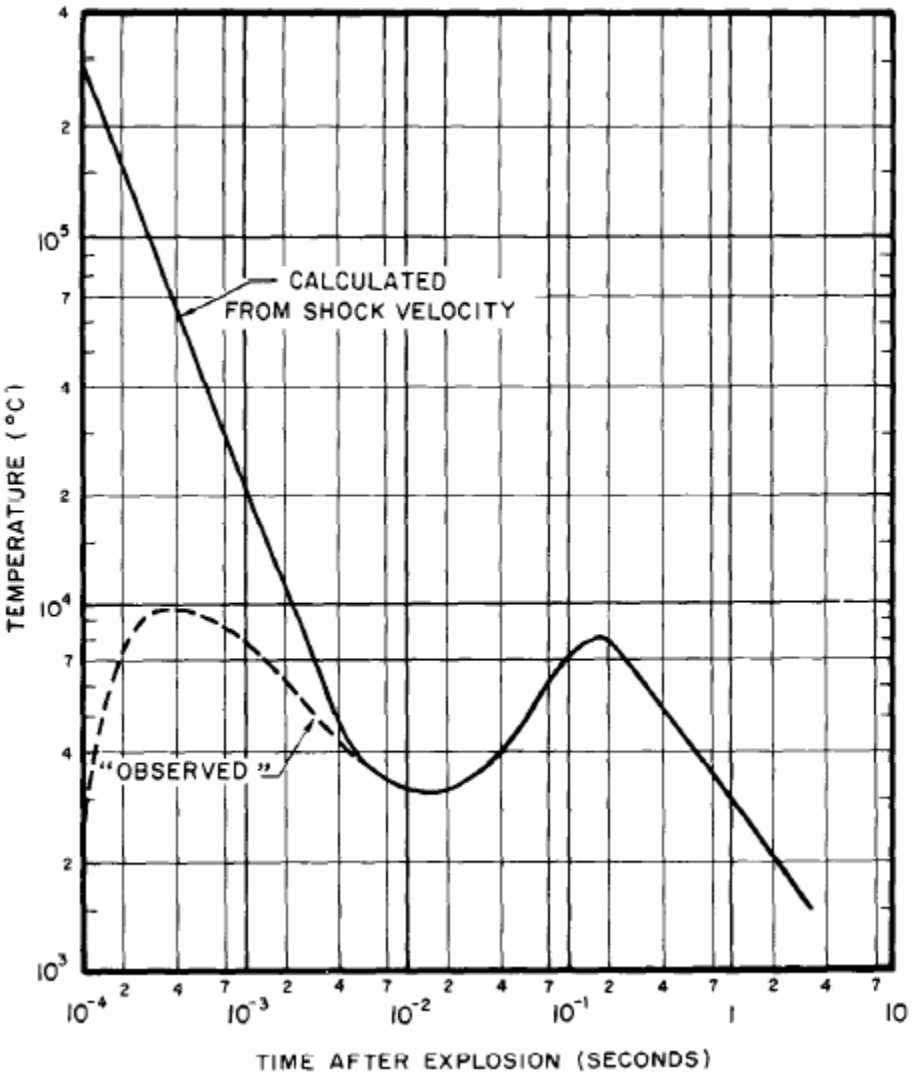

Figure 4.13 Observed blast temperature vs time [1]

In Figure 4.13 it is noted that the observed temperature is significantly below the calculated temperature. The observed temperatures do not exceed 10,000 Kelvin even at early times when the shock front would be expected to have started expanding at high temperatures. These results are for a 20 KT burst in free air similar to the simulation results. Most historical results were not as concerned with the temperature at the shock front since that is far from the most dominant feature of the shock front. Most historical results were far more concerned with peak overpressure and dynamic overpressure which are the most damaging features of a nuclear blast wave [1].

However, there is a relationship between temperature and pressure as shown in one of the first pictures of a nuclear blast in Figure 4.14 below.

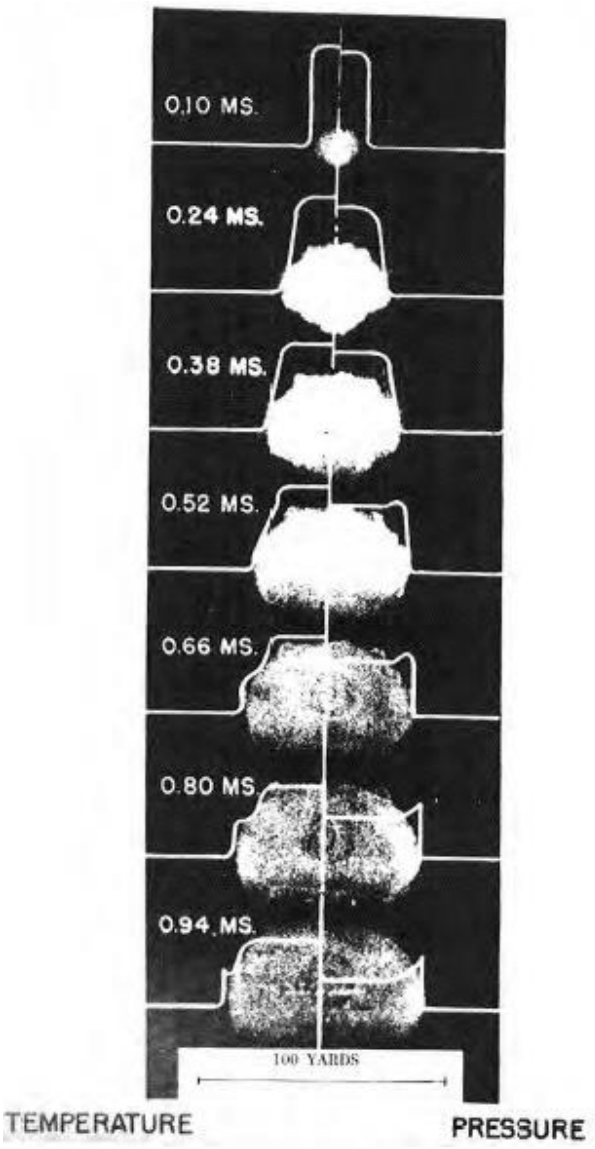

Figure 4.14 Pressure vs Temperature of a 20 KT Blast [1]

The picture in Figure 4.14 has a time scale from .1 ms to .94 ms out to an estimated distance of approximately 100 yards. Most of the shock front forms around approximately .1 ms [1]. This is significantly longer than the prompt radiation which has long since deposited its energy and left the area meaning the radiation being seen is mostly from the shock front. The curves overlayed on the photo show the relative

scale of pressure and temperature. This is a useful depiction of how the shock front forms over time and what the temperature gradient at the shock front looks like as the pressure forms. Temperature is continuously affected by absorbing thermal radiation from the fireball while most of the pressure is generated in the initial shock front causing some of the discrepancies seen in the profiles.

Figure 3.3 presented earlier in the methods sections also shows peak overpressure for a 1 KT blast in free air. Figure 3.3 has a max peak overpressure of 2000 pounds/inch^2 which is the equivalent of 13.79 MPa at a distance of 100 feet or 30.48 meters. At 100 meters or approximately 328 ft Figure 4.8 gives a peak overpressure between 1 and 2 psi. This would be the equivalent of about .0103 MPa. These figures were generated for a 1 KT free air burst. These can be compared to the results listed in Figure 2.3 from Northrop "Handbook of Nuclear Weapons Effects" which were also generated for a 1 KT blast [3]. At 10 meters Figure 2.3 shows a peak overpressure of approximately 300 MPa [3]. At 50 meters it is closer to approximately 150 MPa and at 100 meters the peak overpressure is approximately 1 MPa [3]. Interestingly, this is close to results from the "Blast Wave" report from LANL shown in Figure 4.15 below.

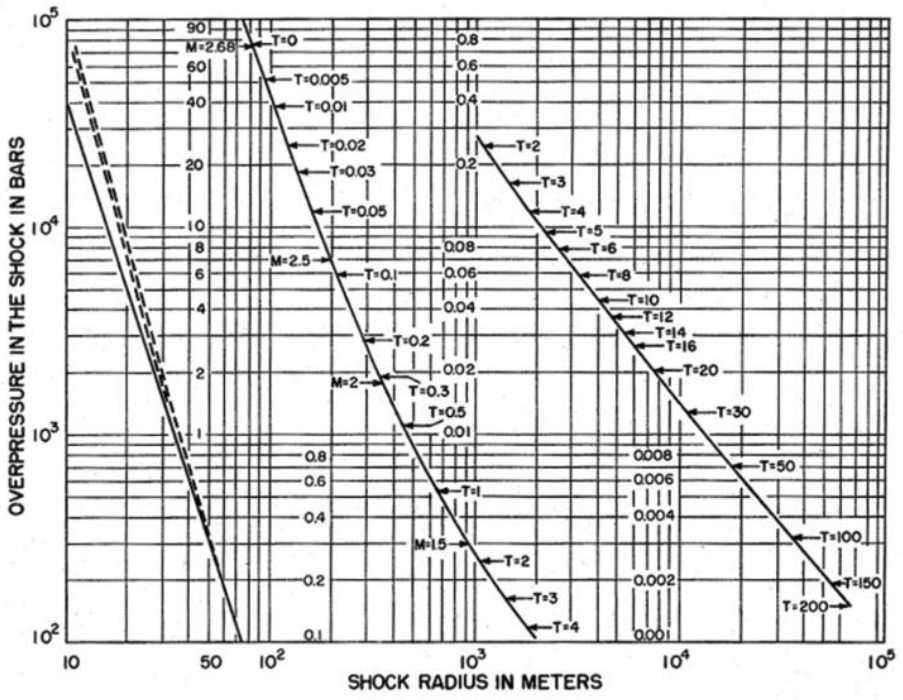

Figure 4.15 Peak overpressure (bars) vs shock front radius (m) [2]

This chart was generated using a IBM computer in 1947 to simulate overpressures of a 10 KT blast. At ten meters this chart supports that the peak overpressure of approximately $40x10^4$ bars which is 4000 MPa. The results in this table are calculated prior to T=0 which is when the IBM simulation started running. T=0 is actually .012 seconds after the explosion. This means at approximately .1 seconds the shock radius would already be at 100 meters and have a peak overpressure of approximately 40 bars or 4 MPa [2].

The final two values that have significance are the dynamic overpressure and the shock front velocity. For both figures the best models are found in the Northrop book. Dynamic pressure is given with peak overpressure in Figure 2.3 [3]. It is shown that within the first 100 meters that the dynamic pressure is slightly higher than the peak overpressure and after 100 meters the overpressure quickly outpaces the dynamic pressure. At 10 meters, the peak overpressure is estimated to be approximately 350 MPa. The estimated dynamic pressure at 10 meters is approximately 787 MPa which is 437 MPa higher than the peak overpressure [3]. These two values start to converge somewhere around approximately 100 meters. At this point, the dynamic pressure is approximately 1.5 MPa where the peak overpressure is 1 MPa [3].

The shock front velocity is displayed in Figure 2.9 of the Northrop handbook[3]. It shows that the shock front velocity of a free air 1 KT blast at 10 meters is approximately 5.50E+03 m/s [3]. This drops down to approximately 6.00E+02 m/s at 100 meters [3]. Another historical that shows the relationship between peak overpressure is shown in Figure 4.16 below:

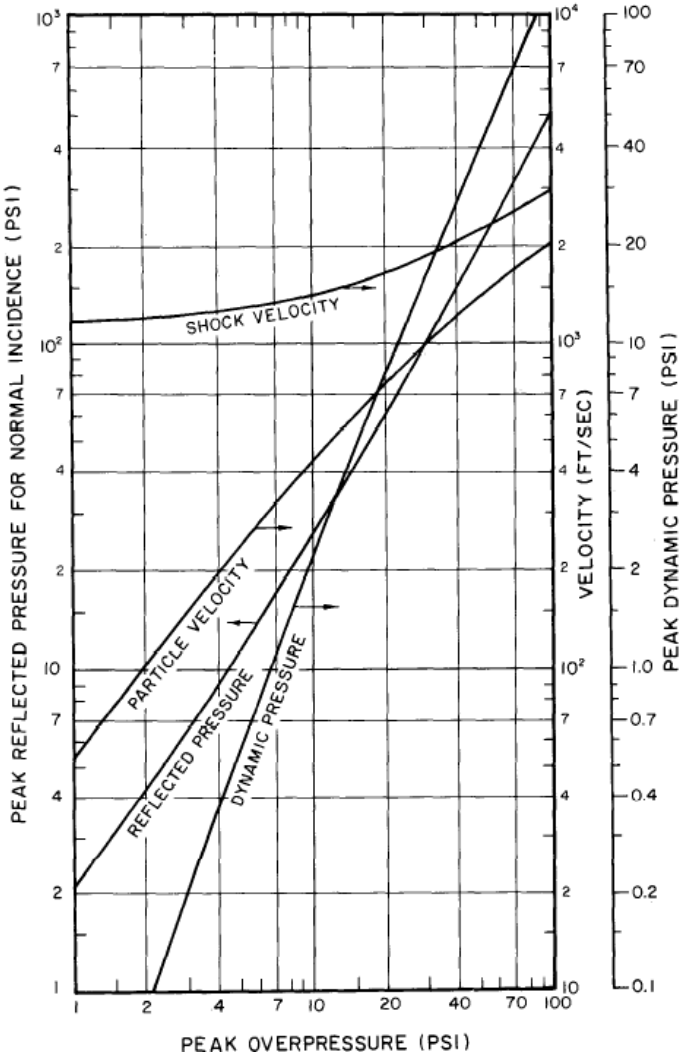

Figure 4.16 Relationship between peak overpressure and particle velocity

Figure 4.16 estimates that at a peak overpressure of 100 psi the particle velocity (or material velocity) is approximately 2,000 ft/sec. This pressure is the equivalent of .689 MPa which is significantly below most the values generated in Table 4.25. The peak overpressure of a 1 KT blast does not drop below this pressure until approximately 100 meters. The material velocity at this point is 517 m/s which close to the ~610 m/s given in Figure 4.16. This gives us a scale to understand how peak overpressure relates to other blast wave features. It should also be noted that the values generated in each of these historical results are for 1 KT blasts at standard temperatures and pressures[1,2,3]. All blasts are considered free air standard burst

which means it is a blast simulated at sea level altitudes with no ground[1]. These historical tables and numbers give the ability to compare the simulation results and determine if the changes calculated are realistic.

5 Discussion

Modeling or simulating the extreme forces present in a nuclear blast is never a simple or easy task. There are multiple variables that are difficult to accurately account for such as the state of air at high temperatures and pressures, the reflection from a surface, or the change in density due to elevation. These difficulties are accounted for with assumptions that introduce error into the simulation. In many cases the results can only be compared to historical data in order to verify the validity of the simulation. It becomes an important task to highlight the differences between what was observed against what might be expected. Additionally, the limitations of the model used in the simulation must be explored to show the possible sources or error. Finally, it is important to explore the future of the work in this field.

5.1 Expected Results vs. Observed Results

There were many possible outcomes for this research. Based on historical analysis of the issue it was expected that prompt radiation could play a role in the early stages of blast wave formation. However, it was documented prior to this research that over time and distance the blast wave formation characteristics become uniform [2]. This indicates that while there could be a short term impact to blast wave formation, at greater distances prompt radiation would become less important. Additionally, there are multiple different types of weapons that yield different amounts of neutron and gamma prompt radiation at different energy levels. To differentiate between devices MCNP6 was used to simulate the devices under equal conditions. These results could then be used in analytical solutions to blast wave variables. From these results the overall impact of simulating prompt radiation could be inferred.

5.1.1 MCNP Results

In order to make the best analysis of the potential impacts of prompt radiation on blast wave mechanics it must first be determined what type of device is most appropriate for analysis. To do this the initial MCNP6 simulations were ran out to a distance of 10 meters. This was conducted for four distinct weapon types and their results compared to see if there is a significant difference in temperature change. Once the results can be compared, one device type is selected to do a larger simulation out to 100 meters to generate results to use in the blast wave analytical solutions.

The amount of energy deposited within the first 10 meters of each of the simulations ranged from millions of degrees (K) at close distances down to tens of thousands of degrees (K) at 10 meters. Within the first few meters it can be seen in Figure 4.5 that temperatures might increase into the millions of kelvins for each device type with only the Type 13 device having a significant difference in output. These are temperatures levels that are fully expected close to the blast [1]. As expected, there was a decrease of energy deposited as distance increased. Historical models show that while prompt radiation can travel hundreds of meters in air, the quickly expanding volume of air present would significantly dampen any effects that radiation would have on temperature [1]. This is evident in Figure 4.6 which shows the sharp drop of temperature in the first few meters followed by a more steady cooling over the next 90 meters. This result is expected as neutrons are not able to travel as far in air as gamma radiation. This can be observed in Table 4.16 in a Type 3 device which has a lower radiative yield of gamma rays. At 1 meter, the neutrons account for 2.09E+04 C of temperature change compared to 7.36E+03 C from the gamma radiation. By 100 meters, the change in air from neutrons is 1.23 C compared to .596 C from gamma radiation. The gap between the neutron and gamma radiation decreases with distance.

In Table 4.16 at a distance of 1 meter the total contribution to temperature change between neutrons and gamma radiation is not even on the same order of magnitude. The change in temperature from neutrons is almost 10 times higher than the changes

from gamma radiation. This ratio quickly changes by 10 meters the change in temperatures from neutrons is only double the change from gammas. Gamma radiation is becoming more impactful on air temperature over larger distances.

The difference in temperatures for each device was expected to increase for each device type as they grew in complexity of design and available radiation energy spectrum. However, it was not anticipated how much of an impact the Type 8 gamma ray yield limitations would have. The Type 3 device is the simplest of the devices simulated, it used only fission as a source for neutrons and gamma rays [3]. Yet, despite its limitations it produced higher temperature changes than the more modern Type 8 device which also included higher energy neutrons from fusion. When Table 4.13 is compared to Table 4.11 it can be observed that at 10 meters the Type 3 device yields almost 8% more temperature change than the Type 8 device. From this we can make a few implications about the design of the Type 8 device that make it less suitable to use in the larger blast wave simulation.

The Type 8 device uses a thermonuclear secondary which increase both the energy and number of neutrons and gamma rays produced [3]. However, the yields were calculated according to Table 8.5 and 8.6 given by the Northrop handbook for nuclear weapons [3]. These tables show that there is a limiting factor in Type 8 devices that must be accounted for [3]. The Northrop manual does not specify why this limit exists, only that it does. One possible factor is the size of the device. In order to physically accommodate the space for the thermonuclear secondary the overall mass of the design might have been increased. This increased amount of mass would absorb gamma radiation at a much higher rate than any device that is smaller [2]. This limiting factor reduces the overall amount of prompt gamma radiation in a 100 KT blast by 26.3%. This reduction in overall available gamma rays is what reduces the temperature changes to below those generated even in a pure fission device like the Type 3 device. Initially it was expected that the higher energy levels of neutrons from fusion would overcome the limited gamma radiation escaping the device. This was not the case, as the Type 3 and Type 8 devices had extremely similar results. Despite up to half of the energy of a Type 8 device coming from

fusion, it did not change the impact of the prompt radiation as expected. Compare those results to the results of Type 13 device, which yielded significantly higher amounts of radiation. The Type 13 device had by far the highest temperature yields which would be expected. The Type 13 device had the highest average neutron and gamma energy level, as well as the highest number of prompt radiation particles released. This is within expectations for this device type which is specifically designed to increase the radiative yields [3].

Multiple previous studies have identified a few different key temperature milestones in blast wave formation [1]. It was expected that prompt radiation would have a significant ability to increase the temperature of air up to or past those critical temperatures [2]. The highest threshold for temperature was around 3E+05 K [2]. It is expected that below this temperature the blast wave would be able to form. It would be expected then that based on the initial conditions set by the prompt radiation that the blast wave would form at or beyond the shells that had their temperature increased above this amount. Some historical models have estimated the shock front forms anywhere from 5-10 meters away from the blast for a 1 KT blast[2].

In the Type 3, 5, and 8 devices it is seen in Figure 4.5 that the temperature of the air is heated to over 300,000 K at approximately 3 meters from the blast. The Type 13 device in Table 4.14 produces these same temperatures out to 6 meters. This is due to the much higher amount of prompt radiation as well as a higher average energy level of that radiation. Based on the limited understanding of the mechanics and individual designs of these weapon types it is only possible to rely on given historical data. The Type 3, 5, and 8 devices are all more limited in the amount and energy of prompt radiation. The Type 13 has significantly higher available energy levels as well as available amount of neutrons and gamma rays produced. The temperatures shown in the simulation would imply that the shock front would form at the distances between 3-6 meters. This is generally in line with expectations of the front forming between 5-10 meters for a 1 KT blast.

Since there is variation between the temperature change of different device types, it is possible to simply choose one type in order to model blast wave effects. This

will allow a simulation with the most accuracy possible to compare to available historical charts and figures. The Type 3 device yielded similar results to both the Type 5 and Type 8 designs without the added energy from fusion. Many of the historical charts were generated with fission devices in mind[1,2]. The Type 13 device was the most modern and the most likely therefore to exceed the historical charts due to the higher radiative yield. For these reasons the Type 3 device was selected to continue the simulation out to100 meters as shown in Table 4.15. The results of that simulation show a temperature change as great as 775 K at distances of 100 meters prior to the shock front moving through the area. This is for the higher 100 KT yield. This rate is consistent with the results of the earlier simulation shown in Figure 4.6. The way this simulation was conducted the main driving factor for the scale of temperature change was purely yield of the device. The decrease in energy was at the same rate for the Type 13 (with the highest temperature change) and the Type 8 device (with the lowest temperature change) over the first 10 meters. The results for the Type 3 device are consistent with all the other simulated outputs and are considered reliable temperature changes to be used in the blast wave calculations.

5.1.2 Blast Wave Analytical Solution Results

The analytical solutions to blast wave effects implement ambient pressure, temperature, and density of the air ahead of the blast wave. There were multiple assumptions that were vital to implementing these equations. The first assumption was that the detonation was done in free, homogenous air. This means that no ground was present and the energy could be deposited as if the only elements present were natural air. This eliminates factors like reflection which are significant factors but also allow for simpler and more straightforward calculation to be made. This assumption also includes the starting density of air to be sea level and dry air. Blast wave effects vary significantly with elevation as the density of air changes[1,2,3]. Placing the blast at sea level conditions prevents the need for excessive scaling laws in combination with other assumptions already made to make the calculations possible [1]. This serves the purpose of reducing error in the calculations. It is also consistent with the conditions set in historical charts like the Figure 4.13 as well as

the result contained in the Northrop manual. Each of these used the same assumptions in order to generate historical results of different effects[1,2,3]. The final assumption used was the constant volume and density of air. This is an important assumption because the state of air close to the blast varies widely with temperature and pressure. In order to account for the state of air to some extent, a separate case study was conducted where pressure was kept constant. It is important to note this was simply to give an understanding of the potential impact of changing air density, not to generate the most accurate results. The truth likely lies somewhere between the density of air changing while pressure increases simultaneously. Finally, the last case study to be analyzed was simulating a 1 KT blast. This will allow for observing the changes in the ability of prompt radiation to impact blast wave effects based on yield.

To generate a baseline for calculations, each calculation was done for two separate conditions. The first set of calculations were done considering the initial conditions created by prompt radiation. The second, were done for STP to give a minimal value expected for each calculation. Looking at Table 4.17 there is a slight difference between the peak overpressure of the prompt radiation simulation and the STP. This difference is from the increased ambient pressure of air that is a results of the prompt radiation increasing the temperature. Table 4.22 shows that modeling prompt radiation for a 100 KT yield increases the peak overpressure from the STP outputs by as much as .20% at a distance of 100 meters. This is small in comparison to the change generated at 100 meters by a 1 KT blast. Table 4.26 shows that at 100 meters the prompt radiation increases the STP peak overpressure in a 1 KT blast by as much as .55%. That isn't to say that peak over pressure of a 1 KT blast is .55% higher than a 100 KT blast at 100 meters. The percentage change represents the change in peak overpressure that was calculated for STP based on the respected yields of the device.

What this indicates is that prompt radiation has a decreasing impact on peak overpressure as yield of the device increases. At 100 KT the peak overpressure at 100 meters is an estimated 33.4 MPa ash shown in Table 4.18. The ambient pressure

due to prompt radiation at this distance is .169 MPa. The ratio between peak overpressure and ambient pressure is roughly 197.6 meaning the peak overpressure has so much energy it dominates the relationship. Compare the 100 KT pressures, to the pressures at the same distance in the 1 KT results shown in Table 4.24. At 100 meters, the peak overpressure is .600 MPa. The ambient pressure which was calculated but not shown is .105 MPa. The ratio between peak overpressure and ambient pressure is only 5.71. The lower ratio means that the ambient pressure caused by increasing temperatures from prompt radiation are able to have a higher influence on blast wave systems. This is especially true at greater distances as shown in Figure 4.8. This would indicate that the increase in temperature cause by modeling prompt radiation has more of an impact at 1 KT than 100 KT.

Comparing results in Tables 4.20 and 4.25 to those displayed in the Northrop handbook there are similar results in the prompt model for a 100 KT blast at equal distances. In order to compare equally it is important to use the scaled distance as shown in Table 4.17. This means using scaling laws to estimate the difference between blast yields that 10 meters in the Northrop Figure 2.3 is the equivalent pressure at 50 meters for a 100 KT blast[3]. At 50 meters in Table 4.18 the peak overpressure is estimated to be 254 MPa for a 100 KT blast. At 10 meters in the Northrop Figure 2.3 the peak overpressure is approximately 350 MPa. For the 1 KT results in Table 4.24 at 10 meters the estimated peak overpressure is 316 MPa. All of these estimates are significantly below Figure 4.15 given from the LANL "Blast Report" from 1947 which estimates a value closer to 3000 MPa [2]. Considering how close the results are to the more modern Northrop figures, it would be safe to conclude that the results are relatively accurate for peak overpressure for both the 100 KT and 1 KT blasts.

The next important values to analyze are the air density and the shock front density. Table 4.19 compares the prompt and STP solutions at 100 KT. The STP density of air is a constant 1.23 kg/m^3 which makes sense since the temperature and pressure are constant. Regardless of yield, both prompt radiation results actually have slightly lower value of 1.24 kg/m^3. The ambient air density is probably not the

driving factor in the production of the shock front density. The shock front density is also dependent on the ratio of the peak overpressure to the ambient pressure. Due to these relationships, even though the densities of air are relatively constant, the shock front density values converge at approximately 60 meters for the 100 KT blast as shown in Table 4.19. After 60 meters the STP model actually has a higher shock front density. Both the values for density of air and shock front density are within range of calculations done in the LANL "Blast Report" and represent valid values for possible states of air in the shock front at different temperatures and pressures [2]. This can also be compared to the 1 KT results which also drop below STP estimates except at a distance of only 50 meters as shown in Table 4.26. The 1 KT calculations also show that in a lower yield the impacts of implementing prompt radiation into calculations has a more severe effect on shock front density inside 100 meters.

Table 4.26 shows that at 100 meters the 1 KT prompt radiation changes the STP shock front density by as much as -.361%. Compare this to the results of Table 4.22 which show at the same distance the 100 KT calculations change the STP shock front density by only -.234%. At this distance for a 100 KT yield, Table 4.19 shows that the shock front density is 7.20 kg/m^3. At the same distance for a 1 KT yield Table 4.24 has a significantly lower value of 2.88 kg/m^3. This is comparable to an estimated STP shock from density of approximately 3.74 kg/m^3 for a 1 KT blast as shown in Table 4.24. Figure 4.9 shows the difference in how much modeling prompt radiation changes with yield. What this implies is that prompt radiation is more important to shock front density at lower yields.

To answer the question of why the values of the shock front density are higher in the STP simulations compared to the prompt simulations at larger distance there is little research available on what could be occurring. It is mentioned breifly in the "The Effects of Nuclear Weapons" source that there is a certain distance from the blast that the air is at a sufficient density to allow the formation of a sharp shock front similar to the one shown in Figure 2.1[1]. It is possible that this is the point shown at 10 meters that meets this minimal criteria for 100 KT and 1 KT. More study would be needed to verify where exactly the shock front would form. Looking at Figure

4.14 it can be observed that the shock front does begin to form a sharp pressure profile around 50 meters for a 20 KT blast. This picture is not meant to generate exact points of certainty so it is not reliable in giving an exact comparison. It does however give a reference point, it could be expected based on observed blasts that the blast for 20 KT yields and higher in free air form shock fronts by at least 50 meters. This photo also tries to relate the scale of the shock front temperature to the peak overpressure. Shock front temperature is an important aspect of blast wave as it is one of the primary contributors to the light that is used to measure the yield of a nuclear blast using optics.

Shock front temperatures for the STP and prompt models are both given in Table 4.21. It is interesting that the prompt shock front temperatures are lower than the STP outputs by approximately -2.57% at 1 meter. This difference decreases with distance, and at 100 meters the prompt model temperature begins to gradually converge with STP. This difference between STP shrinks to -.994% at 100 meters where the calculations and simulation were stopped. This can be compared to the 1 KT results in Table 4.26 which shows a slightly faster change in shock front temperature. The 1 KT results show that prompt shock front models start -2.57% below STP estimates at 1 meter just like the 100 KT results. By 100 meters the difference has decreased to -.66%. This indicates that the prompt radiation at lower yields is having more of an impact at closer distances than higher yields.

The shock front temperature is dependent on ambient air temperature, ambient pressure, and peak overpressure. The STP model has constants for temperature and pressure, the prompt model used the MCNP6 outputs to generate temperature changes. From those temperature changes, the Ideal Gas Law was used to calculate pressure changes. The higher temperatures and pressures of the prompt simulations cause the shock temperature to drop more slowly than the STP model. Additionally, in the 1 KT results as discussed earlier in this section the ratio between the peak overpressure is lower than the 100 KT calculations. This would indicate that ambient pressure would be more important in lower yields. This effect is also seen in the shock front temperature where again it is observed the simulating prompt radiation at

lower yields has a larger impact than at higher yields. It is also interesting to note that both prompt calculations change at very different rates than the STP calculations. This would indicate that at even greater distances these changes may become even more pronounced.

Figure 4.13 implies that that there is a divergence between expected and optically observed temperatures in the shock front [1]. A large part of this is because air heated over five thousand degrees readily absorbs the thermal radiation behind it [2]. The difference in the curves could be accounted for by the prompt radiation heating the air in advance of the shock front shielding it from optical view. This would increase the time it would take to see the shock front allowing for the front to cool prior to being viewed. It is expected that as understanding of what occurs inside the first 100 meter of a blast grows, the curves in Figure 4.13 would progressively converge to a more accurate answer. This would be especially useful in estimating the yield of a nuclear blast which is reliant on the time between the two peaks shown in Figure 4.13[8].

The constant density of air does not have as great of an impact on the shock temperature at this point in the calculations. However, when an alternate case study was conducted under constant pressure conditions relationships occur. The results shown in Table 4.23 show a large increase of shock temperature and a large decrease in shock front density. Shock front temperatures at 60 meters were almost as high as 2.28E+05 K while the shock front density was as low as 2.27 kg/m^3 for a 100 KT yield blast. While this represents values that are high for shock temperature and low for density, they give an idea of what the ceiling of these values could be if air density changes due to temperature increases. They also might help determine the exact point that the shock front would form in a 100 KT blast. More research would be needed to solve the state of air equations to balance out the exact change in air density and pressure. It would be best to use an advanced radiation hydrodynamics code like the Rochester University “Flash” code which will be discussed more in the following sections.

The last two values generated were the material velocity and the dynamic pressure. These are shown in Table 4.20 and represent blast wave effects that occur in and behind the shock front. The material velocity is how fast particles inside the shock front are moving and dynamic pressure is the drag pressure the wind behind the shock front can create on objects [1]. Dynamic overpressure is the kinetic energy per unit volume of air immediately behind the shock front. Both material velocity and dynamic pressure are related to peak overpressure as shown in Figure 4.16. Figure 4.16 gives an overview of how these pressures are related along with material and shock velocity for a 1 KT blast[1]. Figure 4.16 estimates that at a peak overpressure of 100 psi (~.689 MPa) in a 1 KT blast that max shock velocity is approximately 2,000 ft/sec or 609 m/s. The peak overpressures in the prompt simulation do not drop below 33.3 MPa inside 100 meters as shown in Table 4.18. If the peak model is scaled down to 1 KT yield using scaling laws and the calculations are conducted again the overpressure doesn't drop to .690 MPa until almost 90 meters. At 90 meters in these calculations the material velocity is 600 m/s. This can be compared to the outputs from the actual 1 KT estimates in Table 4.24. In table 4.24 the pressure of .689 is reached around approximately 90 meters for a 1 KT blast. At this distance the estimated material velocity is 604 m/s. This is on the same scale of the estimated velocity for Figure 4.16 as well as the scaled outputs for the 100 KT blast wave calculations.

Looking at Table 4.22, it is evident that there is very little difference between the prompt and STP conditions for material velocity for a 100 KT yield. The greatest impact to the overall results is at 100 meters where the prompt calculations lower the STP values for material velocity by -.572%. This means at 100 KT prompt radiation likely has a very minimal impact on the speed of the shock front. This makes sense since the primary driving factor for the material velocity is the peak overpressure which dominates the energy spectrum at 100 KT. However, at 1 KT the peak overpressure has lower impacts at greater distances as previously discussed. Table 4.26 shows that utilizing prompt radiation in blast wave calculations can lower the material velocity calculated at STP conditions by as much as -.765 percent. This is

greater than the impact of prompt radiation at higher yields. This indicates that like many other blast wave effects, prompt radiation is more important at lower yields for material velocity.

Another way to verify these numbers is to compare them to Figure 2.9 in the Northrop which estimates material velocity as a function of distance from the blast[3]. At 90 meters it estimates that material velocity would be as high as approximately 750 m/s for a 1 KT blast. The difference of 150 m/s is relatively large. This may be more reason to study the state of air which may impact these outcomes. When pressure is kept constant in Table 4.23 the material velocity increases to 7540. This is significantly higher than even the Northrop estimates. What it may show though is that the actual material velocity is influenced by the changing density of air. More research would be needed to make this conclusion.

Figure 4.16, which was used earlier for material velocity, is also useful for comparing the calculated dynamic pressure to the peak overpressure. The chart shows that it would be expected that dynamic pressure would be slightly higher than peak overpressure at high pressures over 100 psi and lower for all values under 100 psi. In Figure 4.16, at a peak overpressure of 2 psi(.0138 MPa) the dynamic pressure is approximately .1 psi (.00689 MPa). This is a ratio between dynamic pressure and peak overpressure of approximately .05 at its lowest measured point. Comparing Tables 4.18 and 4.20 the values for dynamic pressure are approximately two and a half times greater than peak overpressure initially at 1 meter. This decreases over time as the values begin to converge to a minimum at 100 meters where the ratio between dynamic pressure to peak is about 2.40. When the yield is reduced to 1 KT this convergence occurs more quickly. Looking at Table 4.24 for values of dynamic and peak pressures at 1 meter, the ratio between dynamic and peak overpressure is 2.5. At 50 meters the ratio has already decreased to about 1.94. By 100 meters the ratio has increased to .832. meaning that the peak overpressure is almost 1.2 times greater than the dynamic pressure at 100 meters. At 90 meters the peak overpressure is in a 1 KT blast was calculated to be .748 MPa (~108 psi). These values are almost

perfectly in alignment with than Figure 4.16. This may indicate that the calculations made are accurate and usable for further analysis.

The calculations for dynamic pressure were relatively consistent with values contained in the Northrop Figure 2.3[3]. The Northrop results estimate for a 1 KT blast that dynamic pressure would be greater than peak overpressure up to approximately 100 meters[3]. Northrop estimates that at 10 meters the dynamic pressure would be approximately 760 MPa. By 100 meters this drops to ~1.5 MPa. Table 4.25 shows that for a 1 KT blast the estimated dynamic pressure at 10 meters is ~787 MPa. At 100 meters dynamic pressure drops as low as .50 MPa. Northrop gives a confidence interval of $\pm$15% for its estimate. This means at close distances the dynamic pressure outputs are inside what is expect. But at larger distances the simulation results diverge from expected results. This could imply that simulating prompt radiation impacts dynamic pressure simulations.

In terms of the overall impact modeling prompt radiation had on dynamic pressure the different case studies have very different results. Table 4.22 shows that at 100 KT the prompt model only changed the STP values for dynamic pressure by a maximum of -1.37% at 100 meters. This can be compared again to Table 4.26 which shows how much prompt radiation changed dynamic pressure in a 1 KT blast. In the lower yield blast at 100 meters the prompt radiation lowered the STP dynamic pressure by -1.88%. Much like the other analyzed blast wave effect, the influence of prompt radiation was greater at lower yields.

When the dynamic pressure results are compared to the constant pressure case study the results are very similar to the initial 100 KT results. Dynamic pressure in Table 4.23 is 81.2 MPa which is only slightly higher than the 80.1 MPa estimate in Table 4.20 for the original 100 KT results. This would indicate that at close distances and low elevations the density of air has a minimal impact on the dynamic pressure.

5.2 Limitations of Research

There were significant limitations at many different parts of the research conducted. When simulating the extreme physics of a nuclear blast error is inevitable. Some of the largest constraints come down to the limited ability of even modern machines to

perfectly carry out the millions of calculations needed to account for the thousands of variables at each stage of radiation transports. Adding to the complication of the research was the need to utilize two separate codes in order to effectively see the potential impacts of prompt radiation.

First, one of the most limiting factors in the research is the lack of prior interest or simulations done in this area. Most early research on nuclear weapons effects concluded that the most important aspect of prompt radiation was the possible radiative dose in organic tissue. This could be especially important to organic life that survives the extreme blast wave and heat from the thermal radiation. The dose of prompt radiation can indeed be very high as gamma rays propagate at nearly the speed of light and penetrate miles in air. Additionally, Due to the blast wave eventually becoming more uniform over time the early phases of the blast become unimportant when looking at larger distances from the blast. The blast wave more or less propagates the same for each device type according to previously generated models after a certain point regardless of how much prompt radiation changed the initial conditions. As a result, very little available research exists on the air temperatures at range as a result of prompt radiation. This lack of available information makes it difficult to perfectly analyze the accuracy of the simulation.

Second, for the sake of simplicity, many assumptions about the conditions of the air surrounding the blast had to be made. First, the initial starting point of the air temperature was the standard room temperature of 273.15K. This is a relatively safe assumption as the starting temperature of air is not significant when so much energy is present. What is important however is that the blast is simulated as if at sea level but in infinite air. The conditions and characteristics of blast wave formation change drastically with increased elevation. Air becomes significantly less dense, radiation travels further, and in general interacts less frequently due to the thinner atmosphere present at higher elevations. Alternatively, modeling the ground in any capacity increases both the computational time and complexity of the problem significantly.

A third important assumption that limits the overall accuracy of the model is the specific heat capacity of air. For this research a constant value of 1.4 J/g-C was

used. As temperatures increase, the specific heat capacity of air would increase as well. This means that as the air heats up it resists absorbing heat more. At higher temperatures in the millions of kelvins air would significantly resist any changes in temperature. This would potentially push significantly more energy out into shells further from the center of the blast. The main difficulty is that there is not an inherent table built into MCNP that accounts for these extreme temperatures. It would be extremely difficult to capture temperature changes in this infinitely small space of time and large amount of available energy. It is necessary than to assume a constant specific heat capacity in order to generate a reasonable estimate of how much the temperature could change. This estimate is still reliable as long as temperatures do not significantly vary from historical estimates. Most historical models account for temperatures inside the shock front of the blast wave. The blast wave is expected to contain more energy and higher temperatures than the prompt radiation.

5.3 Future of Model

While the simulation was able to give a very basic representation of the impact of prompt radiation, there is significant room for future growth. Many of the improvements that can be made to the research involve the assumptions used to generate multiple different results. Perhaps the largest assumption that can be improved upon is the burst occurring in free open air. By removing in surfaces from the equation it simplified the model significantly, but it also took away from the ability of the research to be used in what might be its most significant impact. Ultimately simulations like this can be a huge benefit to civil disaster preparedness and response. In a worst-case scenario, if a nuclear detonation occurred in a populated area, civil planners would need blast simulations and models that help them understand the effects on the surface of the earth. How radiation is transported when the surface of the earth is added into the simulation would significantly change many of the outputs. This is even more true in a heavily urban environment with buildings and a variety of different materials for both radiation and blast wave effects to interact with. To improve upon this model the first step would be to implement the earth in both the MCNP6 simulation and the calculations done for blast wave effects. The

final solution would include a city environment with dense materials like concrete and steel included. The dense materials would significantly change the impacts of prompt radiation and would also deform the blast wave effects.

Including a surface burst would also make it possible to analyze another prompt radiation impact. In surface bursts, what is known as a "precursor" is formed by prompt radiation heating various materials suspended in the atmosphere [1]. This precursor is a mini-blast wave that propagates in advance of the main blast wave. This would have possibly significant impacts on the ambient air density and temperature ahead of the blast wave. Ambient conditions can be large driving factors in blast wave models and could be key in urban environments as well. Any future models would have to consider this as an impact. This is extremely challenging to simulate in all possible environments, but surely an accurate simulation could be generated for various biomes at a minimum.

Another area of improvement that can be made is improving the simulation for the state of air at high temperatures and pressures. Table 4.23 highlights the highest changes possible if the pressure is kept constant in the simulation. Some of the outputs like the material velocity are unrealistic and do not represent achievable speeds. However, it is also apparent that the air will not remain at a constant density in an environment where the prompt radiation can heat the air up to as much as twice the ambient temperatures at 100 meters. This is also true in the event of a surface burst where a more complicated simulation would be needed to see how the density of the air is impacted by dust, dirt, or other particles that would be heated significantly. It is expected that an advanced radiation hydrodynamics code like FLASH which was mentioned earlier might helped to make significant strides in this specific area. It may be possible for FLASH to simulate blast wave propagation through air or on surfaces. By combining the outputs from MCNP6 and FLASH it may be possible to integrate the impacts prompt radiation into the initial conditions of the code. This may generate more accurate results that could be useful in a variety of purposes for civil planning and response.

Another key area of growth for this simulation may be the inclusion of time as a factor in outputs. As has been mentioned at various points, the time gap between observable energy peaks of a nuclear blast is one key mechanism used to determine the yield of a device. This research assumed there was no time in order to simplify the expansion of the blast wave and make it possible to use existing equations to calculate blast wave effects. In reality, time plays a role in how different nuclear weapons effects scale with yield. This is also true in surface bursts where reflection of the radiation and blast wave alters blast wave propagation in time and space.

To implement time more effectively, the simulation would also need to be ran out to a longer distance. Currently, the simulation was only conducted for radiation inside 100 meters. In order to generate the most accurate results for different yields, it would perhaps be best to simulate out as far as 2000 meters. This would provide better information for larger yields to analyze the impacts of prompt radiation on blast wave effects at larger distances.

Lastly, the radiation transport model used in this simulation can be improved in a variety of ways. Radiation was modeled isotropically in spheres of homogeneous air. In reality, all radiation would be impact by weapon design. Neutrons are less affect by weapon design, but gamma radiation is altered significantly [2]. The dense materials in weapons tends to make the gamma radiation more directional than neutrons [2]. It is not clear what the best geometric distribution of gamma radiation could be in order to account for weapons materials, but clearly it is not perfectly spherical. The main impact could be an increase in gamma radiation in the directions that the blast wave propagates. An increase in available gamma rays would have a higher impact on ambient air temperatures and pressures. Those temperatures and pressures could in turn have more significant impacts on blast wave outputs, especially at lower yields. As was seen in this research, gamma radiation has increasing importance at large distances. A better understanding of the radiative release of different modern weapons may drive better simulations of blast wave effects.

There is plenty more research to be done to perfect modeling and simulation nuclear weapons effects. This is especially true for urban environments with more complicated interactions with buildings and various materials not seen in rural environments are upper atmospheric conditions. Better simulation tools would help civilian leaders plan and respond to nuclear blast events in order to minimize the loss of life and improve disaster response.

6 Conclusion

This research was started with the goal of analyzing the impacts of prompt radiation from nuclear weapons. Specifically, the focus was on the impacts to the unique blast wave formed by nuclear explosions. The hope is that by better understanding nuclear weapons effects it would develop better tools to use in civil disaster planning and response. To accomplish this, many assumptions had to be made to simplify the problem including limiting the potential yield, altitude, eliminating time, and modeling the blast in open air with no surfaces. Additionally, a constant specific heat capacity of air was utilized to attempt to account for the extremely high temperatures present in the model. To account for the broad spectrum of weapons designs, four different design types were selected to be modeled initially. These designs came from previously generated research which gave neutron and gamma weapon outputs based on the yield of each device. The first task was to simulate the neutron and gamma prompt radiation that would be released for each device at 100 KT.

The prompt radiation was modeled using MCNP6 code which provided highly accurate radiation transport results in open air. The blast was modeled as .5 meter void that would radiate neutrons and gamma rays isotropically in standard open air at STP conditions. The radiation was transported through a series of expanding concentric spheres of air. These spheres of air started at 1 meter and ran as far as 10 meters with 1 meter gaps of air between them. The MCNP6 code was then able to handle millions of particle interactions and estimate how much average energy (in MeV/g) would be deposited in the volume of each shell of air. The code also

generated accurate volumes and masses of the air which could be utilized in the post production calculations. These calculations would generate the first set of results that would be needed to accurately compare the different device designs.

Once the amount of energy deposited in air for each device was known, it needed to be determined how much that energy would increase the temperature of air. To determine this, the energy deposited was converted from MeV to Joules, and finally from Joules using a constant specific heat capacity, to degrees Celsius. The temperature was then converted from Celsius to Kelvin since most thermodynamic equations required air to be in units of Kelvin. The results for each device showed that more modern devices that were designed to have higher radiative releases also had higher impacts on air temperatures. The difference between the most advanced design and the simplest designs were not significant. The simplest device type analyzed was a Type 3 Device which was based on pure fission devices. The highest temperature analyzed at 1 meter for this device was 2.83E6 K. The most advanced device was the Type 13 Device which at the same distance yielded a temperature of 7.42E6 Kelvin. These results are more than twice as high as the Type 3 device, which would be expected. The Type 13 device was optimized to increase radiative release. To give a solid baseline for results, and since most of the oldest blast wave models were made for older weapons designs it was determined that the best device to use for further analyses would be the Type 3 Device. This would give a set of outcomes that would ideally be the smallest possible change. If there is significant change for the most simple design it would follow that more advanced designs would have higher impacts.

With a device selected, it was important to first do another simulation using MCNP6. The difference in the simulation was the distances simulated. This second simulation was done the same for the first 10 meters. After the first ten meters the simulation was continued with more spheres of air this time at 10 meter intervals out to 100 meters. Many historical blast wave charts and figures start at ten meters and have markers at 100 meters. This data was also converted into temperature using previously mentioned equations. At this point in time the temperature calculations

were done for two different yields of devices. This was to show the difference in impact of radiation at different yields. The calculations were done for both a 100 KT and 1 KT device. Since the temperature was modeled based on average energy deposited by particles in the MCNP6 code the results were similar for both yields. The real difference in their impacts occurred in the calculations of the blast wave effects.

In order to calculate blast wave effects, a set of equations that were given in previous weapons effect research had to be utilized. These equations generated values for peak overpressure at different radii, shock front density, material velocity, shock front temperature, and dynamic pressure. To use these equations multiple variables had to be calculated for different distances. The most important value calculated here was the ambient pressure of air. Ambient pressure and air were key contributors to many of the equations. These same calculations were also made using standard temperature and pressure conditions to give a baseline for outputs. As a final experiment, a third set of calculations were done at constant pressure conditions to see how the density of air would impact blast wave effects.

What was found was that prompt radiation at higher yields had relatively low impacts on blast wave effects inside 100 meters. The values for peak overpressure were so dominant in many of the calculations at this yield and distance that the radiation simply did not contain enough energy to be relevant. However, in the constant pressure calculations done for the 100 KT yield there were larger changes to many of the blast wave effects. Many of these effects, such as material velocity, produced unrealistic results. This indicates that air density could play a factor but it is not the sole deciding factor in these calculations. Further research would be needed to understand the state of air near the blast before impact of the air density could be better understood.

The second conclusion from these blast wave calculations is that prompt radiation does have a more significant impact at lower yields. Most of the changes had increasing impacts with distance with a max at 100 meters. For example, 1 KT results lowered the outputs of shock temperature by only -.660% at 100 meters. It

also lowered the dynamic pressure behind the shock front by as much as -1.8% at the same distance. All the 1 KT impacts were higher than the same calculations done at 100 KT. It was evident that prompt radiation (especially gamma rays) increased in importance at lower yields since radiation propagates in air much more readily than blast wave effects. Many of those blast effects are dependent on the relationship between peak overpressure and ambient conditions. At lower yields, prompt radiation increases ambient conditions, while peak overpressure drops drastically with distance. This indicates that modeling prompt radiation can have more importance as lower yields.

More research is be needed to determine the exact point at which prompt radiation would be completely negligible. It is at least clear that at 100 KT the energy released in the blast wave is significantly higher than the energy from prompt radiation making it irrelevant to blast wave analysis. There is a spectrum of the importance of prompt radiation by device type starting near 1 KT and decreasing the higher the yield.

The next step in this research is to utilize more advanced computer codes that may more accurately simulate these complex blast wave equations. Using may grant a better clarity of how much of an impact that prompt radiation may have on blast wave effects.

References

[1] Samuel Glasstone and Philip Dolan, “The Effects of Nuclear Weapons,” United States Department of Defense and United States Department of Energy, 1977.

[2] H.A. Bethe, K. Fuchs, J. Hirschfelder, J.L. Magee, R.E. Peierls, and J. Von Neumann, “Blast Wave,” Tech. rep., Los Alamos Scientific Laboratory, 1947.

[3] John Northrop, “Handbook of Nuclear Weapon Effects: Calculation Tools Abstracted from DSWA’s Effects Manuel One (EM-1),” Defense Special Weapons Agency, 1996.

[4] Paul Whalen, “Source and Replica Calculations,” Tech. rep., Los Alamos Scientific Laboratory, 1994.

[5] R.L. Holmes and S.W. White, “Standardized Unclassified Little Boy and Fat Man Outputs,” Tech. rep., Defense Threat Reduction Agency, 2013.

[6] Office of the Undersecretary of Defense for Acquisition, Technology, and Logistics, “Report of the Defense Science Board Task Force on Nuclear Weapons Effects Test, Evaluation, and Simulation,” Tech. rep., Defense Science Board, 2005.

[7] C.J. Werner(editor), "MCNP Users Manual - Code Version 6.2," Los Alamos National Laboratory, report LA-UR-17-29981 (2017).

[8] Guy E. Barasch, “Light Flash Produced by an Atmospheric Nuclear Explosion,” Los Alamos National Laboratory, report LASL-79-84 (1979).

Appendix A

Example MCNP6 Neutron Simulation Input Card

```
circular area 100 meter of air, 10 cm inner area currently air
c cell cards
1 1  -.001225 -1  imp:n=1 $source area
2 1  -.001225 1 -2  imp:n=1
3 1  -.001225 2 -3  imp:n=1
4 1  -.001225 3 -4  imp:n=1
5 1  -.001225 4 -5  imp:n=1
6 1  -.001225 5 -6  imp:n=1
7 1  -.001225 6 -7  imp:n=1
8 1  -.001225 7 -8  imp:n=1
9 1  -.001225 8 -9  imp:n=1
10 1  -.001225 9 -10  imp:n=1
11 1  -.001225 10 -11  imp:n=1
12 1  -.001225 11 -12  imp:n=1
13 1  -.001225 12 -13  imp:n=1
14 1  -.001225 13 -14  imp:n=1
15 1  -.001225 14 -15  imp:n=1
16 1  -.001225 15 -16  imp:n=1
17 1  -.001225 16 -17  imp:n=1
18 1  -.001225 17 -18  imp:n=1
19 1  -.001225 18 -19  imp:n=1
20 1  -.001225 19 -20  imp:n=1
21 0           20  imp:n=0 $vacuum outside boundary

c Surface Card, creates concentric spheres of air centered at 0, each cell will be analyzed for energy deposition
1  so  50
2  so  100
3  so  200
4  so  300
5  so  400
6  so  500
7  so  600
8  so  700
9  so  800
10  so  900
11  so  1000
12  so  2000
13  so  3000
14  so  4000
15  so  5000
16  so  6000
17  so  7000
18  so  8000
19  so  9000
20  so  10000

c Data Cards, we want only prompt nuetrons that would be from fission (early blast time) and we want f6 tallies to see how much E is deposited
c source definition cards
SDEF CEL 1 erg=D1 PAR=1 $prompt neutrons using watt spectrum for energy distribution
SP1 -3 .988 10 $Energy of each neutron drawn from the watt fission spectrum between .988 and 10 MeV
mode n $determines what kind of particles are used
nps 100000 $number of generations to simulate
+f6 2 3 4 5 6 7 8 9 10 11 12 13 14 15 16 17 18 19 20 $adds together energy deposition (MeV/g) of all particles averaged over each cell
M1  6000  -.000124  7014 -.755268  8016 -.231781  18000 -.012827 $natural air, infinite free air simulation
```

Appendix A (continued)

Example MCNP6 Gamma Simulation Input Card

```
circular area 100 meter of air, 50 cm inner area currently air
c cell cards
1 1  -.001225 -1  imp:p=1 $source area
2 1  -.001225 1 -2  imp:p=1
3 1  -.001225 2 -3  imp:p=1
4 1  -.001225 3 -4  imp:p=1
5 1  -.001225 4 -5  imp:p=1
6 1  -.001225 5 -6  imp:p=1
7 1  -.001225 6 -7  imp:p=1
8 1  -.001225 7 -8  imp:p=1
9 1  -.001225 8 -9  imp:p=1
10 1  -.001225 9 -10  imp:p=1
11 1  -.001225 10 -11  imp:p=1
12 1  -.001225 11 -12  imp:p=1
13 1  -.001225 12 -13  imp:p=1
14 1  -.001225 13 -14  imp:p=1
15 1  -.001225 14 -15  imp:p=1
16 1  -.001225 15 -16  imp:p=1
17 1  -.001225 16 -17  imp:p=1
18 1  -.001225 17 -18  imp:p=1
19 1  -.001225 18 -19  imp:p=1
20 1  -.001225 19 -20  imp:p=1
21 0            20  imp:p=0 $vacuum outside boundary

c Surface Card, creates concentric spheres of air centered at 0, each cell will be analyzed for energy deposition
1  so  50
2  so  100
3  so  200
4  so  300
5  so  400
6  so  500
7  so  600
8  so  700
9  so  800
10  so  900
11  so  1000
12  so  2000
13  so  3000
14  so  4000
15  so  5000
16  so  6000
17  so  7000
18  so  8000
19  so  9000
20  so  10000

c Data Cards, we want only prompt nuetrons that would be from fission (early blast time) and we want f6 tallies to see how much E is deposited
c source definition cards
SDEF CEL 1 erg=1.5 PAR=2 $prompt gammas from fission produced ave E of 1.5 MeV
mode p e $determines what kind of particles are used
nps 100000 $number of generations to simulate
f4:p 2 3 4 5 6 7 8 9 10 11 12 13 14 15 16 17 18 19 20 $track length estimate of cell flux
f14:e 2 3 4 5 6 7 8 9 10 11 12 13 14 15 16 17 18 19 20$track length estimate of cell flux
f6:p 2 3 4 5 6 7 8 9 10 11 12 13 14 15 16 17 18 19 20$track length estimate of energy deposition.
f16:e 2 3 4 5 6 7 8 9 10 11 12 13 14 15 16 17 18 19 20$track length estimate of energy deposition from electrons
M1  6000  -.000124  7014 -.755268  8016 -.231781  18000 -.012827 $natural air, infinite free air simulation
```